Reductive Alkylation Reactions Using Tetramethyldisiloxane and Potassium *tert*-Butoxide via Reductive-Radical Polar Crossover

HANA NUGRAHA

Thesis submitted to the University of Ottawa
in partial fulfillment of the requirements for the
Accelerated Master's degree in Chemistry

Department of Chemistry and Biomolecular Sciences
Faculty of Science
University of Ottawa

Abstract

Hypervalent silicon compounds have shown increasing applications and synthetic versatility throughout recent years due to their unique reactivity. In this study, the combination of alkoxide base and silicon hydride species – potassium tert-butoxide (KO^tBu) and 1,1,3,3-tetramethyldisiloxane (TMDSO) – facilitates two different reactions involving the formation of $C(sp^3)$-$C(sp^3)$ bonds: the hydroalkylation of vinylarenes (chapter 2), and the cross-electrophile coupling of alkyl halides (chapter 3). This simple system of commonly available reagents is suspected to form a hypercoordinate silicon complex capable of acting as a single-electron donor as well as a hydrogen-atom donor. In each chapter, the process of discovery, optimization, scope, and mechanistic investigations are described. In chapter 2, mechanistic studies suggest the dual radical and polar characteristic of the benzyl nucleophile reactive intermediate, proving the system undergoes the process of reductive-radical polar crossover (RRPC) Ultimately, the TMDSO and KO^tBu reagent pair is thought to be synthetically useful in performing reactions in transition-metal-, photoredox-, and electrochemistry-free conditions, with a potentially larger number of transformations that have yet to be discovered. The formation of $C(sp^3)$-$C(sp^3)$ bonds is fundamental in organic synthesis and continues to be an ongoing field of research. Overall, novel routes towards the hydroalkylation of vinylarenes and cross-electrophile coupling of alkyl halides was successful using commercially cheap and synthetically available starting materials.

Acknowledgements

First and foremost, I would like to thank my research supervisor, Professor Steve Newman, for his guidance throughout my three years in his research group as a BSc and MSc student. Truly, my time in this lab has been very monumental for my academic and professional career, and I was able to learn so much valuable skills both inside and outside of the lab and research setting. Steve's example as a scientist and mentor has left a lasting impression on how I view research, learning, and my own potential, and I am sincerely grateful for having had this opportunity.

I would like to thank all of the members of the Newman lab that I have had the chance to overlap and work with: Eric, Adam, Piers, Aisha, Zichuan, Aref, Piyas, Shajia, Kian, Fran, Kostya, Isuru, and Mario. I am grateful to have had an amazing and supportive to both work and goof with, and I found myself friends that I'm sure I will be seeing long after the Newman days are past. A special thank-you-for-everything to Piers, with whom I shared this journey of the base and hydrosilane projects with from day 1. I was lucky to get a mentor who taught me a great deal about being a chemist, and a colleague who was always open to collaborate and chat about anything. Good luck on your next chapter, I'm sure it will be a great one!

I want to thank my parents for making the decision to allow me to come to Canada for university. I would not be here without my family's overwhelming trust, love, and support, and alhamdullilah for everything. As I wrap up my degree here, I wish for the same love, support, and success for my sister Zahira as she starts her university life this fall semester. Lastly, I want to thank my newly wed husband, Irbaz. I didn't expect to come out of this Master's already married, but I can't imagine a better way to begin this next chapter of my life. Thank you for your love and support.

Table of Contents

List of Schemes

List of Tables

List of Figures

Statement of Contribution

Unless otherwise noted, all work was performed by the author of this thesis. The work in Chapter 2 was performed under the direct supervision of PhD candidate Piers St. Onge during the Honours Project course (BPS 4006). The work described in Chapter 3 were performed solely by the author of this thesis. The research presented in this thesis is original and, where indicated, has been incorporated into peer-reviewed publications.

Abbreviations

4CzIPN	1,2,3,5-tetrakis(carbazol-9-yl)-4,6-dicyanobenzene, 2,4,5,6-tetrakis(9H-carbazol-9-yl)isophthalonitrile
Ac	acetyl group
Ar	generic aromatic ring
Bn	benzyl group
Boc	*tert*-butyloxycarbonyl group
Bu	butyl group
C(+)	graphite cathode
Cat	catalyst
CCRI	Centre for Catalysis Research and Innovation
$CDCl_3$	deuterated chloroform
CPME	cyclopentyl methyl ether
Cy	cyclohexyl group
d	doublet
DCM	dichloromethane
DMF	dimethylformamide
DMSO	dimethylsulfoxide
DTBP	di-*tert*-butyl peroxide
E.g.	for example
Equiv	equivalents
Et	ethyl group
Et	ethyl group
EtOH	ethanol
GC-MS	gas chromatography-mass spectroscopy
HAT	hyrogen atom transfer
HMDSO	hexamethyldisiloxane
HTE	high-throughput experimentation
Hz	hertz
I.S.	internal standard
^{i}Pr	isopropyl group
KHMDS	potassium bis(trimethylsilyl)amide
L	generic L-type ligand
LG	leaving group
L_n	generic L-type ligand; unspecified number around metal centre
M	metal
m	multiplet
m	meta substituent

Me	methyl group
MeOH	methanol
MHz	megahertz
Ms	mesyl group
Nap	napthyl group
Mg(+)	magnesium anode
nm	nanometer
NMR	nuclear magnetic resonance spectroscopy
o	ortho substituent
OAc	acetate
OMs	mesylate
O^{t}Bu	*tert*-butoxide
OTf	triflate (trifluoromethane sulfonate)
p	para substituent
pent	pentet
Ph	phenyl group
PhMe	toluene
PMHS	polymethylhydroxysilane
Ppm	parts-per-million
Py	pyridine
q	quartet
R	generic carbon chain
s	singlet
sBu	*sec*-butyl group
SET	single electron transfer
SI	supporting information
t	triplet
^{t}Bu	*tert*-butyl group
THF	tetrahydrofuran
TLC	thin-layer chromatography
TMDSO	1,1,3,3-tetramethyldisiloxane
Tol	tolyl group
TS	transition state
UV	ultraviolet
X	generic Cl, Br, I, or (pseudo)halide
XAT	halogen-atom transfer
µL	microliter
C(–)	graphite cathode

Chapter 1: INTRODUCTION

In this thesis, two projects are presented in which new synthetic transformations are identified, which are discussed independently in chapters 2 and 3. This introduction chapter serves to describe concepts that apply to both projects. The purpose and importance of pursuing research and development in finding new synthetic routes to add to the chemist's synthetic toolbox is described in chapter 1.1. Chapter 1.2 will present the reagent class that enables both transformations: organosilanes. Chapter 1.3 will present the key mechanistic step in which the reaction is hypothesized to proceed with: reductive-radical polar crossover. Chapter 1.4 serves to discuss research goals consistent with both projects with the purpose of understanding the uniquely reactive reagent system.

1.1: Expanding the synthetic toolbox

Expanding the synthetic toolbox refers to the discovery and development of new synthetic methodologies, granting access to a new chemical space for chemists to use worldwide. It remains as an ongoing field of research as it opens up new or alternative synthetic routes to accessing certain bonds, allowing chemists to expand their ability to create novel molecules that were previously inaccessible.

In fields such as drug discovery, agrochemicals, natural product analogues, and similar fields that require small molecule synthesis, this is particularly useful when traditional methods fail in providing routes to complex structures, sensitive functional groups, or stereochemical challenges.[1] In such fields, the speed in which more compounds can made and tested will increase the chances for success.[2] Therefore, with the discovery of new synthetic routes, chemists can have more "tools" from the synthetic library of transformations to access new

molecules and overcome challenges. Additionally, innovative methods can offer better selectivity and reaction efficiency , eliminate the need for expensive or toxic reagents, attain higher yields, minimize step-count to preserve atom-economy, or have the option to generate fewer waste products for improved sustainability.[3] Ultimately, expanding the synthetic toolbox enables diverse chemical processes that benefit both academia and industry.

In this thesis, the reagent combination of hydrosilane and alkoxide base remain a recurring theme in the facilitation of two different transformations: the hydroalkylation of vinylarenes (chapter 2), and the cross-electrophile coupling of alkyl halides (chapter 3). While these two transformations are not particularly novel transformations, we present a new route (and thus expanding the synthetic toolbox) for conducting these transformations in a manner that is more cost-effective, simple, and mechanistically unexplored compared to previous reports.

The following section (chapter 1.2) introduces these silanes as an intriguing class of compounds that exhibit an alternate reactivity to other carbon-based organic compounds due to silicon's character. Importantly, this section highlights their activation by the alkoxide base into the hypervalent state, and how this moiety is reported to be highly productive in conducting a diverse set of transformations. Based on mechanistic studies in the hydroalkylation work (chapter 2), we hypothesized that the unique combination of TMDSO and KO^tBu facilitated the transformation via a process called reductive-radical polar crossover (RRPC), a concept introduced in further detail in chapter 1.3. Previous research that reported this mechanism inspired the search for other transformations that can be done with the TMDSO and KO^tBu system, which led to the discovery of the cross-electrophiles coupling (XEC) of alkyl halides (chapter 3) mediated by this same reagent system.

1.2: Organosilanes

Organosilanes are a broad class of chemical compounds that contain at least one direct silicon–carbon (Si–C) bond, typically represented as R_nSiX_{4-n}, where R is an organic substituent (alkyl, aryl, or functionalized groups) and X is usually a halide, alkoxy, or hydrogen.[4] Organosilanes occupy a distinctive niche between purely inorganic silicon compounds (such as silicates and silica) and organic molecules because the silicon–carbon (Si–C) bond confers both compatibility with organic chemistry and silicon-specific properties. Their hybrid nature enables diverse applications in materials science, coatings, electronics, and advanced functional materials, and biomedical applications.[4,5]

From a synthetic perspective, organosilanes are particularly valuable due to their versatility in acting as reagents, intermediates, and protecting groups. Silicon's electropositive character compared to carbon alters the reactivity of adjacent atoms, enabling unique transformations such as hydrosilylation, cross-coupling, and silyl-directed C–H functionalization.[6-9] Importantly, organosilanes are often less toxic than analogous organotin reagents, making them an attractive alternative in the synthetic toolbox. Silyl protecting groups (like TMS, TBDMS, or TIPS) are essential for selectively masking hydroxyl, amino, or carboxyl groups during multi-step syntheses[6], while silyl enol ethers are key intermediates in carbon–carbon bond-forming reactions such as the Mukaiyama aldol reaction.[10] Overall, their ability to act as mild and selective reagents makes them indispensable tools in modern synthetic methodology. The following section introduces "hydrosilanes" as category of organosilanes containing Si–H bonds as efficient and versatile reducing agents.

1.2.1 | Silicon, hydrosilanes, and accessing hypervalency

Located directly under carbon on the periodic table, both silicon and carbon are group 14 elements designated by 4 valence electrons and form tetrahedral geometry in normal tetra-coordinate bonding. This additional valence orbital of silicon leads to certain attributes of the atom that allow for reactivity unseen with carbon.

Silicon's larger valence orbital relative to carbon translates to longer bonds (C–H = 1.09 Å, Si–H=1.48 Å,). With weaker electron withdrawing power, its electronegativity is similar to that of boron (Si = 1.9, B = 2.0) and lower than that of carbon (C = 2.5) and hydrogen (H = 2.2).[7] Consequently, silicon-element bonds are more polarized where electron density is decreased around silicon, leading to partial negative charges on surrounding atoms.[11] A prevalent example of this phenomenon is seen with the Si–H bond, which is moderately polar, exhibiting *reverse polarity* compared to the C–H bond (**Figure 1**).

Figure 1. Relative polarization of C–H and Si–H bonds

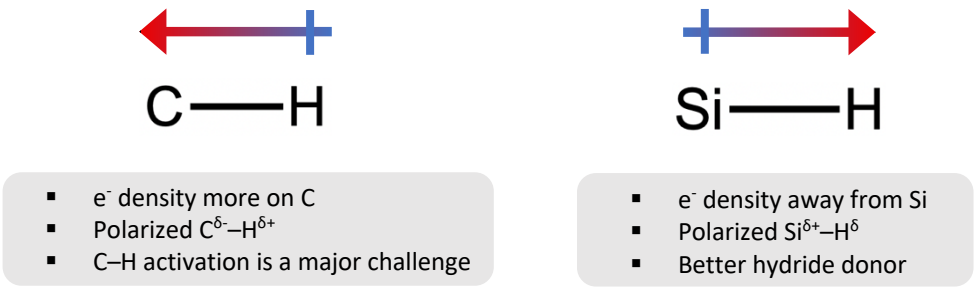

Hydrosilanes are a class of organosilicon compounds that contain one or more silicon–hydrogen (Si–H) bonds, with the general formula $R_3Si–H$ (where R is typically an alkyl or aryl substituent). With silicon's lower electronegativity and polarization of the bond $Si^{\delta+}–H^{\delta-}$, this enables hydrosilanes to be hydride donors in many reactions.[7] Additionally, the bond dissociation

energy (BDE) of a Si–H bond (~90 kcal/mol) is weaker than a typical C–H bond (~100–105 kcal/mol), making it easier to cleave under catalytic or radical conditions.[12] This combination of polarity and relative bond weakness gives the Si–H bond unusual reactivity, in addition to its hydridic character, may also undergo homolytic cleavage to generate radicals or add across unsaturated bonds in hydrosilylation reactions.[13]

Carbon is strictly limited by the octet rule, and its small size cannot stabilize more than four electron pairs. On the contrary, hydrosilanes can enter hypervalent states as silicon readily expands its coordination number beyond four. This hypervalency of silicon arises from its energetically accessible empty 3d orbital, allowing for the central silicon atom to exceed the traditional octet rule. With this d orbital, tetra-coordinated silicon complexes can readily expand into relatively stable penta- and hexacoordinated species (e.g., SiF_6^{2-}, hypervalent silicates, or transition-metal–bound silanes).[14] (**Scheme 1**)

Scheme 1. Hypervalent silicon structures

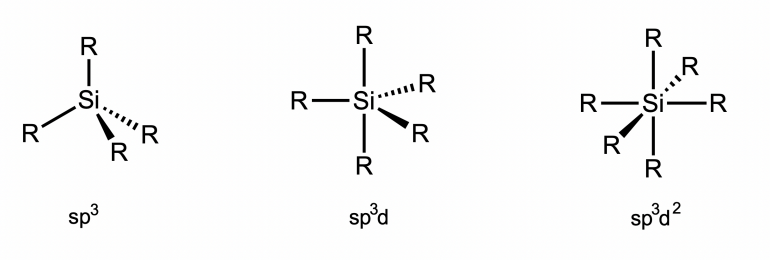

As seen in Scheme 1, hyper-coordination into the penta- and hexavalent state show reduced s-character. With the addition of an R group, the central silicon atom becomes more polarized with higher electropositive character, and the hydride-donor ability is enhanced. Alternatively, these systems with increased negative partial charges at the R group and as well its elongated bonds allow the transfer of the R group as a carbanion or hydride equivalent to an acceptor.[14] This

hypervalency of silicon is extremely valuable as it enables hydrosilanes to serve as efficient reducing systems, as well as unlocking reactivity, selectivity, and stability that carbon-based analogues cannot achieve.

One way to achieve a hypercoordinate silicon species is by the addition of a Lewis base (e.g., fluoride, alkoxide, amine, NHC) to a hydrosilane, wherein the base can donate electron density into silicon, giving rise to the hypervalent state (**Scheme 2**). In effect, the otherwise stable Si–H bond is "activated" by the Lewis base, unlocking strong hydride donor ability.[14,15]

Scheme 2. Pentacoordinate expansion of organosilane with KO^{t}Bu as Lewis base

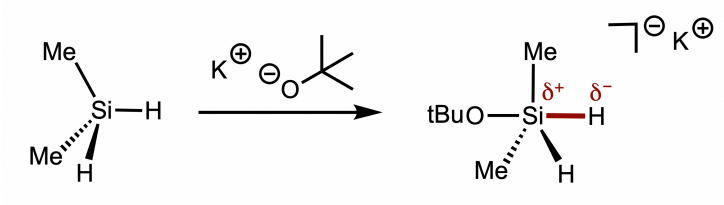

By this method, activated hydrosilanes can become potent sources of nucleophilic hydride, and unlike classical metal hydrides ($LiAlH_4$, $NaBH_4$), Lewis base and hydrosilane systems are milder, safer, and more chemoselective.[16] In organocatalysis, the Lewis base and hydrosilane combination mimics transition-metal hydride reactivity.[17,25]

1.2.2 | Examples of hydrosilane and base-enabled transformations

A number of hydrosilane-base reagent combinations have been reported in literature to produce a diverse array of transformations. A pioneering example of this is the Grubbs-Stoltz reagent system comprised of Et_3SiH and KO^{t}Bu. It was reported as an effective reagent pair for the cleavage of strong C–O bonds in aryl ethers (**Scheme 3A**) and particularly useful for the degradation of lignin.[18] Following this seminal discovery, the desulfurization of hydrocarbon fuels can be attained using the same combination of reagents, where heterocyclic sulfur is removed

via reductive cleavage of C–S bonds in thioethers.[19] Additional reductive bond cleaving reactions were reported, including the cleavage of C–N bonds in *N*-benzyl- and *N*-allylindoles[20] (**Scheme 3B**) as well as the cleavage of C–C bonds in the decyanation of benzyl nitriles.[21] (**Scheme 3C**)

Scheme 3. Grubbs-Stoltz (Et_3SiH/KO^tBu) mediated reductive cleavage transformations

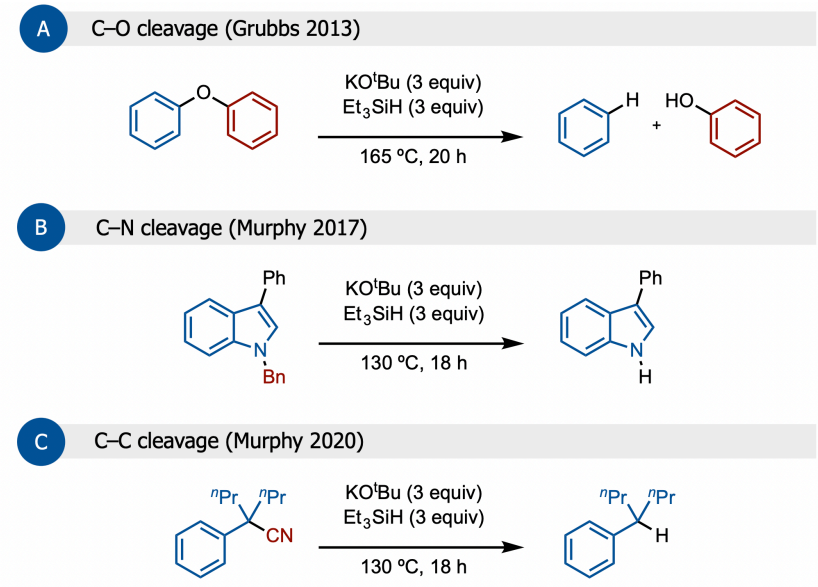

Mechanistically, the reductive cleavage of C–O bonds in diaryl ethers were said to proceed via parallel single-electron transfer (SET) and hydride transfer pathways. [21] First, KO^tBu enables the activation of Et_3SiH, forming a reactive triethylsilyl radical or silanate intermediate in situ. A single-electron transfer (SET) step from occurs from the silanate anion to the aryl ether, producing aryl ether radical anions that fragment at the C–O bond. Then, a silyl radical can directly attack the hydride delivery from a silicon-based species (such as $Et_3Si^{\cdot}$) to the aromatic ring, followed by fragmentation to the phenolic and aromatic hydrocarbon products whilst leaving a silylated byproduct (**Scheme 4**). The other reductive cleavage reactions follow similar

mechanisms involving SET. These reductive conditions enable selective ether bond cleavage even in substrates that resist metal-catalyzed or traditional reductive method.

Scheme 4. Proposed mechanism for the reductive cleavage of diaryl ether and dithioether via Grubbs-Stoltz reagent (Et_3SiH/KO^tBu)

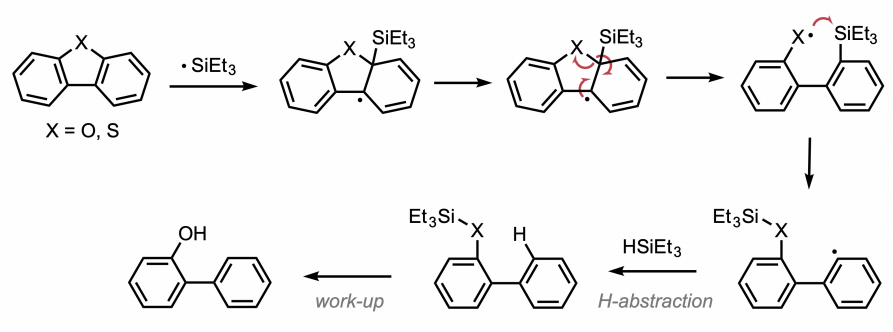

In addition to reductive cleavage reaction, other transformations that non-defunctionalization reaction can be also done with the Grubbs-Stoltz system (**Scheme 5**). These include the C–H silylation of indoles[22] (**Scheme 5A**), intramolecular cyclization[21] (**Scheme 5B**), and rearrangement of o-tolyl aryl ethers[24] (**Scheme 5C**).

Scheme 5. Other Grubbs-Stoltz (Et_3SiH/KO^tBu) mediated transformations

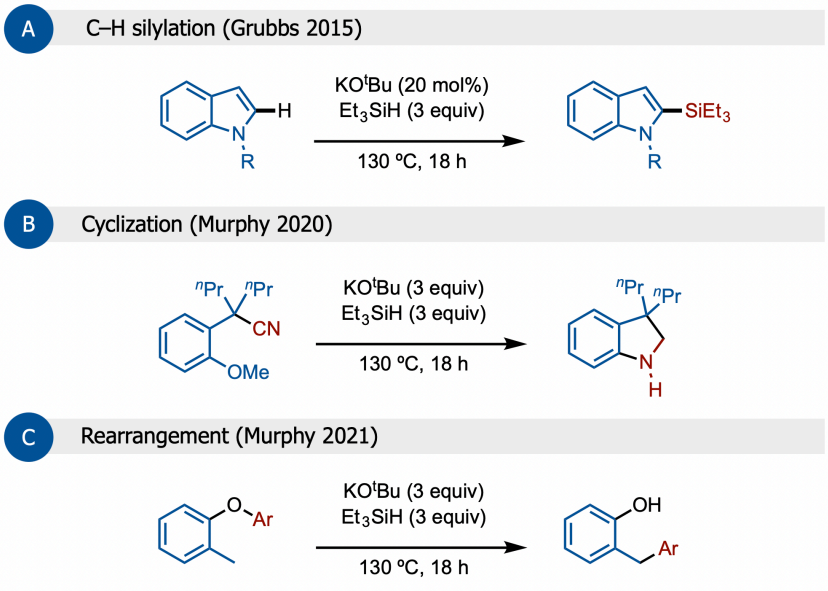

The Grubbs-Stoltz catalyzed C–H silylation of indoles (**Scheme 5A**) bypasses the need for transition-metal catalysis, which was required with previous literature for similar reactions. Interestingly, silylation occurs with catalytic instead of stoichiometric KO^{t}Bu and works with lower temperatures, which differs from the reductive cleavage examples. C–H silylation was determined to proceed through radical chain mechanism initiated by $Et_3Si\cdot$, formed by cleavage of the weakened Si–H bond from the pentavalent silicon intermediate. $Et_3Si\cdot$ adds to C2 of the indole, forming a benzyl radical. β-H scission would then restore aromaticity to eject H_2, which ultimately drives the entropic force. The silicate radical anion with another equivalent of Et_3SiH can regenerate the triethylsilyl radical.[23] (**Scheme 6**)

Scheme 6. Proposed radical pathway for the C–H silylation of indoles via Grubbs-Stoltz reagent (Et_3SiH/KO^{t}Bu)

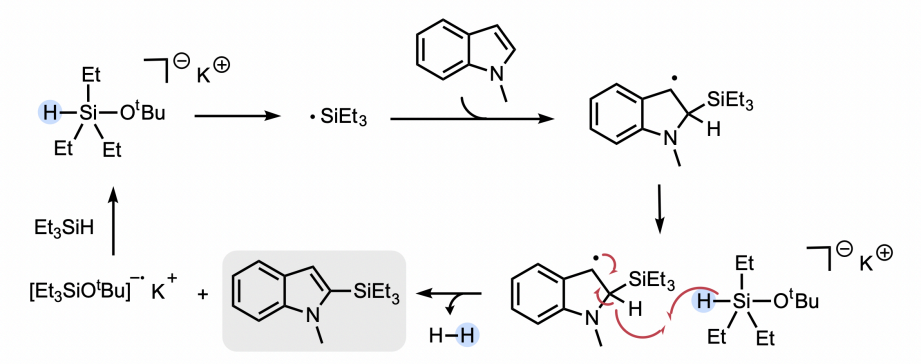

When the benzyl nitriles shown in **Scheme 3C** are ortho substituted with a methoxy group, a different product forms despite using the same conditions. Instead of decyanation, displacement of the methoxy group occurs to yield a cyclized product (**Scheme 5B**).[21] Similarly, dibenzyl ethers with ortho-substituted methyl subjected to the Grubbs-Stoltz conditions lead to rearrangement of o-tolyl aryl ethers into *o*-hydroxydiarylmethanes (**Scheme 5C**). This transformation was proposed to proceed via hydrogen atom abstraction by a $Et_3Si\cdot$ to form a benzyl radical, where

5-*exo*-trig cyclication could then proceed to yield a spiro intermediate, followed by fragmentation to afford the phenoxyl radical and form the product upon protonation. [24] (**Scheme 7**)

Scheme 7. Proposed mechanism for the rearrangement of o-tolyl aryl ethers via Grubbs-Stoltz reagent (Et_3SiH/KO^tBu)

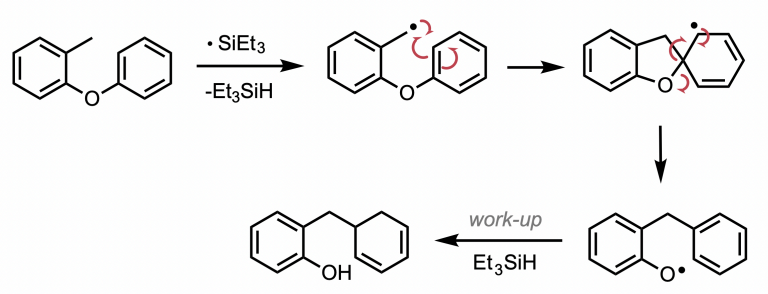

Aside from the Grubbs-Stoltz reagent, other productive hydrosilane and base combinations have been reported, which can lead to other reactive silicon intermediates. One example of this is the hydrosilylation of styrenes reported by Jeon and coworkers (**Scheme 8**). Contrary to the two-electron hydride-transfer mechanism, Jeon et al. proposed that the hydrosilane-base system H_2SiEt_2/KO^tBu forms a silanate complex (**II**) that can participate in H-atom transfer (HAT) onto styrene (**III**), resulting in a benzyl radical (**IV**). The benzyl radical can continue to trap silyl radicals to afford the hydrosilylation product (**V**). When crown-ethers are introduced as a component, this chelates potassium ions and results in the free radical polymerization of the benzyl radical (**VI**).[25]

Scheme 8. Proposed reaction mechanism for the hydrosilylation of styrene by Jeon et al.

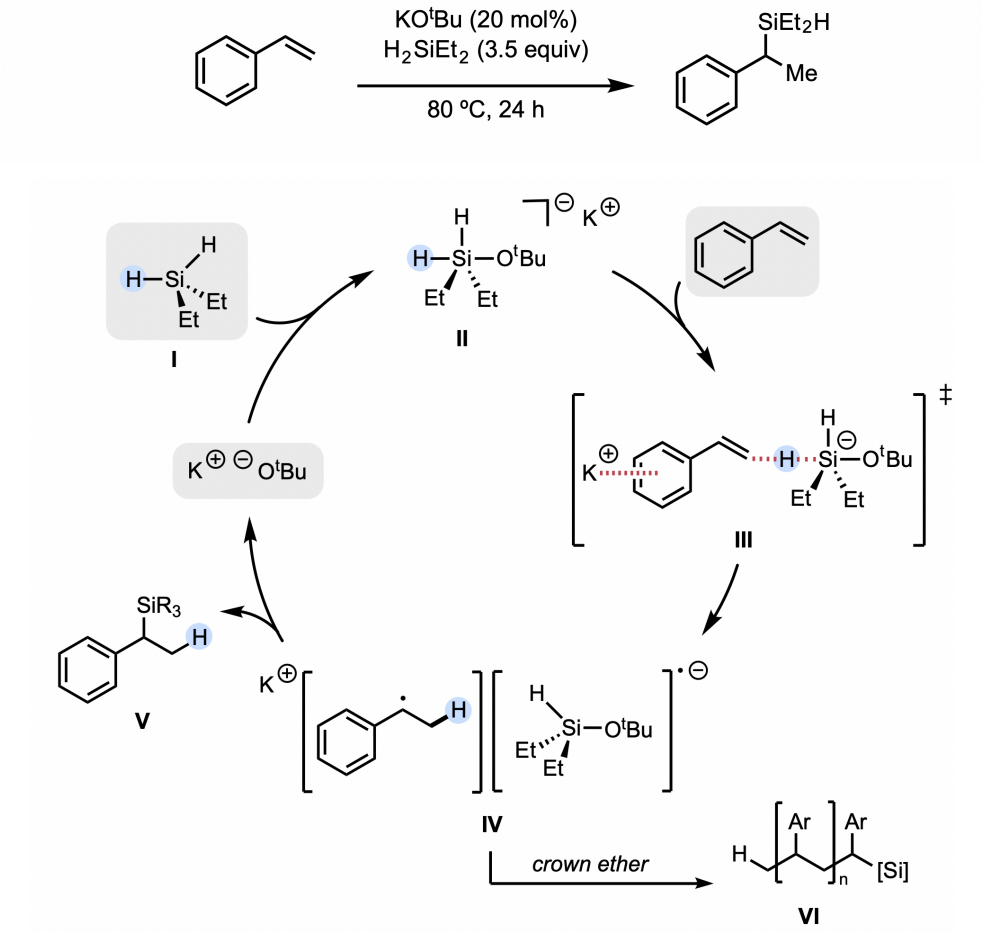

Lastly, a new combination of hydrosilane and base consisting of 1,1,3,3-tetramethydisiloxane (TMDSO) and KO^{t}Bu was found to cleave the strong C–CF_3 bond in 2-methylpyridine, further highlighting the strong reductive character of the system (**Scheme 9**). In this transformation, the reaction proceeds by a key SET step into the pyridine π-system to generate a pyridine radical anion. This is then followed by HAT, where the dearomatized pyridyl anion can then eject CF_3 as an anion to result in the defunctionalized pyridine.[26]

Scheme 9. Proposed reaction mechanism for the C–CF_3 cleavage of 2-trifluoromethylpyridine.

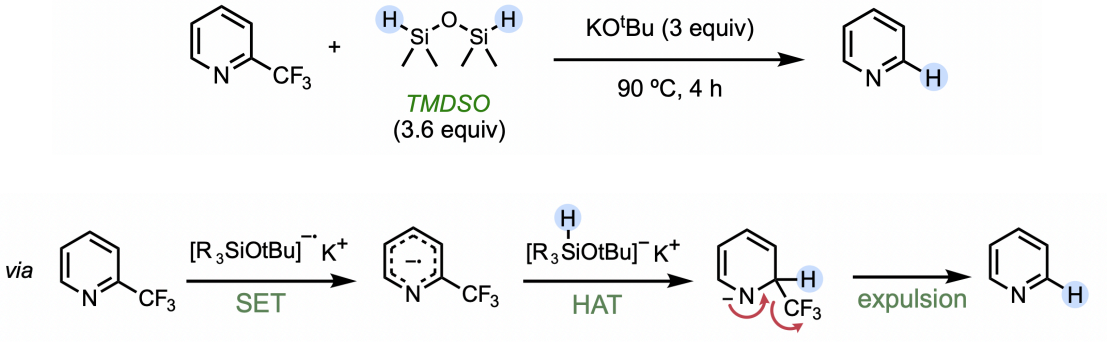

Not only the silane, but KO^{t}Bu also plays a major role in these transformations. From the transformations mentioned, substituting the KO^{t}Bu for other alkoxides such as sodium, lithium and aluminium tert-butoxides, or di-*tert*-butoxide peroxide (DTBP)[23], will cease reactivity. The addition of crown ether in Scheme 8 resulted in the chelation of potassium ions and led to polymerization of the benzyl radical instead of hydrosilylation. With C–CF_3 cleavage, changing the counterion on the butoxide from potassium to sodium or lithium resulted in no reaction. However, changing to another potassium base still allows for reactivity but lowers the yield significantly, from 72% with KO^{t}Bu to 22% with KHMDS.[26] This highlights the importance of KO^{t}Bu and complementary to the silane, with reactivity enabled by the counter anion effect specifically provided by potassium as well as the alkoxide. Additionally, KO^{t}Bu is frequently implicated in organic reactions involving SET has also been reported to be a key component in single-electron transfer mechanisms.[27] In studies done by Murphy et al., addition of KO^{t}Bu as a strong base enables the generation of organic electron donors and occasionally as a direct electron donor to substrates with suitable reduction potentials. The stronger basicity and distinct metal-oxygen bonding of KO^{t}Bu (compared to NaO^{t}Bu or LiO^{t}Bu) enhances its role in these electron transfer processes.[27]

While the mechanisms of these transformations are still perplexing, these examples show that the simple combination of hydrosilane and KO^{t}Bu give rise to a multitude of reactive intermediates that can facilitate diverse transformations with simple and commonly available reagents. As seen with these examples, the hydrosilane and base system commonly facilitates various steps by forming these intermediates: single-electron donor, hydride donor, silicon radical, strong base, and discovered more recently as an H-atom donor (**Figure 2**).

Figure 2. Speculated hydrosilane/base-derived intermediates

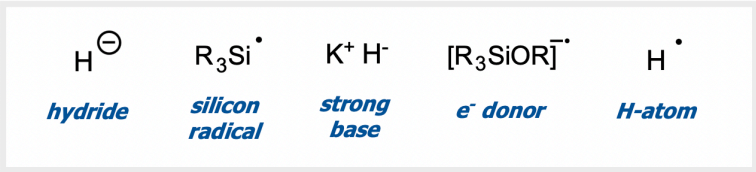

In chapters 2 and 3, TMDSO and KO^{t}Bu are key reagents in facilitating both the hydroalkylation of vinylarenes and the cross-electrophile coupling of alkyl halides. Based on the work done in chapter 2, it was hypothesized that this particular combination of hydrosilane and base conducted the reaction via a mechanism called reductive-radical polar crossover (RRPC). This finding was key to the discovery of the work in chapter 3, and further studies are done to explore if the mechanism remains the same for this different transformation. In this next section, RPPC is introduced and described in greater detail. Examples of transformations that are reported to use this method are given for context and current state of the field.

1.3: Reductive-radical polar-crossover

The oldest published experiment indicating the conversion of a radical to an anion can be traced back to early work in the 1930s and 1940s involving the reduction of conjugated dienes or aromatic compounds by alkali metals in liquid ammonia. In these experiments, a single electron is added to a neutral molecule, generating a radical anion (or anion radical). This species then undergoes further reduction and protonation, leading to the formation of a closed-shell anion. A classic example is the reduction of dienes to alkenes or naphthalene to dihydro derivatives by sodium in liquid ammonia, which was systematically studied around the time of Arthur J. Birch's work in the 1940s.[28] (**Scheme 10**) These experiments provided clear mechanistic evidence for the stepwise reduction of radicals to anions under controlled experimental conditions.

Scheme 10. Birch reduction of aromatic rings

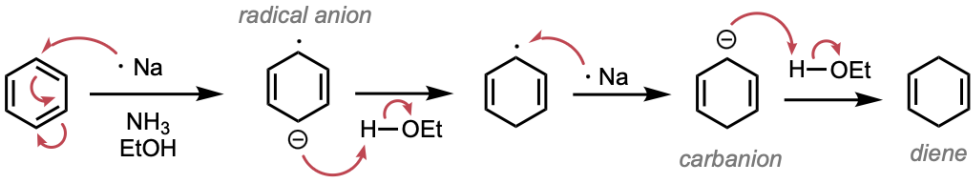

The mid-20th century continued to observe early examples of the foundational principles of radical reductions through single-electron transfer (SET) processes. Kornblum's observations in the 1960s on the benzylation of nitronate anions (i.e. 2-nitropropane) with nitro-substituted benzyl halides (i.e. *p*-nitrobenzyl chloride) revealed unexpected products of *C*-alkylation over *O*-alkylation, which was inconsistent with S_N2 and rather suggesting a radical pathway. A SET-initiated chain was proposed, where the aryl halide $ArCH_2X$ accepts an electron from the nucleophile, Nu^-, forming a radical anion species $[ArCH_2X]^{\bullet -}$ that fragments into $ArCH_2\bullet$ and X^-. The aryl radical then couples with Nu^- to yield radical anion $[ArCH_2Nu]^{\bullet -}$, which can

propagate the chain by reducing another $ArCH_2X$ while yielding the product $ArCH_2Nu$. Addition of nitrobenzene or other radical traps sharply supressed *C*-alkylation while diverting products to *O*-alkylation[29].

Building on this study and other reports and observations of that time, elucidation of the radical-nucleophilic aromatic substitution mechanism, or $S_{RN}1$, ensued in 1970 by Bunnet and Kim[30]. They definitively identified and named the $S_{RN}1$ process, describing it as a unimolecular radical chain reaction initiated by SET where substitution is achieved via intermediary free radical species, establishing its distinction from S_N1 or S_NAr mechanisms.

Photochemical initiation became a method that increased the utility of $S_{RN}1$. In the 2010s, visible-light photoredox enabled precise control over single-electron transfer events, allowing for radicals to be generated and selectively reduced to anions under exceptionally mild conditions.[31] Seminal studies showed that carbon-centered radicals formed by addition to alkenes, decarboxylation, or halide abstraction can be intercepted by a second reduction event to form carbanions. Subsequently, the carbanion can engage in polar reactions such as protonation, substitution, or carbonyl addition.

Cumulative reports of the radical-to-anion conversion ultimately led to the formalization of reductive radical polar crossover (RRPC) as a distinct mechanistic and strategic concept. While early radical-to-anion reductions (such as the Birch reduction) relied on stoichiometric, strong reductants and direct electron transfer in harsh environments, [28] RRPC allows for a more refined, catalytic, and mild approach that merges radical and polar chemistries to enhance control.[32,33] RRPC was described thoroughly as a concept in a 2019 review article by Frank Glorius and coworkers.[33] This article systematically introduced the term, discussing the merger of radical

and polar pathways to convert radical intermediates into nucleophilic anions in catalytic reactions. It highlighted how this strategy overcomes the limitations of radical or polar chemistry alone and summarized important recent transformations that exemplify this approach.

In the RRPC synthetic strategy, catalytic methods (often photoredox or electrochemical) are employed to generate radicals under mild conditions. These radicals then undergo controlled electron transfer to become anions within the same catalytic cycle. This "crossover" allows the reaction to proceed through radical intermediates with the mildness and functional group tolerance typical of radical chemistry with its ability to engage in selective bond activations, radical additions, or C–X bond cleavages, while simultaneously harnessing the selectivity and versatility of nucleophilic anions reactions that can can engage in classical ionic reactions such as substitutions, eliminations, or additions to electrophiles.[32,33]

By joining radical and polar pathways in a controlled and strategic manner, RRPC enables use of common radical precursors alongside classical electrophiles like carbonyls and alkyl halides, enhancing functional group compatibility and broadening synthetic utility.[28] This method allows for enhanced selectivity, mild reaction conditions, and broader substrate scopes. This approach has unlocked new complex molecule constructions, enabling radical-initiated additions followed by nucleophilic substitution, cyclization, or C–C bond formations that are otherwise difficult to achieve.

Essentially, RRPC deliberately exploits radical-to-anion conversion as a strategic synthetic approach to enable selective bond formations under mild conditions, allowing for a new approach towards challenging synthetic problems and marking a breakthrough in radical and polar reaction integration. Moreover, the single electron redox control in RRPC enables

developing diastereo- and enantioselective radical transformations by combining photoredox or transition metal catalysis with organocatalysis. [28]

1.3.1 | Fundamentals of RRPC

The process of RRPC typically begins with a single electron transfer (SET) from a reductant to an electrophile like an alkyl halide, producing a carbon-centered radical. This can be done using a transition-metal catalyst, a photocatalyst under visible light, or an electrochemical cathode. Instead of engaging exclusively in radical-radical coupling or hydrogen atom transfer, this radical undergoes a second reduction event to form a carbanion. At this stage, the reactivity switches from radical to polar, and the carbanion can engage in ionic processes such as nucleophilic substitution, addition to carbonyls, or C–C bond formation with other electrophiles (**Scheme 10**). This dual character enables bond constructions that are difficult or impossible with purely radical or ionic approaches alone. [32]

Scheme 11. General scheme for RRPC and common strategies

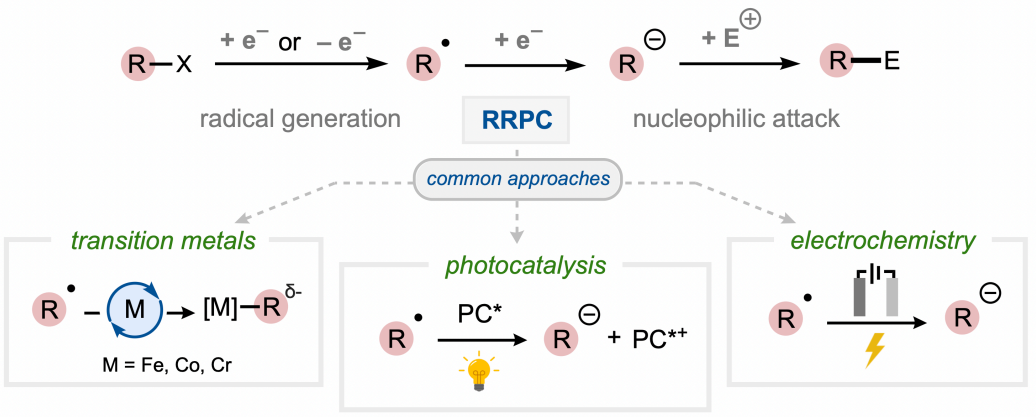

The RRPC framework has become increasingly important in synthetic methodology, especially in the context of cross-electrophile coupling, photoredox catalysis, transition-metal catalysis, and electrochemistry, where controlled single electron transfers can mediate these transitions. From

a process perspective, RRPC can simplify synthetic routes by reducing the need for protecting groups and minimizing step count, all of which align with the growing demand for efficient and scalable chemical manufacturing.

1.3.2 | Transformations mediated by RRPC

Utilization of the RRPC strategy to conduct various transformations have increased in number in the past decade. The groups of Ryu and Sonoda were the first major group to present a mechanistic demonstration of RRPC in the 1990's for the synthesis of bicyclic octanols via a three-component system of alk-4-enyl iodines, CO, and alkene in the presence of zinc.[33,34]

The Martin group in 2017 was the first group to report RRPC via visible-light photoredox catalysis to conduct the dicarbofunctionalization of styrenes. The Ir-photocatalyst generates trifluoromethyl radicals, which can then add to styrene to result in benzyl radicals. As benzyl radicals are relatively stabilized radicals, reduction by the photocatalyst can ensue to form a benzyl anion that traps CO_2 to lead to the carboxylic acid product.[35]

Scheme 12. Dicarbofunctionalization of styrenes via photoredox catalysis by Martin et al.

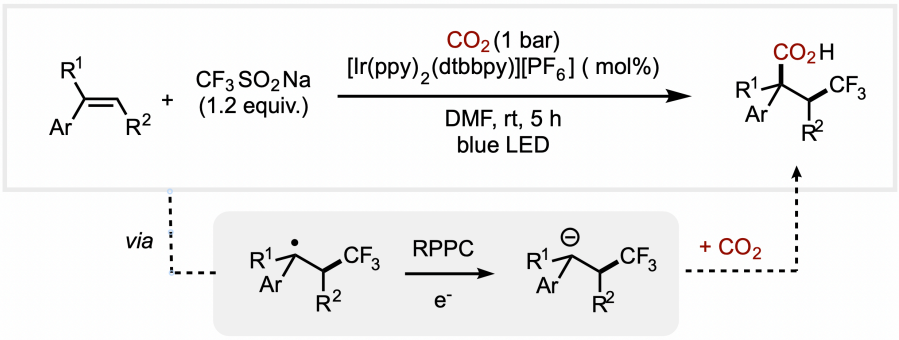

Carbonyls also present as great S_N2 electrophiles for RRPC. The group of Zuo reported a cerium- and photoredox-catalyzed bridged lactone formation from cycloalkanols and Michael acceptors.[36] Here, cerium(IV)-mediated ligand-to-metal charge transfer produces an alkoxy

radical, where its instability results in C–C beta-scission to a more stabilized alkyl radical. Following this, radical addition to the Michael acceptor takes place, and SET to the radical generates the anion. Nucleophilic addition of the anion to the pendant aldehyde moiety results in an isolable cyclized product and work-up with *p*TsOH will yield the lactone product.

Scheme 13. Ce- and photoredox-catalyzed lactone formation by Zuo et al.

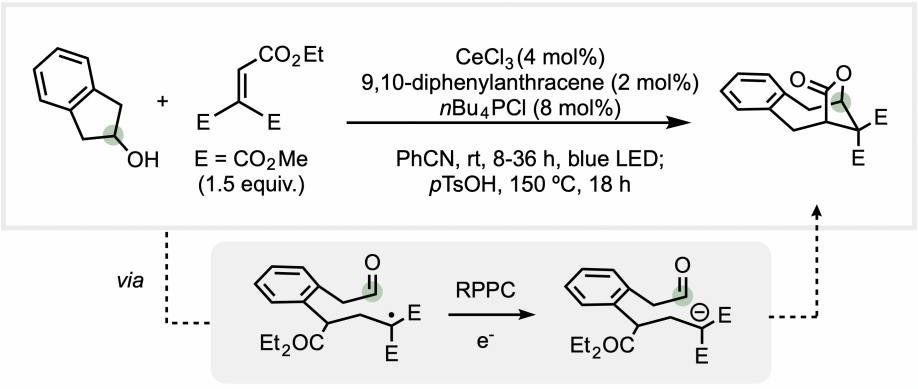

Alternatively, the two electron transfer steps in RRPC can also be done using transition-metal catalysis. In one example by the Baran group in 2019, the decarboxylative Nozaki-Hiyama-Kishi reaction was conducted via RRPC.[37] In this report, redox active esters (RAE) were used to generate the alkyl radical after SET from the chromium(II) species. Next, RRPC occurs with the trapping of the radical with the excess chromium(II) salt to form a Cr(III)-alkyl complex as an active nucleophile. Following this, subsequent addition to aldehydes in situ leads to the formation of TMS-protected alcohol products.

Scheme 14. Nozaki-Kiyama-Kishi reaction of redox-active esters to form TMS-protected alcohols

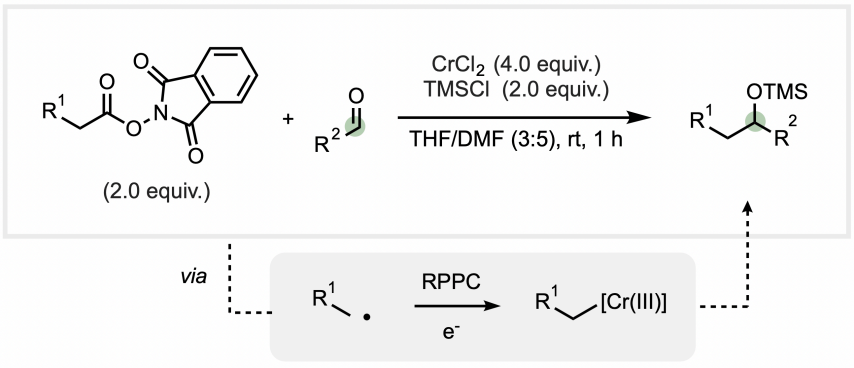

Lastly, alkyl halides have also been reported to be a viable electrophile choice with RRPC. Published by Molander 2018, the cyclopropanation as well as the cyclobutanation of alkenes using iodomethyl silicates was done via visible-light photoredox catalysis.[38] Here, the photocatalyst 4CzIPN oxidizes the radical precursor. A final step involving S_N2 involving the halide leads to ring-closure and cyclopropanation product.

Scheme 15. Intramolecular cyclopropanation using iodomethyl silicates by Aggarwal et al.

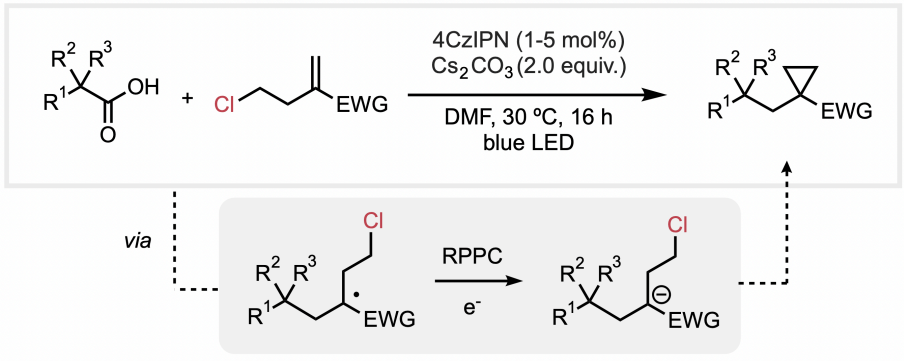

RRPC is also an excellent method to harness cross-electrophile coupling as it enables control over the generation of anion from a radical, and an example using electrochemistry will be discussed in the introduction to chapter 3.

1.4: Research Goals

As shown in chapter 1.2.2, most of the reported hydrosilane and base transformations are reductive defunctionalization reactions. The few examples of complexity-building reactions only involve C–Si bond formations during hydrosilylation or C–H silylation. No reports have been made on C–C bond formation using this reagent combination, which is a harder bond to attain and is also important avenue to pursue in medicinal chemistry and other small molecule synthesis fields alike. Similarly, no reports have been made on RRPC transformations without using photochemistry, transition-metal catalysis, or electrochemistry.

In this thesis, we hypothesize that the combination of hydrosilane and base of TMDSO and potassium alkoxide can form reactive intermediates capable of facilitating complexity-building transformations that would otherwise require much more complex and costly set ups. As reported by Jeon et al. and discussed in chapter 1.2, the combination of H_2Et_2Si and KO^tBu can form a silanate complex, and acting as an H-atom donor, conducts hydrosilylation upon styrene. Supporting this, the combination of TMDSO and KO^tBu was reported to conduct both HAT and SET for the reductive CF_3 cleavage of 2-trifluoromethylpyridines. Based on this reactivity, we hypothesized that other transformations can be mediated by this combination of hydrosilane and base by facilitating HAT and SET steps.

With this hypothesis, two distinct transformations were discovered facilitated by a system of potassium alkoxide base (namely KO^tBu and KOEt) and TMDSO. In these two transformations, functionalization was achieved through $C(sp^3)$–$C(sp^3)$ bond formation. In chapter 2, the functionalization of styrenes and other vinylarenes via hydroalkylation will be explored. In

chapter 3, the cross-electrophile coupling of alkyl halides will be explored. In each chapter, the goal was to explore the scope of reactivity and identify possible reactive intermediates.

Scheme 16. Two novel transformations mediated by TMDSO and KO^{t}Bu (this work)

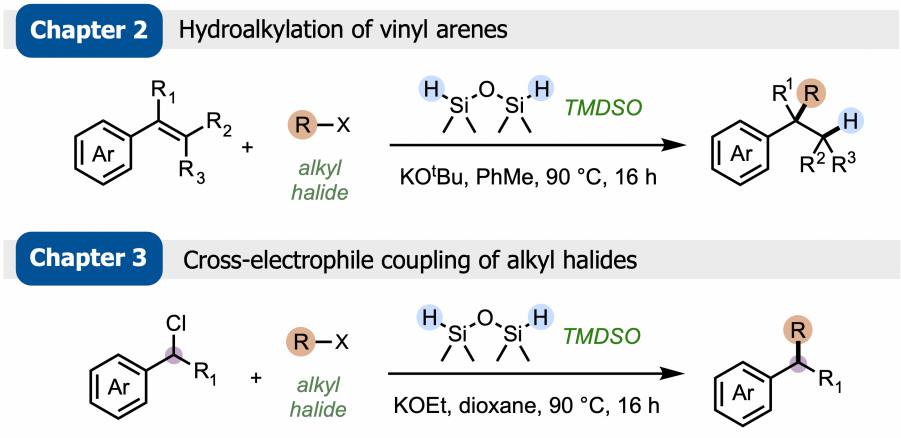

1.5: References

(1) Atanasov, A. G.; Supuran, C. T.; Taskforce, the I. N. P. S. et al. Natural Products in Drug Discovery: Advances and Opportunities. *Nat. Rev. Drug Discov.* **2021**, *20*, 200–216.

(2) Boström, J.; Brown, D. G.; Young, R. J.; Keserü, G. M. Expanding the Medicinal Chemistry Synthetic Toolbox. *Nat. Rev. Drug Discov.* **2018**, *17*, 709–727.

(3) Campos, K. R.; Coleman, P. J.; Alvarez, J. C.; Dreher, S. D.; Garbaccio, R. M.; Terrett, N. K.; Tillyer, R. D.; Truppo, M. D.; Parmee, E. R. The Importance of Synthetic Chemistry in the Pharmaceutical Industry. *Science.* **2019**, *363*, eaat0805.

(4) Antonucci, J. M.; Dickens, S. H.; Fowler, B. O.; Xu, H. H.; McDonough, W. G. Chemistry of Silanes: Interfaces in Dental Polymers and Composites. *Journal of research of the National Institute of Standards and Technology*. **2005**, *110*, 541–558.

(5) Shivhare, H. Applications of Organosilanes: (A Comprehensive Review). *Journal of Fundamental and Comparative Research.* **2022**, 10, 20.

(6) Acros Organics. A Review of Organosilanes in Organic Chemistry; Thermo Fisher Scientific: India, 2024. http://www.thermofishersci.in/lit/Acros%20White%20Paper%20Organosilanes.pdf.

(7) Petkowski, J. J.; Bains, W., Seager, S. On the Potential of Silicon as a Building Block for Life. *Life (Basel, Switzerland)*. **2020**, *10*, 84.

(8) Barton, T. J.; Boudjouk, P. Organosilicon Chemistry: A Brief Overview. In Silicon-Based Polymer Science. *American Chemical Society: Washington, DC.* **1989**, 224, 3–46.

(9) Lal, N.; Shirsath, S. B.; Singh, P.; Deepshikha; Shaikh, A. C. Allylsilane as a Versatile Handle in Photoredox Catalysis. *Chem. Commun.* **2024**, *60*, 4633–4647.

(10) Srimani, D.; Bej, A.; Sarkar, A. Palladium Nanoparticle Catalyzed Hiyama Coupling Reaction of Benzyl Halides. *J. Org. Chem.* **2010**, *75*, 4296–4299.

(11) Corey, J. Y. Historical Overview and Comparison of Silicon with Carbon. In *Organic Silicon Compounds (1989)*; PATAI'S Chemistry of Functional Groups; **1989**; pp 1–56.

(12) Zakarian, A. Bond Dissociation Energies; Chemistry Faculty Order No. 11; Department of Chemistry and Biochemistry, University of California, Santa Barbara, 2013. https://labs.chem.ucsb.edu/zakarian/armen/11---bonddissociationenergy.pdf.

(13) Chuit R J P; Perz, R; Reyé, C, C. C. Improved Procedure for the Selective Reduction of Carbonyl Compounds and Carboxylic Acid Esters by Potassium Salt-Induced Hydrosilylation. *Synthesis (Stuttg).* **1982**, *1982*, 981–984.

(14) Rendler Martin, S. O. Hypervalent Silicon as a Reactive Site in Selective Bond-Forming Processes. *Synthesis (Stuttg).* **2005**, *2005*, 1727–1747.

(15) Chuit, C.; Corriu, R. J. P.; Reye, C.; Young, J. C. Reactivity of Penta- and Hexacoordinate Silicon Compounds and Their Role as Reaction Intermediates. *Chem. Rev.* **1993**, *93*, 1371–1448.

(16) Pesti, J.; Larson, G. L. Tetramethyldisiloxane: A Practical Organosilane Reducing Agent. *Org. Process Res. Dev.* **2016**, *20*, 1164–1181.

(17) Iglesias, M.; Fernández-Alvarez, F. J.; Oro, L. A. Non-Classical Hydrosilane Mediated Reductions Promoted by Transition Metal Complexes. *Coord. Chem. Rev.* **2019**, *386*, 240–266.

(18) Fedorov, A.; Toutov, A. A.; Swisher, N. A.; Grubbs, R. H. Lewis-Base Silane Activation: From Reductive Cleavage of Aryl Ethers to Selective Ortho-Silylation. *Chem. Sci.* **2013**, *4*, 1640–1645.

(19) Tang, L.; Chen, S.; Wang, S.; Tao, X.; He, H.; Zheng, L.; Ma, C.; Zhao, Y. Heterocyclic Sulfur Removal of Coal Based on Potassium Tert-Butoxide and Hydrosilane System. *Fuel Process. Technol.* **2018**, *177*, 194–199.

(20) Smith, A. J.; Young, A.; Rohrbach, S.; O'Connor, E. F.; Allison, M.; Wang, H.-S.; Poole, D. L.; Tuttle, T.; Murphy, J. A. Electron-Transfer and Hydride-Transfer Pathways in the Stoltz–Grubbs Reducing System (KO^tBu/Et_3SiH). *Angew. Chemie Int. Ed.* **2017**, *56*, 13747–13751.

(21) Smith, A. J.; Dimitrova, D.; Arokianathar, J. N.; Clark, K. F.; Poole, D. L.; Leach, S. G.; Murphy, J. A. Et3SiH + KOtBu Provide Multiple Reactive Intermediates That Compete in the Reactions and Rearrangements of Benzylnitriles and Indolenines. *Chem. Sci.* **2020**, *11*, 12364–12370.

(22) Toutov, A. A.; Liu, W.-B.; Betz, K. N.; Fedorov, A.; Stoltz, B. M.; Grubbs, R. H. Silylation of C–H Bonds in Aromatic Heterocycles by an Earth-Abundant Metal Catalyst. *Nature* **2015**, *518*, 80–84.

(23) Liu, W.-B.; Schuman, D. P.; Yang, Y.-F.; Toutov, A. A.; Liang, Y.; Klare, H. F. T.; Nesnas, N.; Oestreich, M.; Blackmond, D. G.; Virgil, S. C.; Banerjee, S.; Zare, R. N.; Grubbs, R. H.; Houk, K. N.; Stoltz, B. M. Potassium Tert-Butoxide-Catalyzed Dehydrogenative C–H Silylation of Heteroaromatics: A Combined Experimental and Computational Mechanistic Study. *J. Am. Chem. Soc.* **2017**, *139*, 6867–6879.

(24) Kolodziejczak, K.; Stewart, A. J.; Tuttle, T.; Murphy, J. A. Radical and Ionic Mechanisms in Rearrangements of O-Tolyl Aryl Ethers and Amines Initiated by the Grubbs–Stoltz Reagent, Et_3SiH/KO^tBu. *Molecules* **2021**, *26*.

(25) Asgari, P.; Hua, Y.; Bokka, A.; Thiamsiri, C.; Prasitwatcharakorn, W.; Karedath, A.; Chen, X.; Sardar, S.; Yum, K.; Leem, G.; Pierce, B. S.; Nam, K.; Gao, J.; Jeon, J. Catalytic Hydrogen Atom Transfer from Hydrosilanes to Vinylarenes for Hydrosilylation and Polymerization. *Nat. Catal.* **2019**, *2*, 164–173.

(26) St. Onge, P.; Khan, S. I.; Cook, A.; Newman, S. G. Reductive Cleavage of $C(Sp^2)–CF_3$ Bonds in Trifluoromethylpyridines. *Org. Lett.* **2023**, *25*, 1030–1034.

(27) Barham, J. P.; Coulthard, G.; Emery, K. J.; Doni, E.; Cumine, F.; Nocera, G.; John, M. P.; Berlouis, L. E. A.; McGuire, T.; Tuttle, T.; Murphy, J. A. KO^tBu: A Privileged Reagent for Electron Transfer Reactions? *J. Am. Chem. Soc.* **2016**, *138*, 7402–7410.

(28) Birch, A. J. 117. Reduction by Dissolving Metals. Part I. *J. Chem. Soc.* **1944**, No. 0, 430–436. https://doi.org/10.1039/JR9440000430.

(29) Kornblum, N.; Pink, P.; Yorka, K. V. THE LEAVING GROUP AS A FACTOR IN THE ALKYLATION OF AMBIDENT ANIONS. *J. Am. Chem. Soc.* **1961**, *83* (12), 2779–2780. https://doi.org/10.1021/ja01473a049.

(30) Bunnett, J. F.; Kim, J. K. Evidence for a Radical Mechanism of Aromatic "Nucleophilic" Substitution. *J. Am. Chem. Soc.* **1970**, *92*, 7463–7464. https://doi.org/10.1021/ja00728a037.

(31) Shaw, M. H.; Twilton, J.; MacMillan, D. W. C. Photoredox Catalysis in Organic Chemistry. *J. Org. Chem.* **2016**, *81*, 6898–6926. https://doi.org/10.1021/acs.joc.6b01449.

(32) Müller, N.; Magauer, T.; Kováč, O. Natural Product Synthesis Enabled by Radical-Polar Crossover Reactions. *J. Org. Chem.* **2025**, *90*, 5083–5092..
(33) Pitzer, L.; Schwarz, J. L.; Glorius, F. Reductive Radical-Polar Crossover: Traditional Electrophiles in Modern Radical Reactions. *Chem. Sci.* **2019**, *10*, 8285–8291.
(34) Tsunoi, S.; Tanaka, M.; Tsunoi, S.; Ryu, I.; Yamasaki, S.; Sonoda, N.; Komatsu, M. Tandem Annulations: A One Operation Construction of Bicyclo[3.3.0]Octan-1-Ol and Bicyclo[3.2.1]Octan-1-Ol Skeletons by a Three-Component Coupling Reaction of Alk-4-Enyl Iodides with CO and Alkenes in the Presence of Zinc. *Chem. Commun.* **1997**, No. 19, 1889–1890.
(35) Yatham, V. R.; Shen, Y.; Martin, R. Catalytic Intermolecular Dicarbofunctionalization of Styrenes with CO^2 and Radical Precursors. *Angew. Chemie Int. Ed.* **2017**, *56*, 10915–10919.
(36) Hu, A.; Chen, Y.; Guo, J.-J.; Yu, N.; An, Q.; Zuo, Z. Cerium-Catalyzed Formal Cycloaddition of Cycloalkanols with Alkenes through Dual Photoexcitation. *J. Am. Chem. Soc.* **2018**, *140*, 13580–13585.
(37) Ni, S.; Padial, N. M.; Kingston, C.; Vantourout, J. C.; Schmitt, D. C.; Edwards, J. T.; Kruszyk, M. M.; Merchant, R. R.; Mykhailiuk, P. K.; Sanchez, B. B.; Yang, S.; Perry, M. A.; Gallego, G. M.; Mousseau, J. J.; Collins, M. R.; Cherney, R. J.; Lebed, P. S.; Chen, J. S.; Qin, T.; Baran, P. S. A Radical Approach to Anionic Chemistry: Synthesis of Ketones, Alcohols, and Amines. *J. Am. Chem. Soc.* **2019**, *141*, 6726–6739.
(38) Shu, C.; Mega, R. S.; Andreassen, B. J.; Noble, A.; Aggarwal, V. K. Synthesis of Functionalized Cyclopropanes from Carboxylic Acids by a Radical Addition–Polar Cyclization Cascade. *Angew. Chemie Int. Ed.* **2018**, *57*, 15430–15434.

Chapter 2: Hydroalkylation of vinylarenes

This chapter presents the first project in this thesis: the study of a new transformation facilitated by the hydrosilane-base reagent system, namely the hydroalkylation of vinylarenes. In Chapter 2.1, an introduction to the functionalization of alkenes is given, followed by specific examples of prior hydrofunctionalization and hydroalkylation to give insight to existing methods. In chapter 2.2, results and discussion for the hydroalkylation of vinylarenes via the hydrosilane/base reagent system will be discussed in chapter 2.2. In this section, the process of discovery, scope, and mechanistic insights are discussed.

2.1: Contributions

The final published work for this chapter is in the manuscript " Hydroalkylation of Vinylarenes by Transition-Metal-Free In Situ Generation of Benzylic Nucleophiles Using Tetramethyldisiloxane and Potassium Tert-Butoxide." by Piers St. Onge, Hana Nugraha, and Stephen G. Newman *Angew. Chemie Int. Ed.* **2025**, *64* (10), e202421077. The thesis author is the second author of this work. Results not produced by the thesis author mentioned in this chapter will be explicitly stated and only used to add further context to the work.

2.2: Background

Alkenes and other unsaturated bonds alike are highly convenient scaffolds for functionalization. With relatively weak π-bonds, they can be compatible with many reactants to allow for site-specific modifications, transforming inexpensive starting materials into higher-value and structurally diverse molecules. The mono-, hydro-, or di-functionalization of alkenes can occur by electrophilic, nucleophilic, or radical addition onto the π-system.[1,2]

In hydrofunctionalization reactions, the addition of a functional group to an unsaturated bond occurs in the presence of a hydrogen source, commonly transition-metal hydrides or silanes, and can be regioselective. Common hydrofunctionalization reactions include hydroboration, hydroamination, hydrosilylation, hydroalkoxylation, and in our particular interest, hydroalkylation.[3] The di-functionalization of alkenes via hydroalkylation enables simultaneous $C(sp^3)$–$C(sp^3)$ and C–H bond formation across a C=C bond in a single step, allowing for a higher efficiency and step economy.

2.2.1 | Existing methods for the hydrofunctionalization of unsaturated bonds

A number of catalytic strategies enable hydrofunctionalization, including radical pathways, metal-hydride hydrogen atom transfer (MHAT), and polar addition mechanisms (**Scheme 17**). Radical approaches are often driven by photoredox catalysis or thermal/chemical initiators. In this approach, a carbon- or heteroatom-centered radical is generated and adds across the double bond, followed by hydrogen atom transfer (HAT). Transition-metal catalysis provides another powerful strategy, with metals like palladium, nickel, copper, or cobalt enabling hydroarylation, hydroamination, or hydroboration through organometallic intermediates that guide both regio- and stereoselectivity. More recently, dual catalytic systems, such as photoredox–metal cooperativity, have emerged to merge radical and polar modes, unlocking highly selective hydrofunctionalization reactions under mild conditions. Polar mechanisms typically involve electrophilic activation of the alkene, such as in hydrohalogenation or acid-catalyzed hydration, where the double bond acts as a nucleophile toward an electrophile, followed by capture of the resulting carbocation by a nucleophile. Together, these methods provide complementary routes to install various functional groups directly onto alkenes. [3-5]

Scheme 17. Common approaches to the hydrofunctionalization of alkenes

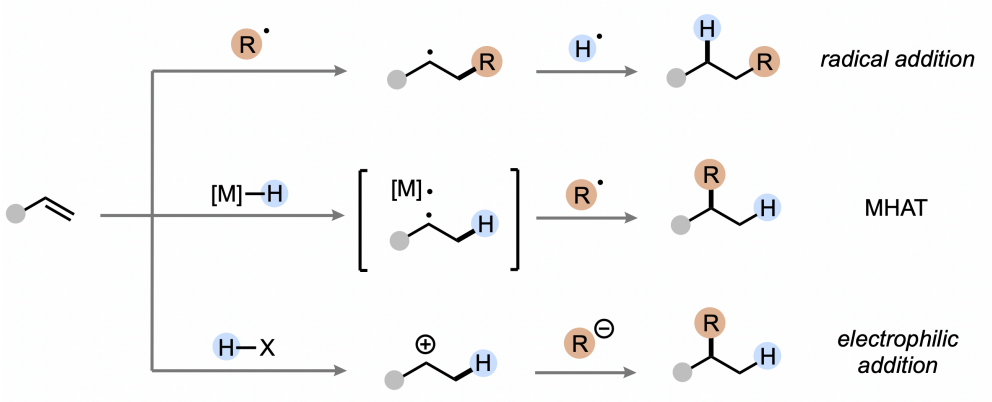

Various alkenes can undergo hydrofunctionalization, and the type of alkene often dictates both the reactivity and the selectivity of the transformation. Terminal alkenes are among the most common substrates, as their electronic and steric environment allows for relatively predictable regioselectivity often favoring addition at the terminal carbon. Internal alkenes (including both linear and cyclic systems) can also undergo hydrofunctionalization but typically require more sophisticated catalysts or directing groups to achieve high selectivity due to the possibility of multiple different addition sites. Electron-rich alkenes like enol ethers and allyl silanes can be activated toward electrophilic addition, while electron-deficient alkenes, such as acrylates, acrylonitriles, and vinyl ketones, are predisposed to nucleophilic attack. Strained alkenes such as norbornene or cyclopropenes can also undergo hydrofunctionalization with unique regio- and stereochemical outcomes due to their ring strain. Of particular interest, styrenes and other conjugated alkenes such as dienes and enones are exceptionally reactive due to the adjacent aromatic or electron-withdrawing groups that are capable of stabilizing carbocationic or radical intermediates formed during hydrofunctionalization.[5,6]

Regioselectivity in the hydrofunctionalization of alkenes is ultimately dependent on the stability of the resulting intermediate, whether a radical, metal-alkyl complex, or carbocation. For example, regioselectivity of radical addition to the alkene is dependent on the stability of the resulting radical. With vinylarenes, addition onto the olefin leads to a stabilized benzylic radical. In polar reactions like hydrohalogenation, Markovnikov's rule is followed because addition occurs in a way that stabilizes the carbocation or radical intermediate at the more substituted carbon. Conversely, anti-Markovnikov selectivity can be achieved when radical pathways or certain metal catalysts (i.e., hydroboration with BH_3, or nickel/iron systems) override this preference by favoring addition to the less substituted site. Steric effects also play a major role, as bulky substituents or catalysts can hinder approach to certain carbons, directing the functional group to the less hindered position. Lastly, reaction mechanism and catalyst design strongly influence outcome. Transition-metal catalysts often enforce regioselectivity through coordination and migratory insertion pathways, while ligand environments and directing groups can guide bond formation toward specific carbons. Therefore, regioselectivity is an important aspect to control in hydrofunctionalization, and is a balance of intermediate stability, steric accessibility, and the nature of the catalytic or mechanistic pathway used.[5-10]

In Scheme 18, two examples each of regioselective linear or branched hydrofunctionalization of vinylarenes products are shown. The radical approach to the linear (anti-Markovnikov) hydro(amino)alkylation of vinylarenes via photoredox catalysis was reported.[7] In this work, vinylarenes are coupled with oxidizable substrates such as organoborons (X = BF^3K), which gets activated via SET by the photocatalyst to generate a carbon-centered radical. Addition of this radical onto the vinylarene would yield the linear product (**Scheme 18A**). Hydrosilanes may also

be used as a hydrogen-atom source, and are often used in this regard. Using a dual metal catalytic system of nickel and copper, hydrosilane, and alkylhalide, the linear selective hydroalkylation of vinylarenes was reported.[8] (**Scheme 18B**)

Alternatively, branched hydrofunctionalization can be achieved through MHAT processes. The Pd-catalyzed hydroalkylation of styrenes was reported using organozinc reagents under oxidative conditions.[9] (**Scheme 18C**) The reaction initiates with transmetallation of the alkyl group onto Pd(II), followed β-hydride elimination to afford an equivalent of Pd–H. Then, the styrene alkene inserts into the Pd–H bond, forming a stabilized Pd-alkyl intermediate. Oxidative coupling occurs with subsequent reductive elimination forming the new C(sp^3)–C(sp^3) bond between the alkyl group and the benzylic carbon to afford the hydroalkylated product. An oxidant is required to regenerate Pd(0) to Pd(II).

In another method, the copper hydride (CuH)-catalyzed regio- and enantioselective hydroformylation of styrenes take place.[10] In this method, the alkene inserts into the Cu–H bond, producing a chiral alkyl copper intermediate with high regio- and enantioselectivity favoring the branched product. Reaction between the alkyl copper intermediate and electrophilic oxocarbenium ion results in the formation of a new C–C bond, producing a chiral acetal compound that can be converted into other functional groups (**Scheme 18D**).

Scheme 18. Strategies for regioselective linear and branched hydrofunctionalization of styrene

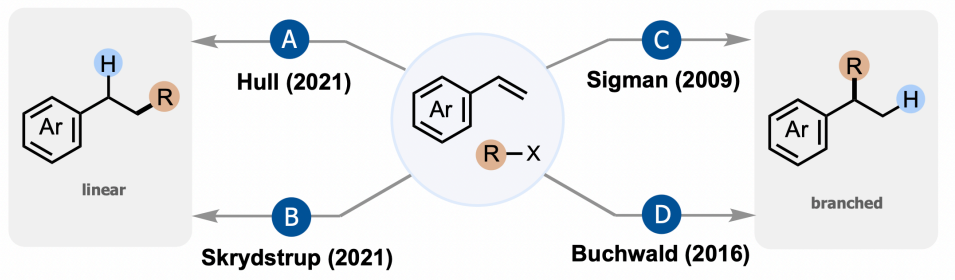

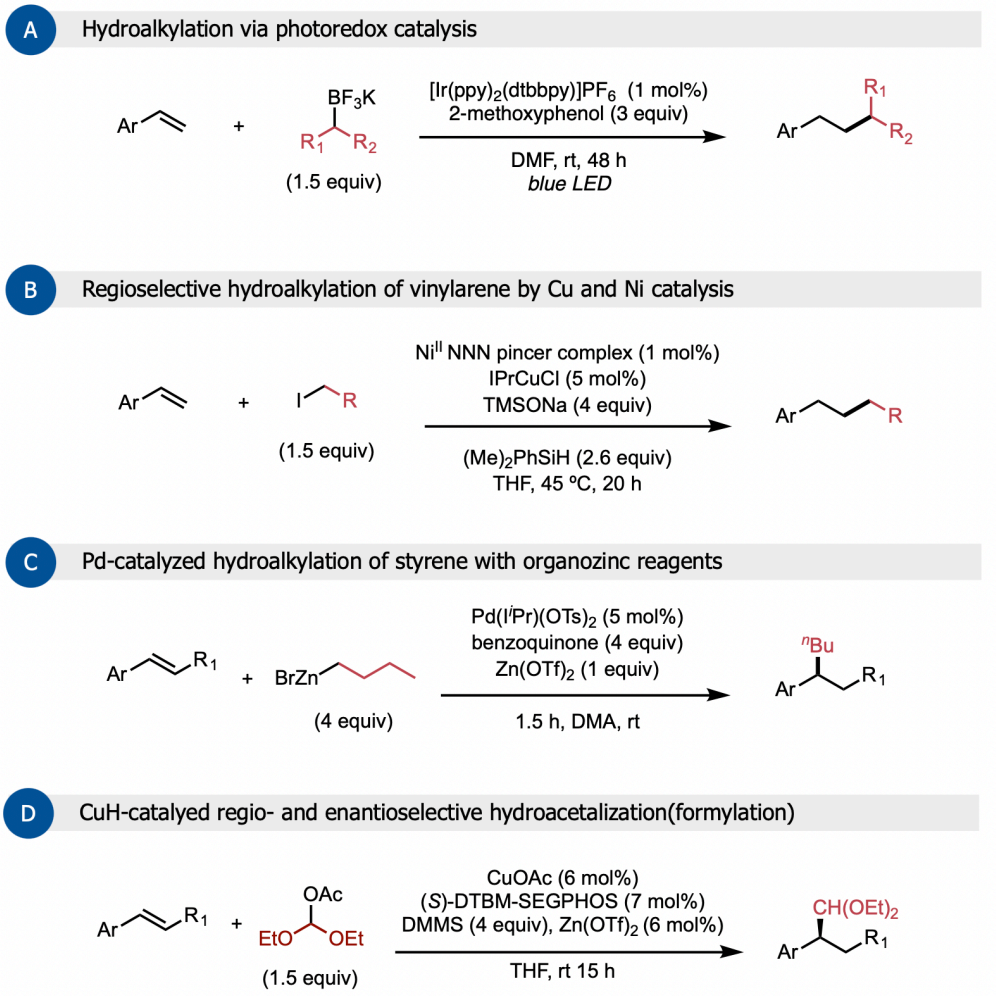

2.2.2 | Early reactions in our group with the TMDSO and KO^{t}Bu reagent system

Recent efforts in our group towards Ni-catalyzed reductive defunctionalization reactions led to the discovery of the C–C bond cleavage of the CF_3 group in 2-trifluoromethylpyridines in the

presence of TMDSO and KO^{t}Bu.[11] Control experiments showed that the Ni catalyst was not involved in this transformation. Due to this unexpected reactivity and rarity of these strong bond cleavages, the study and optimization of the "Reductive Cleavage of C(sp^2)–CF_3 Bonds in Trifluoromethylpyridines" was pursued and published in 2023.

The author of this work, Piers St. Onge (PhD candidate), discovered during mechanistic investigations that the TMDSO and KO^{t}Bu system was capable of reducing *trans*-stilbene into 1,2-diphenylethane with 93% yield, and diphenylacetylene into 1,2-diphenylethane with 78% yield, indicating the strong reductive nature of the reagent system (**Scheme 19A**). Furthermore, subjecting α-cyclopropyl styrene under the conditions of TMDSO and KO^{t}Bu resulted in the ring-opening of the cyclopropyl group in 15% yield, with no detection of the ring-retained product, suggesting a radical pathway towards the transformation (**Scheme 19B**). Based on these discoveries, it was hypothesized that a reactive benzyl intermediate must be formed in situ, and that the addition of an electrophile could trap this intermediate. Upon introducing an alkyl bromide to the reaction with *trans*-stilbene, TMDSO, and KOtBu, Piers St. Onge discovered hydroalkylation of the *trans*-stilbene in 76% yield (**Scheme 19C**). From these discoveries, this hydroalkylation pathway was studied in greater detail, which will be discussed in Chapter 2.3.

Scheme 19. Initial discoveries of the TMDSO and KO^{t}Bu mediated reactions

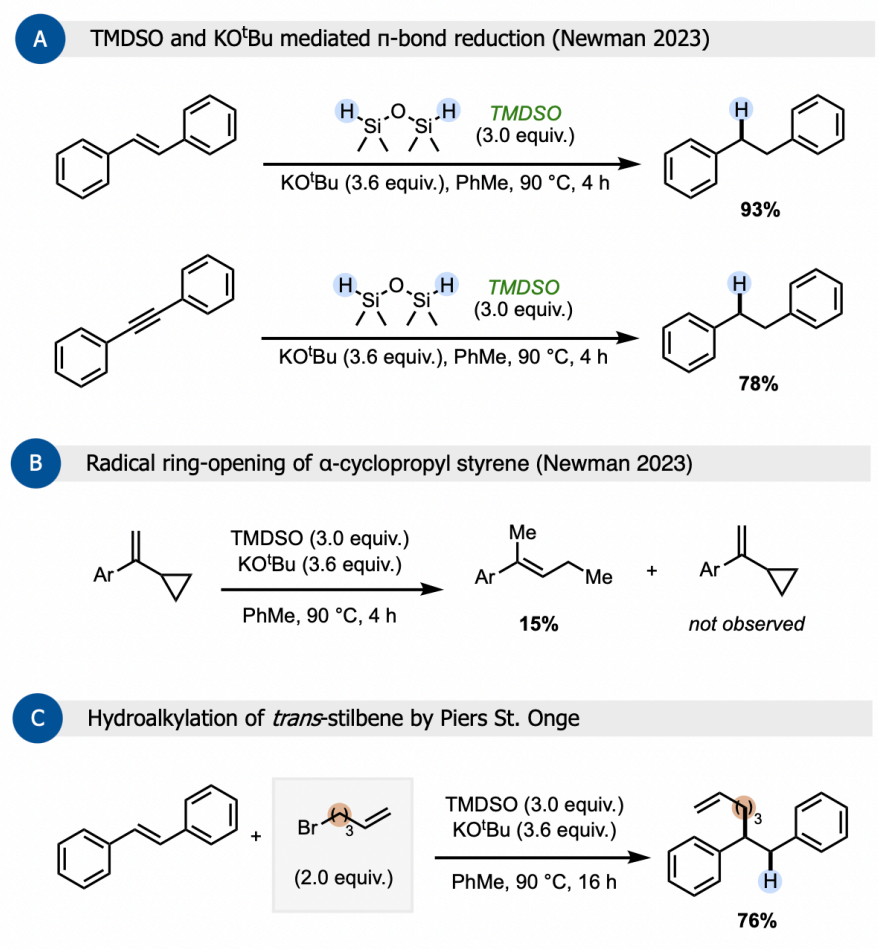

2.2.3 | Research goals

In this chapter, a new route to the hydroalkylation of vinylarenes was explored using a system of potassium tert-butoxide (KO^{t}Bu) and 1,1,3,3-tetramethyldisiloxane (TMDSO). As discussed in chapter 2.1.1, methods already exist in prior literature for the hydroalkylation of various alkene systems. However, as the formation of C(sp^3)-C(sp^3) bonds is fundamental for many disciplines of chemistry[12], the study of novel routes remain important and crucial in gaining access to complex molecules.

The combination of KO^{t}Bu and TMDSO was hypothesized to form a hypercoordinate silicon species that can initiate HAT by delivery of a hydrogen atom to a vinylarene, forming a benzyl

radical. We suspect that subsequent SET by a silicon-derived electron donor can then form the benzyl anion and thus the nucleophile for alkylation via S_N2. The goal of this project was to explore the substrate scope of both vinylarenes and alkyl halides and gather mechanistic insight on how the transformation occurs.

This alternative route presents novel reactivity that can give insight into hypervalent silicon mediated transformations. This system of reagents utilizes cost-effective materials that are both synthetically and commercially available, allowing for quick accessibility to hydroalkylated vinyl arenes and ease of reproducibility.

2.3: Results and Discussion

2.3.1 | Strategies

As previously described in Chapter 2.2.2, mechanistic discoveries in the reductive cleavage of C–CF_3 work showed the strong reductive nature of the TMDSO and KO^{t}Bu system, capable of fully reducing an alkene and alkyne into their alkane counterparts. More interestingly, the introduction of an alkyl bromide into the reaction vessel afforded the hydroalkylation product. In this study, efforts were mostly spent on searching for substrates that can participate in hydroalkylation. We used substrate choice, parameter modification, percent yield of product, and side product identification to gather insight towards the mechanism by which this transformation occurs.

2.3.2 | Initial reactions

The TMDSO and KO^{t}Bu mediated reduction of trans-stilbene into 1,2-diphenylethane, as well as its hydroalkylation with alkyl bromide were first discovered by Piers St. Onge (PhD candidate). Following this discovery, these two reactions were repeated to initiate the start of the project.

The reduction of *trans*-stilbene by the system of KO^{t}Bu and TMDSO into 1,2-diphenylethane (**2.1**) was observed with 95% yield (**Scheme 20**). The combination of these reagents observed an intense color change to dark pink. Similar to the rapid and vivid coloration of ylides in Wittig reactions[13], this color change may be suggestive of the generation of a carbanion nucleophile suspected to be a reactive intermediate. The addition of an alkyl halide 1-bromo-3-phenylpropane turned the mixture to colorless and afforded the hydroalkylated product (**2.2**) with 72% NMR yield.

To observe for the effects of temperature, the reaction was repeated to run overnight at room temperature. The yield of the hydroalkylated product decreased significantly to 15%, with 83% starting material recovery. Although subtle, a color change (from colorless to light pink) was seen when the olefin, KO^{t}Bu, and TMDSO was combined. This color change may have been indicative of the formation of the nucleophile, even at room temperature. This could suggest that the reaction rate was much slower without sufficient heating and a higher reaction temperature would provide more energy for the transformation to occur in a shorter time span.

Scheme 20. Reduction and hydroalkylation of *trans*-stilbene using KO^{t}Bu and TMDSO.

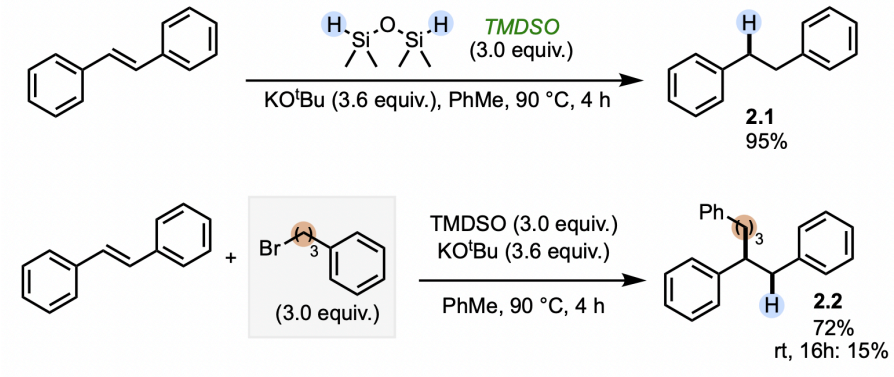

According to Jeon and coworkers, Lewis-base activation of the hydrosilane can function as HAT initiator, in which the presence of an olefin can lead to a benzyl radical.[14] The combination of Et_3SiH and KO^tBu was also found to be competent electron donating system.[15] Subsequent SET by our silicon complex to the benzyl radical could then form the nucleophilic benzyl anion. We predicted that pre-mixing *trans*-stilbene with KO^tBu and TMDSO for a period of time would allow for the active nucleophile to generate in the mixture, where quenching with the alkyl halide would yield the reaction the same way as the simultaneous addition of all reagents. To do this experiment, *trans*-stilbene was stirred in a solution of KO^tBu and TMDSO for one hour before adding 1-bromo-3-phenylpropane (**Scheme 21**). Upon pre-mixing *trans*-stilbene with KO^tBu and TMDSO, the reaction appeared to be a pink mixture, bubbling vigorously before turning clear with the addition of the alkyl halide.

Scheme 21. The stepwise addition of reagents for the hydroalkylation of *trans*-stilbene.

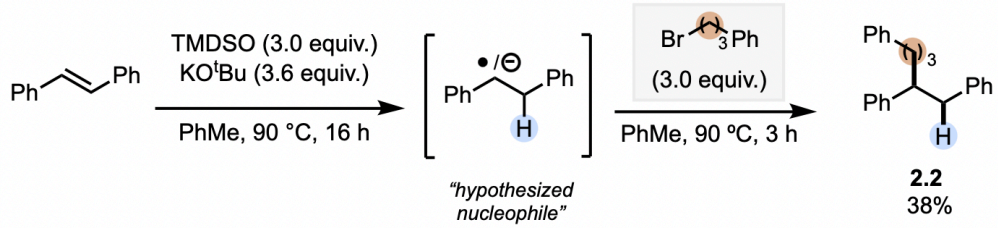

This procedure led to 38% NMR yield of the hydroalkylated product (**Scheme 21, 2.2**), which was lower than the yield from the one-pot addition. While this may have resulted from the reaction not yet running to completion at 3 hours, a multitude of other side-products were observed by GCMS, including reduced *trans*-stilbene (1,2-diphenylethane), homocoupling of 1-bromo-3-phenylpropane, and the cross-coupling product between the 1-bromo-3-phenylpropane and toluene. In the presence of a single electron donor, weak C–Br bonds of the alkyl halide can

undergo homolysis. This can lead to carbon-centered radicals that recombine to form the homocoupled alkyl halide side product. Alternatively, these radicals can also abstract benzylic protons to produce tolyl radicals to form the alkyl halide and toluene side product.

From the step-wise addition of reagents shown in scheme 11, we predict that the combination of olefin, KO^{t}Bu, and TMDSO formed a benzyl radical and silicon radical anion. The radical anion could then continue to react with the benzyl radical, or with weak C–X bonds found in the mixture, turning alkyl halides into radicals . Based on these results, the one-pot addition of reagents was maintained for subsequent experiments for higher yield of product formation, procedural convenience, and less side product formation.

2.3.3 | Exploration of Other π-systems

To determine if hydroalkylation via KO^{t}Bu and TMDSO can be compatible with other pi-systems, various substrates such as polycyclic aromatics, alkynes, and an asymmetric alkene were tested under the same reaction conditions as *trans*-stilbene in Scheme 10. A variety of alkyl halides were also tested.

Results from these experiments showed unsuccessful hydroalkylation of polycyclic aromatic substrates, where phenanthrene was recovered with a yield of 77% (Scheme 20). We predicted that 1,10-phenanthroline would enhance the lewis basicity of KO^{t}Bu by chelating potassium ions[16], leading to a stronger interaction with Si–H and thus promoting HAT. Instead, an intractable mixture of products that we suspect are derived from 1,10-phenanthroline was observed. Grubbs and coworkers have stated that the counter ion plays an important role in the generation of the active silicon species and possibly in the activation of the vinylarene. Therefore, chelation of the potassium ions by 1,10-phenanthroline can explain the lack of conversion.

Furthermore, alkynyl substrates did not undergo hydroalkylation. Phenylacetylene was recovered at 68%, and similarly to the step-wise addition of reagents shown in scheme 11, the reaction formed a mixture of side products with no hydroalkylation.

Interestingly, 1,1-diphenylethylene afforded the branched hydroalkylated product at 60% NMR yield with no linear product observed (**Scheme 22, 2.3**). Similar to Markovnikov alkylation, this indicated that the reactive nucleophile must be more stabilized at the benzylic carbon. From these experiments, the unsuccessful hydroalkylation of alkynes and polycyclic aromatic systems using this reagent system directed the focus of the project towards alkenes.

Scheme 22. Exploration of various π-systems for hydroalkylation.

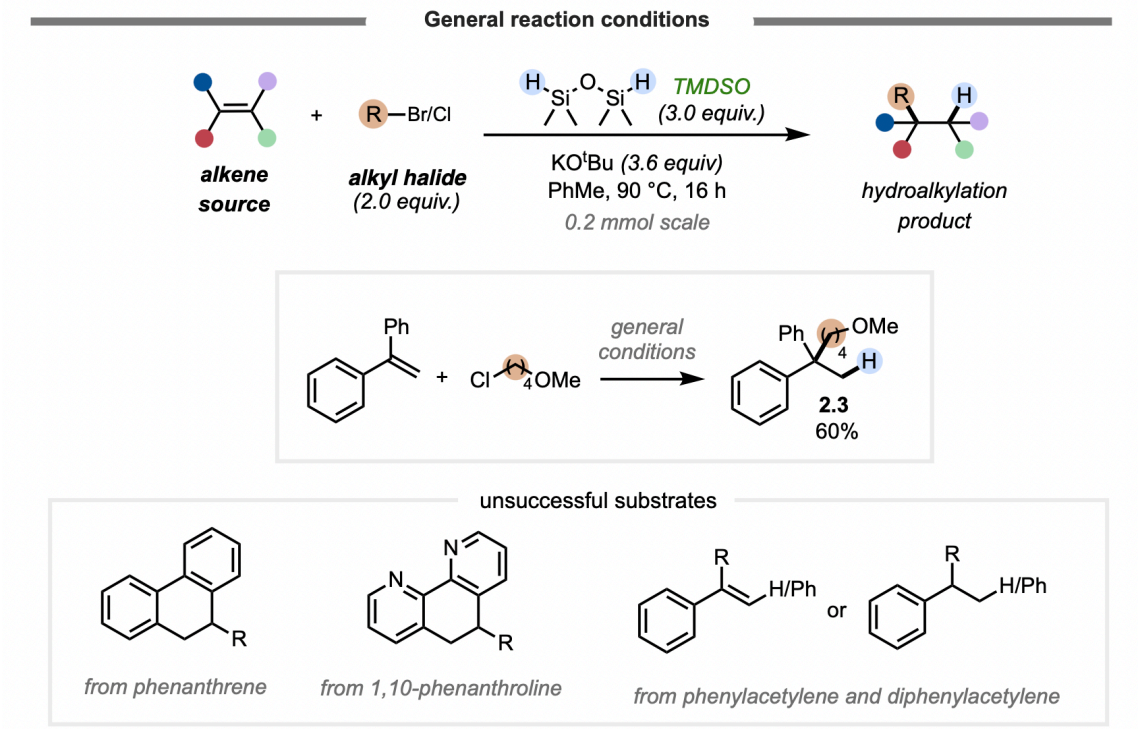

2.3.4 | High-throughput experimentation for substrate screening

High-throughput experimentation (HTE) is a technique used to conduct a large number of experiments simultaneously and analyze them in a short amount of time. To do this, high-throughput plates are utilized so that an array of reactions can be run in parallel. By this method, reactions can be kept mostly constant and changes to reaction parameters can be compared relative to each other for trends that would otherwise not be observed in sequential reactions. For the purposes of this study, a 24-well HTE plate was done for substrate screening where 6 alkenes loaded into each column can react with each alkyl halide charged in each row. Reactions that were successful could easily be identified qualitatively and substrates in scope could be ascertained.

For control experiments, *trans*-stilbene (**Scheme 21**, **1**) and 1-bromo-3-phenylpropane (**B**) were included. Other substrates chosen for a diverse selection of alkene were: styrene (**2**), allylbenzene (**3**), cyclohexene (**4**), tetramethylethylene (**5**), and benzofuran (**6**). An additional primary alkyl halide, 4-choro-1-methoxybutane (**A**), was included. Furthermore, secondary and tertiary alkyl halides, 1-bromocyclopentane (**C**) and 1-bromoadamantane (**D**) respectively, were included to determine if alkylation can still occur with increased steric hindrance.

The success of reactions were determined by GCMS integration of the target product's parent ion relative to 0.2mmol of 1,3,5-trimethoxybenzene as internal standard. With different target products having different ionization constants, the goal of this plate was not to obtain quantitative yields, but rather for qualitative analysis of substrates in scope. The peak intensity of parent ions corresponding to the target product was assumed to be representative of the

amount of product actually formed. Using this information, the hydroalkylated yield of each run could be compared relative to each other to note trends.

Scheme 22. HTE plate conditions for screening other π-systems for hydroalkylation

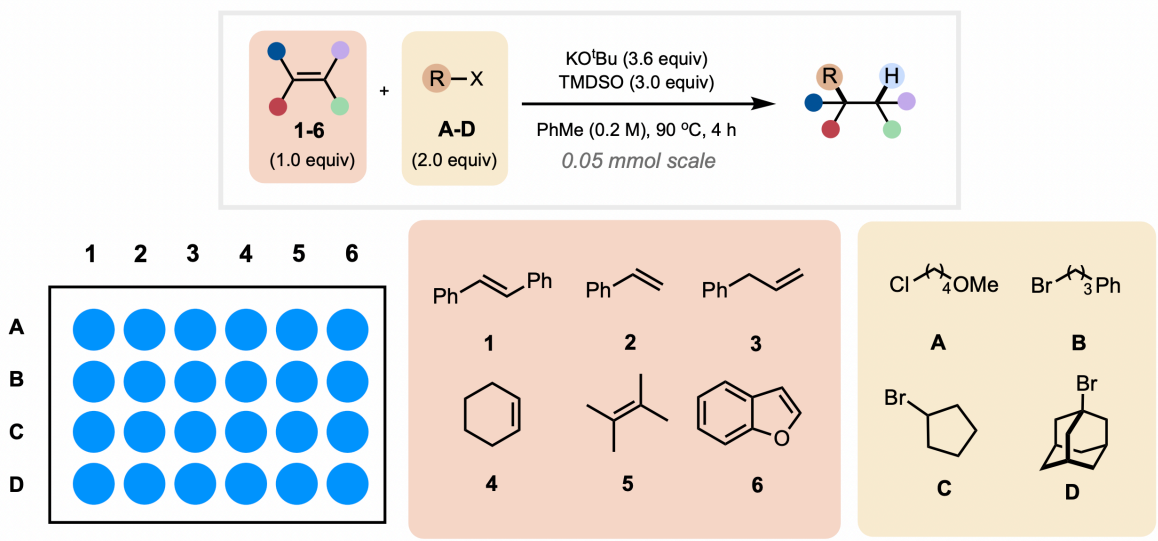

Figure 3. GCMS relative integration of hydroalkylation product with 0.2mmol 1, 3, 5-trimethoxybenzene from HTE plate.

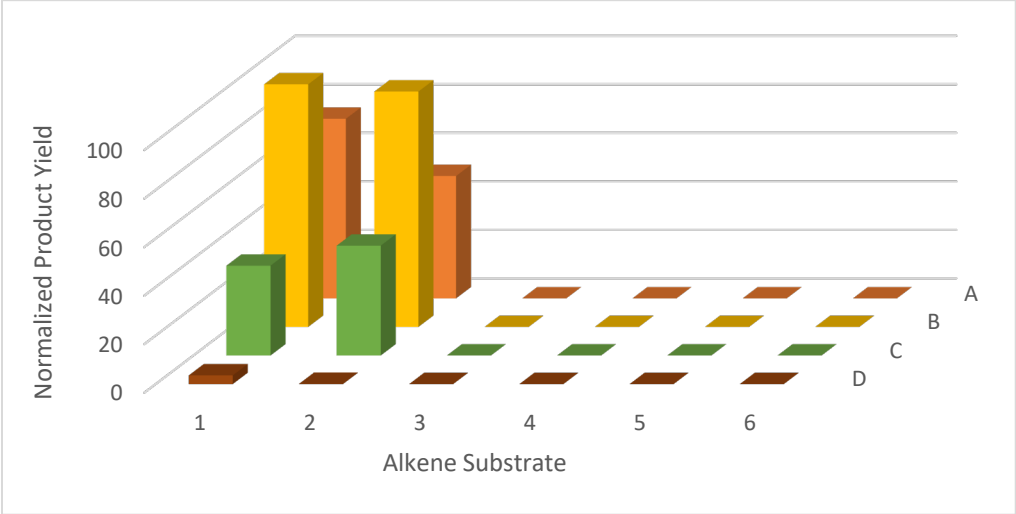

The results obtained from the plate confirmed the consistent reactivity of *trans*-stilbene with both primary alkyl halides (**Figure 4**, **A1** and **B1**), as well as alkylation with the secondary alkyl halide to a smaller degree (**C1**), and even less so with the tertiary alkyl halide (**D1**). Styrene was

observed to follow this reactivity pattern where alkylation occurred to a greater extent with primary alkyl halides (**A2**, **B2**) compared to a secondary alkyl halide (**C2**), but with no tertiary alkyl halide alkylation (**D2**). The highest level of hydroalkylation was observed with 1-bromo-3-phenylpropane for both *trans*-stilbene (**B1**) and styrene (**B2**). The decreasing alkylation yield with increasing hindrance of the alkyl halide is consistent with an S_N2 mechanism of alkylation, corroborating our hypothesis of an in situ generated carbanion intermediate.

Interestingly, the homodimerization of *trans*-stilbene and styrene was observed in the presence of 1-bromoadamantane (**D1** and **D2**). In these reactions, reduced 1-bromoadamantane was also seen which may explain the lack of alkylation. We can predict that a single electron donor present in the mixture can homolyze weak C–Br bonds and form relatively stable tertiary radicals, and subsequent HAT with Si–H can afford the reduced adamantane. With the alkyl halide reduced, this may explain the dimerization of both *trans*-stilbene and styrene.

Allyl benzene showed different reactivity. Parent ions of major products in **A3** through **D3** showed two mass units lower than the hydroalkylated product. Resulting from the basicity of KO^tBu, a benzyl/allylic anion could form upon deprotonation. This anion could then undergo alkylation via S_N2 and lead to a product 2-units mass deficient of the expected product due to the retention of the olefin. GCMS ionization peaks showed that a linear alkylated regioisomer was also present in **A3**, **B3**, and **D3** (**Scheme 23**).

Scheme 23. Alternate reactivity pattern of allyl benzene from HTE plate (Figure 4, Substrate 3)

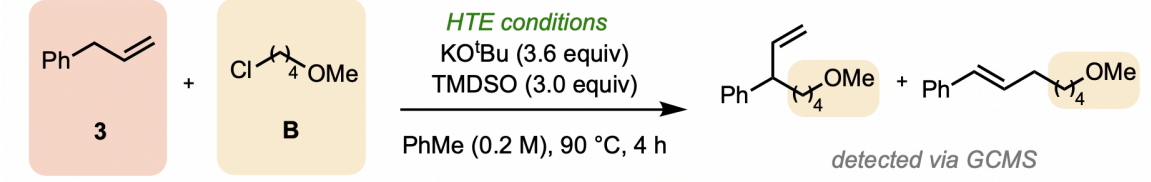

Cyclohexene (**Figure 4**, **4**) and tetramethylethylene (**5**) did not yield hydroalkylated product. In the case of *trans*-stilbene and styrene, harnessing a benzylic nucleophile would be favorable due to resonance stabilization. Contrary to this, HAT towards cyclohexene and tetramethylethylene would generate a fairly unstable nucleophile due to the lack of major stabilizing functional groups. This aligns with our hypothesis, where no hydroalkylation could occur without the generation of a nucleophile.

Lastly, benzofuran (**6**) was not observed to afford the target hydroalkylated product. GCMS data of **B6** showed the parent ion as two mass units lower than the hydroalkylated product, and no other alkyl halide beside 1-bromo-3-phenyl propane was seen to react with benzofuran. Benzofuran is known to exclusively undergo electrophilic substitution at the alpha-position.[22] This suggested that electrophilic substitution of benzofuran occurred in the reaction conditions with no hydroalkylation product formation (**Scheme 24**).

Scheme 24. Alternate reactivity of benzofuran from HTE plate (Figure 4, B6)

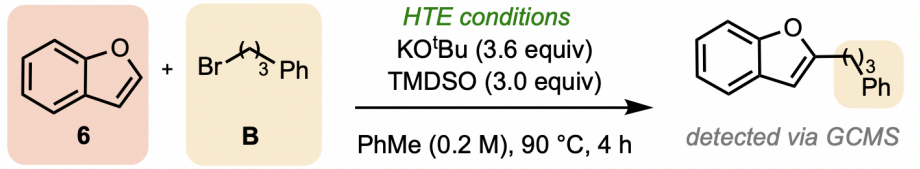

From these results, it was pertinent that a stabilizing functional group is present for the generation of a nucleophile for hydroalkylation to occur. This would explain the consistent benzylic alkylation seen in 1,1-diphenylethylene (**Scheme 20, 2.3**) and styrene (**Figure 4**, **A2**, **B2**), as well as the lack of reactivity with cyclohexene and tetratmethylethlyene. Allyl benzene and benzofuran were not studied any further as they were not observed to participate in the TMDSO and KO^{t}Bu hydroalkylation process. Following this, a scope of vinylarenes was synthesized where both coupling partners were varied.

2.3.5 | Scope of vinylarenes and alkyl halides

Previous experiments showed that styrene had hydroalkylating activity with a number of alkyl halides. To expand this scope, hydroalkylation of various vinylarene derivatives were done using 4-chloro-1-methoxybutane, along with the exploration of a scope of alkyl halides that were coupled with styrene (**Scheme 25**).

The isolation of hydroalkylated products prior to this scope study was often difficult due to the presence of silicon oligomers, which tend to co-elute with the desired product despite being highly non-polar. These impurities were hard to eliminate, likely due to their varying lengths and insolubility in hexanes. In order to remove these silane derived byproducts, tetrabutylammonium fluoride (TBAF) was added to the mixture and stirred for an additional 2 hours. With this change, most silicon-containing byproducts were eliminated from the crude mixture and eased the isolation process

The hydroalkylation of a variety of vinylarenes were done in moderate yields (**Scheme 25**). Tertbutyl and methoxy groups (entry **2.4** and **2.5**) substituted on the aryl ring were tolerated under the reaction conditions and were purified easily, meaning electron species can undergo hydroalkylation. Entry **2.6** using 2-methylstyrene as starting material showed that steric hindrance near the benzylic position was not deleterious for the reaction, with yields comparable to entry **2.4** and **2.5** that have para substitution.

An even more interesting example involved alpha-methyl styrene (entry **2.8**) in which the hydroalkylation of this compound observed the formation of a quaternary carbon. This showed substitution directly on the alpha carbon did not hinder the reaction and had an isolated yield comparable to that of other vinylarene scope examples. Decreased yield was noted using 4-

fluorostyrene (entry **2.7**), reflecting that electron density of the aryl group can influence nucleophilicity of the benzyl intermediate wherein an electron rich aryl substituent can enhance the nucleophilicity of the benzyl intermediate to promote alkylation.

Scheme 25. Scope of hydroalkylation between vinylarenes and 1-chloro-4-methoxybutane

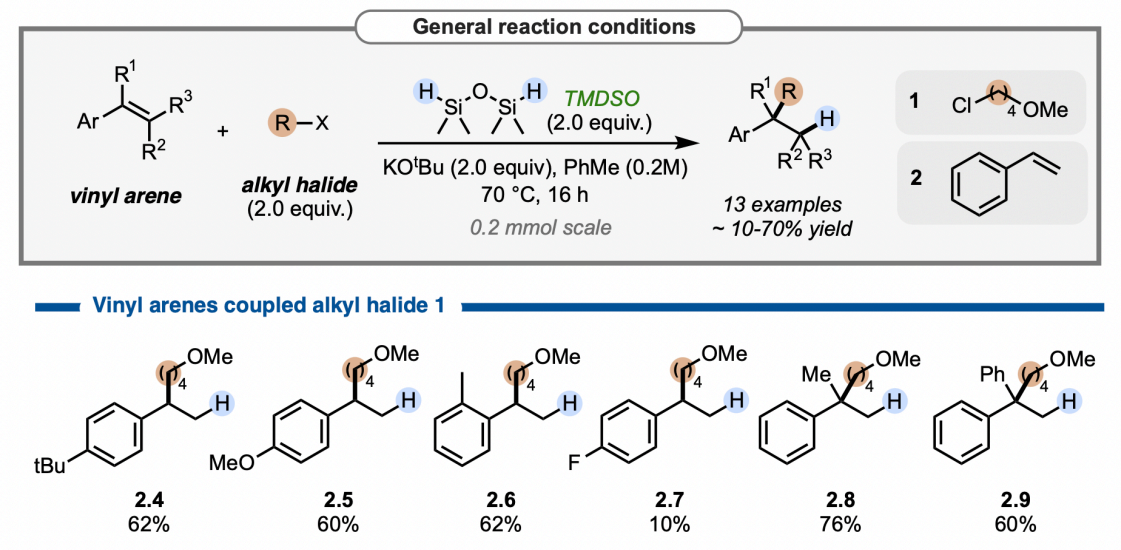

Following this, a scope of alkyl halides was initially done using styrene as the starting material. Then, 4-tertbutylstyrene was also used to test alkyl halides to obtain less volatile compounds with heavier molecular weight.

As seen in scheme 26, functional group tolerance was observed with entries **2.11** and **2.12** containing an acetal and indole group respectively. With the ability of KO^{t}Bu and TMDSO to reduce carbonyl groups, acetal groups withstanding the reaction conditions can be an alternative to using ketones directly. Furthermore, tolerance of indoles in this reagent system is beneficial, as indoles present as useful scaffolds in drug discovery.

Both alkyl chlorides and alkyl bromides were used for these scope examples and did not appear to majorly affect yield. Notably, entry **2.12** was obtained by reacting styrene with either 1-(4-

chlorobutyl)-1H-indole or 1-(4-bromobutyl)-1H-indole with 32% and 35% isolated yields respectively. Additionally, the reduced form of the alkyl halide used in entry **2.12**, n-butyl indole, was calculated at 8% in the isolated sample. Reduced alkyl halides were not seen in other scope examples. N-butyl indole may have been persistent in the sample due to its molecular weight, while other reduced alkyl halides would be more volatile.

Scheme 26. Scope of hydroalkylation between styrene and various alkyl halides

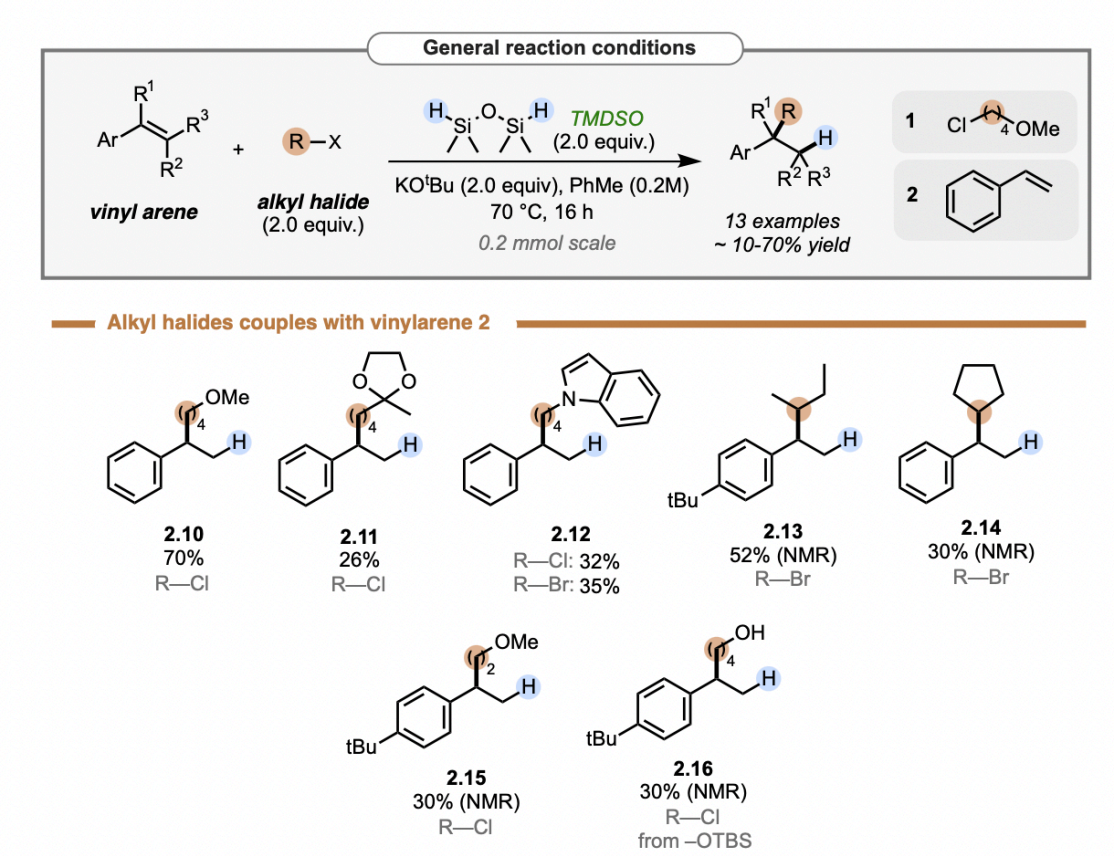

Secondary alkyl bromides (entries **2.13**, **2.14**) were also successful as electrophiles for hydroalkylation. This was observed previously from the 24-well plate results in scheme 22, where both primary and secondary alkyl halides can undergo hydroalkylation, but yields decrease as steric hindrance is increased with the reaction failing when substituted with a tertiary alkyl halide.

Entries **2.13** and **2.14** indicated that both cyclic and acyclic secondary alkyl halides are possible electrophiles for this reaction, showing that steric hindrance did not hamper reactivity.

Entry **2.16** showed that protected alcohols may also be in scope. In this example, (4-Chlorobutoxy)(1,1-dimethylethyl)dimethylsilane as the starting alkyl halide was reacted with 4-tertbutylstyrene. As the alkyl halide contained a silyl protecting group, deprotection occurred with the addition of TBAF to afford the alcohol product.

Observing the reactions of these scope examples, a minor byproduct formed in the majority of the experiments. In cases where dimer formation was more pronounced, purification was harder as it eluted with the target product. Notably, entry **2.10** using styrene as the starting material had the largest dimer byproduct formation estimated to be 15-20%. Aside from this example, dimer presence in all other isolated samples were dilute enough to be undetectable via NMR. The hypothesized mechanism for dimer formation is later discussed in Chapter 2.3.6 and provided additional insight for the overall mechanism of the reaction.

This scope study showed that functional groups on both the alkyl halide and vinylarene could be tolerated, and a number of selected examples were isolated for characterization by ^{1}H NMR and ^{13}C NMR (**Appendix A**).

2.3.6 | Mechanistic Insights and Discussion

Information gathered from literature pretext as well as our own substrate screening done in duration of this project can provide clues towards our hypothesized mechanism. Initially, it was known that the combination of hydrosilane and base is a powerful reducing agent that can form silyl radicals, act as a hydride donor, and as a single electron donor. Adding to this, research by Jeon and Newman also showed that other reactive intermediates exist, and the system of

hydrosilane and base can also act as an H-atom donor. Taking this into consideration, the mechanism of this reaction can be hypothesized and elucidated (**Scheme 28**).

In a report by Nikonov et al., the combination of KO^tBu and PMHS leads to the decomposition of PMHS into methylsilane (H_3SiMe). Analogous to this, the report also states that the addition of KO^tBu upon TMDSO leads to the decomposition of TMDSO into dimethylsilane (H_2SiMe_2). Excess KO^tBu would convert dimethylsilane into the hypervalent state, from which we hypothesize this silanate complex to be the active reducing agent for the H-atom transfer step.

Our method of hydroalkylation via the TMDSO and KO^tBu system is regioselective for the branched (Markovnikov) product, with no trace of the linear (anti-Markovnikov) product. This suggests the reactive intermediate lies on the benzylic carbon. Furthermore, based on HTE screening in Scheme 22, reaction does not occur if no stabilizing group (such as a phenyl ring) is adjacent. This aligns with the hypothesis that HAT occurs by the silanate complex to the accepting styrene, which would yield a stabilized benzyl radical that can continue to react.

Murphy and coworkers have stated that the combination of base and hydrosilane to produce a silicon radical anion is a competent single-electron donating system. In consideration of this, the silicon complex can be hypothesized to donate an electron to the benzyl radical to afford the carbanion required for S_N2 alkylation.

Scheme 27. Proposed reaction mechanism of TMDSO and KO^{t}Bu mediated hydroalkylation

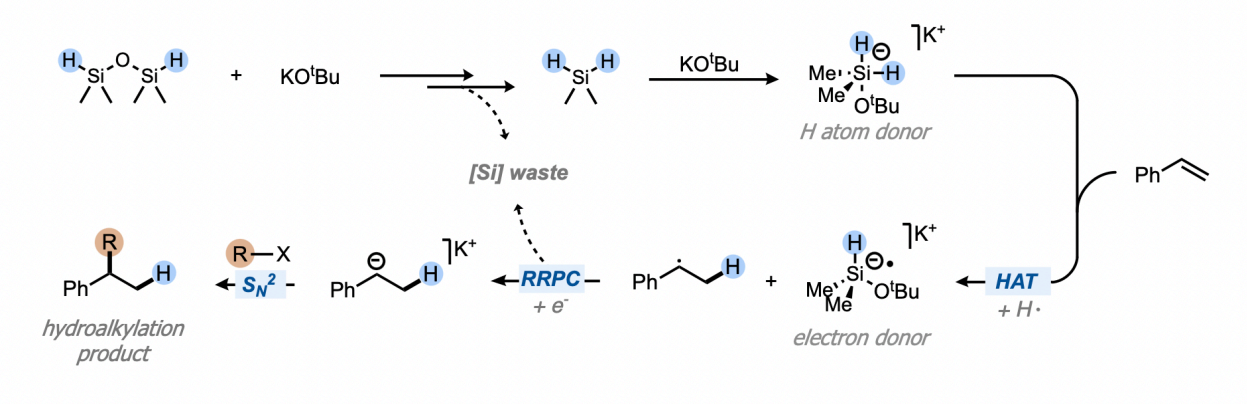

With this hypothesis, the radical and anionic character of the benzyl carbon can be tested through mechanistic probes, through understanding the pathways of unwanted side products. Radical character on the benzylic may be hinted from the presence of styrene dimerization. The nature of the benzyl radical opened the possibility of homocoupling between two vinylarene through Giese addition as a side product. The same steps of SET and S_N2 identical to the product formation can afford the final side product. This was observed during the scope study discussed in the previous Chapter 2.3.5, where dimer formation was seen in a majority of examples via GCMS in varying degrees. The proposed mechanism for dimerization is shown in **Scheme 28**.

Scheme 28. Speculated mechanism for the styrene-derived side product (dimer)

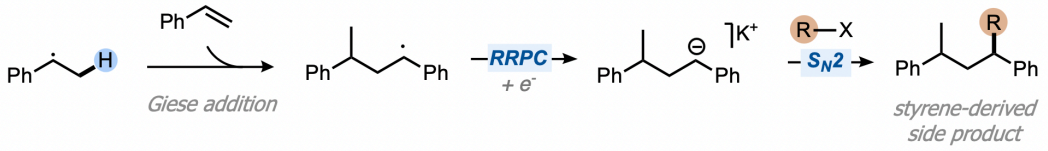

Additionally, to probe for anionic character on the benzylic carbon, a vinyl-ether styrene was tested as a mechanistic probe, where the ejection of benzyl alcohol to form styrene in situ would reflect the presence of a benzyl anion (**Scheme 29**). This results from the benzyl alkoxide being a good leaving group. Running this reaction showed 19% yield of the deoxygenated product,

indicating some anionic character on the benzylic carbon. From the accumulation of literature references and reaction insights, both the radical and anionic character of the reactive intermediate can be argued.

Scheme 29. Ejection of benzyl alkoxide via benzyl carbanion intermediate

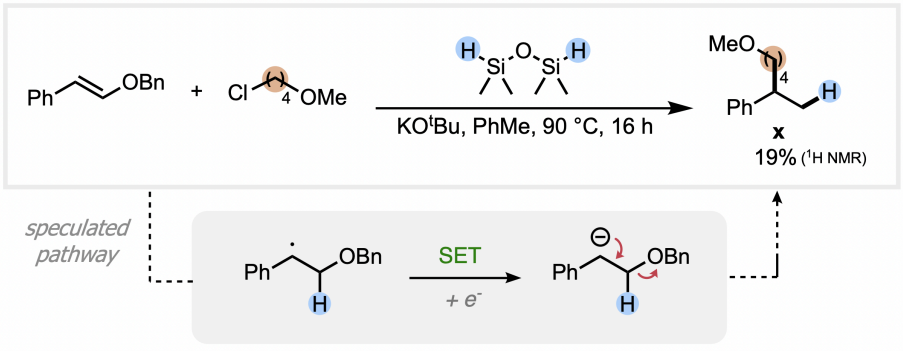

2.4: Summary and future work

In summary, a novel route to the hydroalkylation of vinylarenes via KO^{t}Bu and TMDSO was achieved with exclusive regioselectivity, opting for alkylation at the benzylic carbon. This unusual combination of reagents was hypothesized to form a pentacoordinate silicon complex, facilitating the transformation by initiating HAT and as a source for single electron transfer. Mechanistic insights towards this transformation were gathered from substrate screening experiments and the scope study where both the radical and anionic character of the reactive intermediate can be argued, indicating the process of RRPC. These experiments showed a relatively broad scope where various functional groups on both the vinylarene and alkyl halide were tolerated, allowing for access to alkylated benzene species via a novel route to C(sp^3)-C(sp^3) bond formation.

Future work for this project can explore reactivity with other aryl substrates to find more hydroalkylating coupling partners. Seeing as benzofuran had an alternate reactivity pattern, the

electrophilic substitution mechanism of this reaction can be further investigated and other substrates that can undergo this reactivity can be explored.

During the scope discovery of this project, various other transformations were found to be catalyzed by the TMDSO and KO^{t}Bu reagent pair. Keeping note of these transformations, each reaction can be studied in much more detail to provide more insight to the hydrosilane-base reagent pair, as well as opening up new routes for potential projects following the hydroalkylation work.

In this pursuit, 3 transformations were identified that can be catalyzed by the TMDSO and KO^{t}Bu reagent pair – hydroarylation of styrene with 2-fluoropyridine (**Scheme 30A**), reductive etherification of aryl aldehydes and aryl ketones (**Scheme 30B**), and lastly the dithiane cleavage and in situ alkylation of protected aryl carbonyls (**Scheme 30C**). Optimization campaigns were run for each of these reactions, but halted due to numerous reasons. For the S_NAr of 2-fluoropyridines, yields were capped at 18% and the scope of 2-fluoropyridines pyridines were extremely limited, indicating low functional group tolerance.

Reductive etherification was successful with moderate yields for aryl aldehydes and diaryl ketone. However, ketones with enolizable α-H could not undergo etherification, and the transformation results in α-H alkylation. Optimization campaigns were not successful in altering reactivity to favor etherification over alkylation.

In the desulfurization procedure, success in dithiane cleavage followed by alkylation with an alkyl halide was only observed with diphenyl dithiane. With monoaryl dithianes (i.e. R^1 = H, alkyl), desulfurization halts after the cleavage of one C–S bond before cleaving both. Instead, a thioether

forms by nucleophilic attack of sulfur onto a free alkyl halide. Due to this, the anticipated scope would have been significantly small, and efforts were stopped into optimizing this reaction.

Scheme 30. Other transformations by TMDSO and KO^{t}Bu reagent system and problems associated

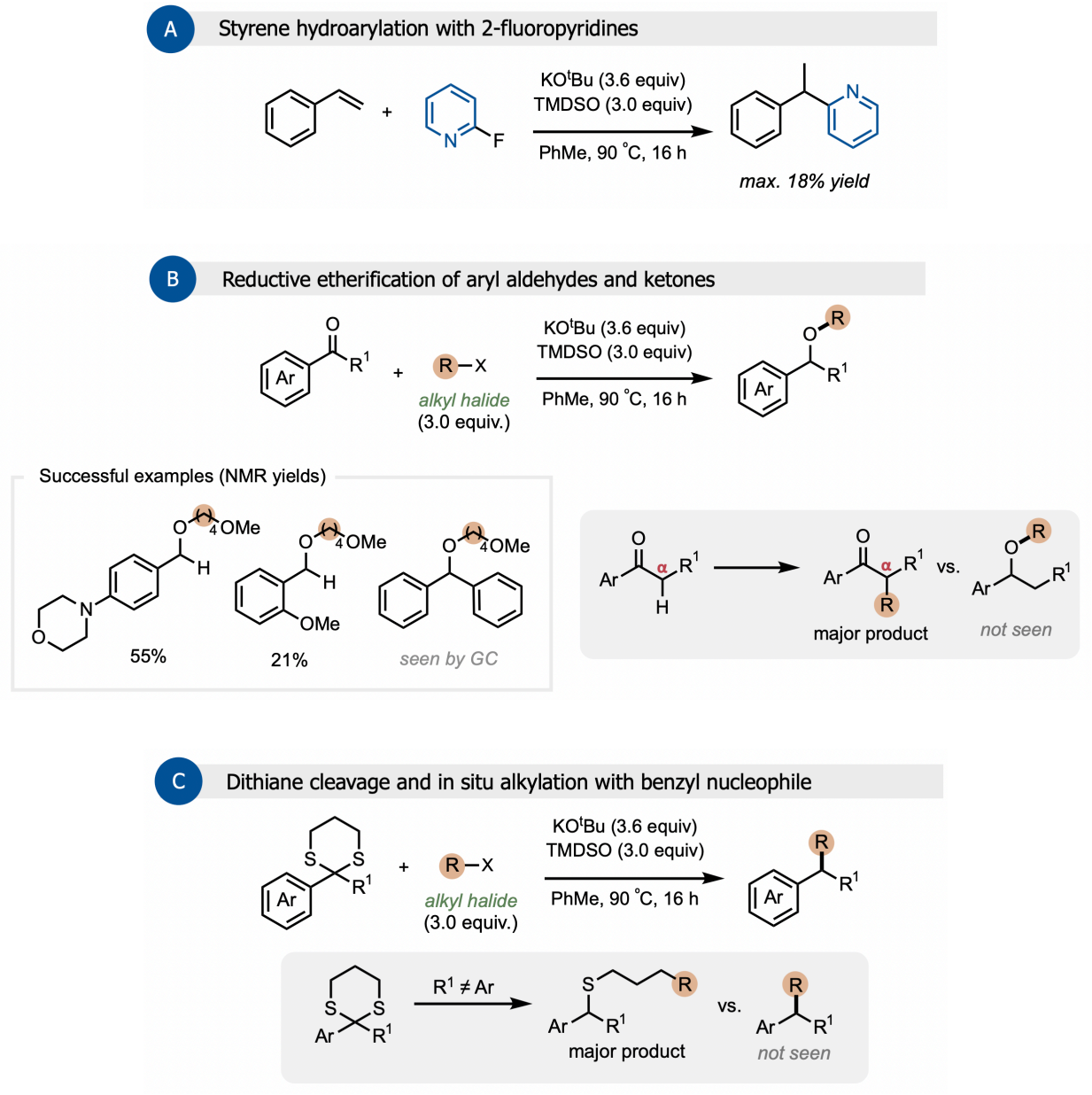

Despite these numerous failed attempts at discovering and optimizing transformations, it can still be argued that the reactivity of TMDSO and KO^{t}Bu is versatile, mechanistically intriguing, and have yet to be fully explored. Moving on from the hydroalkylation work, we decided to put our research efforts into exploring a promising lead – to search in literature for other transformations that take place with RRPC and try to reproduce the reaction in with our reagent system. This led to the discovery of the TMDSO and KO^{t}Bu mediated cross-electrophile coupling of alkyl halides, which will be the main topic in chapter 3.

2.5: References

(1) Wei, G.; Dongmin, F.; Jiying, L.; Wei, Y.; Ruiying, C.; Tao, Z.; Xuebo, C.; Linbin, N.; Shi-Jun, L.; Yu, L. Relay-Hydrogen Atom Transfer Mode for Nickel-Hydride-Mediated Anti-Markovnikov Hydroalkylation of Alkenes. *CCS Chem.* **2024**, *7*, 2409–2418.

(2) Buettner, C. S.; Schnürch, M.; Bica-Schröder, K. Photocatalytic Hydroalkylation of Aryl-Alkenes. *J. Org. Chem.* **2022**, *87*, 11042–11047.

(3) Yin, X.; Li, S.; Guo, K.; Song, L.; Wang, X. Palladium-Catalyzed Enantioselective Hydrofunctionalization of Alkenes: Recent Advances. *European J. Org. Chem*. **2023**, 26, e202300783.

(4) Zhang, S.; Findlater, M. Electrochemically Driven Hydrogen Atom Transfer Catalysis: A Tool for C(Sp3)/Si–H Functionalization and Hydrofunctionalization of Alkenes. *ACS Catal*. **2023**, 13, 8731–8751.

(5) Wang, X.-X.; Xu, Y.-T.; Zhang, Z.-L.; Lu, X.; Fu, Y. NiH-Catalysed Proximal-Selective Hydroalkylation of Unactivated Alkenes and the Ligand Effects on Regioselectivity. *Nat. Commun.* **2022**, *13*, 1890.

(6) Ma, S.; Xi, Y.; Fan, H.; Roediger, S.; Hartwig, J. F. Enantioselective Hydroamination of Unactivated Terminal Alkenes. *Chem* **2022**, *8*, 532–542.

(7) Wu, Z.; Gockel, S. N.; Hull, K. L. Anti-Markovnikov Hydro(Amino)Alkylation of Vinylarenes via Photoredox Catalysis. *Nat. Commun.* **2021**, *12*, 5956.

(8) Ravn, A. K.; Johansen, M. B.; Skrydstrup, T. Regioselective Hydroalkylation of Vinylarenes by Cooperative Cu and Ni Catalysis. *Angew. Chemie Int. Ed.* **2022**, *61*, e202112390.

(9) Urkalan, K. B.; Sigman, M. S. Palladium-Catalyzed Hydroalkylation of Styrenes with Organozinc Reagents To Form Carbon−Carbon Sp3−sp3 Bonds under Oxidative Conditions. *J. Am. Chem. Soc.* **2009**, *131*, 18042–18043.

(10) Garhwal, S.; Dong, Y.; Mai, B. K.; Liu, P.; Buchwald, S. L. CuH-Catalyzed Regio- and Enantioselective Formal Hydroformylation of Vinyl Arenes. *J. Am. Chem. Soc.* **2024**, *146*, 13733–13740.

(11) St. Onge, P.; Khan, S. I.; Cook, A.; Newman, S. G. Reductive Cleavage of $C(Sp^2)$–CF_3 Bonds in Trifluoromethylpyridines. *Org. Lett.* **2023**, *25*, 1030–1034.

(12) Lu, X.; Xiao, B.; Zhang, Z.; Gong, T.; Su, W.; Yi, J.; Fu, Y.; Liu, L. Practical Carbon–Carbon Bond Formation from Olefins through Nickel-Catalyzed Reductive Olefin Hydrocarbonation. *Nat. Commun.* **2016**, *7*, 11129.

(13) Vedejs, E.; Meier, G. P.; Snoble, K. A. J. Low-Temperature Characterization of the Intermediates in the Wittig Reaction. *J. Am. Chem. Soc.* **1981**, *103*, 2823–2831.

(14) Asgari, P.; Hua, Y.; Bokka, A.; Thiamsiri, C.; Prasitwatcharakorn, W.; Karedath, A.; Chen, X.; Sardar, S.; Yum, K.; Leem, G.; Pierce, B. S.; Nam, K.; Gao, J.; Jeon, J. Catalytic Hydrogen Atom Transfer from Hydrosilanes to Vinylarenes for Hydrosilylation and Polymerization. *Nat. Catal.* **2019**, *2*, 164–173.

(15) Revunova, K.; Nikonov, G. I. Base-Catalyzed Hydrosilylation of Ketones and Esters and Insight into the Mechanism. *Chem. – A Eur. J.* **2014**, *20*, 839–845.

(16) Barham, J. P.; Coulthard, G.; Emery, K. J.; Doni, E.; Cumine, F.; Nocera, G.; John, M. P.; Berlouis, L. E. A.; McGuire, T.; Tuttle, T.; Murphy, J. A. KO^tBu: A Privileged Reagent for Electron Transfer Reactions? *J. Am. Chem. Soc.* **2016**, *138*, 7402–7410.

Chapter 3: Cross electrophile coupling of alkyl halides

In this chapter, the study of a second transformation facilitated by the hydrosilane-base reagent system is reported, namely the cross electrophile coupling of alkyl halides. In chapter 3.1, an introduction to the field of cross-electrophile coupling is given, followed by current methods to accessing this transformation. Chapter 3.2 will present results and discussion for the cross-electrophile coupling via the hydrosilane-base reagent system. In this section, the process of discovery, optimization, scope, and mechanistic insights are discussed.

3.1: Background

Cross-electrophile coupling (XEC) modern synthetic method in organic synthesis that enables the direct coupling of two electrophiles under reductive conditions without the need for preformed organometallic nucleophiles. The pioneering example that brought forth the foundation of XEC is the Ulmann coupling, dating back to 1901[1] (**Scheme 31**). Here, we observe the formation a C–C bond between two aryl structures, forming symmetrical biaryl products. This was originally accomplished using two molecular equivalents of aryl halide and stoichiometric copper at high temperatures (above 200 ˚C). These reactions had limited substrate scope, low yields, and harsh conditions and were not widely adopted as synthetic tools.

Scheme 31. Ullman reaction as an early example of XEC

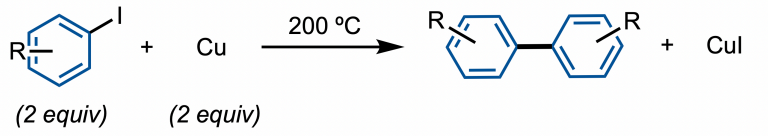

From this point, the field advanced rapidly throughout the 20th century with the rise of catalytic cross-coupling reactions utilizing Pd and Ni catalysts. These include Suzuki-Miyaura, Negishi,

Kumada, Stille, and Heck reactions, which relied on coupling an organometallic nucleophile with an aryl or vinyl electrophile, revolutionizing complex molecule construction in pharmaceutical and material science contexts.[2]

Despite their broad adoption, classical cross-couplings typically require preformed organometallic nucleophiles, often sensitive, air-sensitive, or synthetically challenging. The emergence of XEC coupling introduced an alternative route by enabling the coupling of two electrophiles directly, circumventing the need for pre-formed organometallic nucleophiles.[2,3] From here, innovation in the field drove discovery for cross-coupling between two different electrophilic partners, which brought the challenge of harnessing cross-selectivity over homocoupling (**Scheme 32**).

Scheme 32. General scheme for cross electrophile coupling

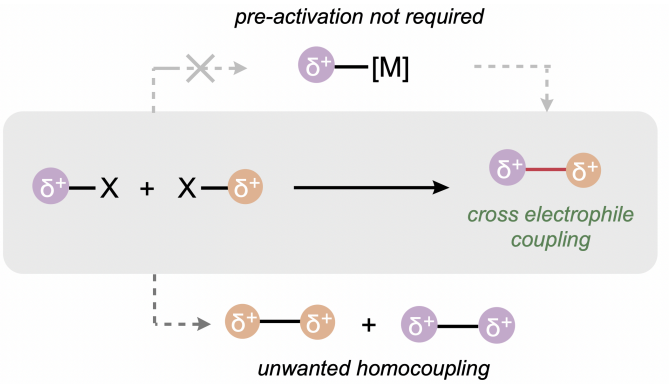

Reports in the early 2010s showed Ni catalysis combined with stoichiometric reductants like zinc or manganese has been central to the development of XEC methodologies.[2] These protocols facilitate selective reductive activation of electrophiles, often involving alkyl or aryl halides under mild conditions. In this way, accessibility and expansion of the chemical space is achieved, including $C(sp^3)$–$C(sp^3)$ bond formations previously elusive due to issues like β-hydride elimination.

3.1.1 | Modern methods towards XEC

Recent advances have expanded the scope to include challenging electrophiles such as alkyl chlorides, pseudohalides, redox-active esters, and heteroatomic electrophiles (nitrogen, boron, silicon, phosphorus-based). Innovations in ligand design, catalyst systems, and mechanistic understanding have addressed challenges in chemo-, regio-, and stereoselectivity, allowing more predictable and efficient couplings.

Most reports on XEC are done by transition metal catalysis, predominantly by 3d transition metals (Ni, Co, Cu, Fe, Cr, and Ti) and with few reports using Pd and Rh.[x] From this list, nickel is by far the most used catalyst. Nickel is favored due to its ability to facilitate electron oxidation and reduction which are necessary steps in transition-metal catalyzed XEC. Alternatively, photochemically-driven XEC usually employs $[(Ir(bpy)(ppy)_2]X$ derivatives as cocatalysts. The photoredox catalyst, upon light excitation, undergoes SET events to generate reactive radical intermediates from one electrophilic partner, often an alkyl halide, via halogen atom abstraction or reduction. In one example by MacMillan in 2016, combines these two approaches to enable the metallaphotoredox catalysis of alkyl halides[3] (**Scheme 33**).

Scheme 33. Cross electrophile coupling of alkyl halides via metallaphotoredox catalysis

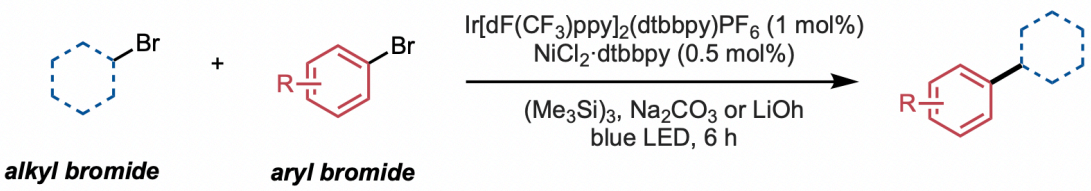

Electrochemical cross-electrophile coupling (eXEC) uses electrochemical reduction to enable C–C bond formation without the use of stoichiometric chemical reductants. In eXEC, an electric current provides the necessary electrons to drive the reductive catalytic cycle, activating two

different electrophiles—often alkyl or aryl halides—for selective coupling. In one example reported by Lin et al, the eXEC of alkyl halides was successfully done with a large scope[4] (**Scheme 34**). In this work, electronically different alkyl halide electrophiles were paired wherein one halide (more substituted) works better as a single-electron electrophile and more prone to homolytic cleavage. The other halide (less substituted) works better as a two-electron electrophile and more prone to nucleophilic attack. With this substrate differentiation, electrochemical reduction will be selective for the single-electron electrophile, and RRPC occurs the carbon-centered radical reduces into an anion before undergoing nucleophilic attack upon the less substituted electrophile. Scope of single-electron electrophiles include but are not limited to: α-halo boron pinacol esters, benzyl chlorides, and allyl chlorides, propargylic chloride, α-chlorosilane. As coupling partners for these substrates, primary alky halides were often employed as the two-electron electrophile. eXEC in this case allows for high control with selective reduction of alkyl halides based on their reduction potential, allowing for cross-coupling to dominate.

Scheme 34. Electrochemically-driven XEC (eXEC) of two electronically different alkyl halides reported by Lin et al.

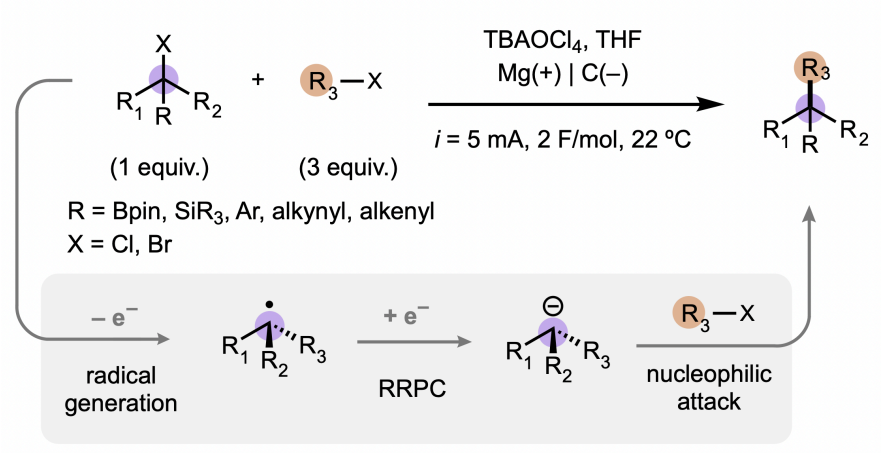

The field of XEC continues to be an exciting field of research, capable of expanding the chemical space in a manner unlike methods before. Modern strategies towards harnessing XEC include controlled reductive activation using transition-metal, electrochemical, or photochemical means to forge diverse C–C bonds.

3.1.2 | Research goals

In this chapter, a new route to the cross-electrophile coupling (XEC) of alkyl halides using potassium tert-butoxide (KO^tBu) and 1,1,3,3-tetramethyldisiloxane (TMDSO). As discussed in chapter 3.1.1, methods already exist in prior literature to harness the XEC of various electrophiles. However, the coupling of two $C(sp^3)$ electrophiles remains challenging and underexplored relative to other C–C bond forming reactions such as $C(sp^2)$–$C(sp^3)$ or $C(sp^2)$–$C(sp^2)$. Importantly, XEC by using the hydrosilane-base system allows for another route to synthesis that omits the use photochemistry, electrochemistry, and transition-metal chemistry, which were the only 3 methods reported in literature for this transformation. In using transition-metal catalysis, $C(sp^3)$–$C(sp^3)$ bond formation may be hindered by β-hydride elimination, or suboptimal conditions for oxidative addition or reductive elimination. In electrochemistry and photoredox catalysis, equipment and reagents can be costly. The hydrosilane-base system efficiently bypasses these issues as it uses cheap and accessible reagents, and require little to no set-up with a one-pot procedure. Therefore, the study of novel routes remain important and crucial in gaining access to complex molecules.

With the same motives as described in chapter 2, as the formation of $C(sp^3)$-$C(sp^3)$ bonds is fundamental for many disciplines of chemistry. Previous chapters allude that the combination of KO^tBu and TMDSO was hypothesized to initiate HAT and SET upon a participating vinylarene and

alkyl halide to afford the hydroalkylation product, where the reactive intermediates exhibit both radical and polar characteristics due to RRPC. We hypothesize that two alkyl halides with different reduction potentials can also undergo RRPC to afford XEC. In specific, one electrophile must a single-electron electrophile with capable of stabilizing radicals, and the other must be a two-electron electrophile, that can act as an S_N2 electrophile for nucleophilic attack on the anion. The goal of this project was to identify potential electrophilic coupling partners and discover a reaction scheme, optimize the transformation, expand the scope of substrates, and gather mechanistic insight on how the transformation occurs. In this way, another transformation by the TMDSO and KO^{t}Bu system can provide us with more information regarding its synthetic capabilities and further our understanding of the perplexing mechanism.

Scheme 35. Research hypothesis for the XEC of alkyl halides via TMDSO and KO^{t}Bu

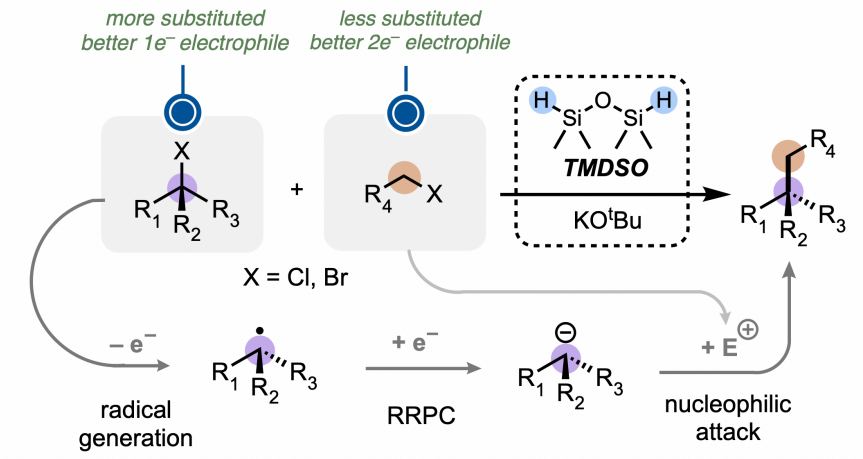

3.2: Results and Discussion

3.2.1 | Strategies

We hypothesized that with two electronically different electrophiles, one will have better stability to be reduced to the radical (single-electron electrophile) before subsequent reduction to the anion, while the other should not be reduced and would only react as an S_N2 electrophile

(two-electron electrophile). As reported in previous literature examples of XEC, matching the rates of radical generation and its addition to the second electrophile are factors that are highly important for selective cross-coupling. Therefore, it was imperative to carefully select halide pairs that were sufficiently different from each other in order to target cross-selectivity.[2.4]

From our understanding of the hydroalkylation work described in chapter 2, the combination of KO^{t}Bu and TMDSO leads to the formation of silicon complexes capable of carrying out both H-atom transfer and single electron transfer, formally conducting RRPC. With this in mind, we sought to find other reports in literature that utilizes RRPC and attempt to harness the same reactivity using the TMDSO and KO^{t}Bu reagent system.

3.2.2 | HTE campaign for XEC discovery

HTE was employed to screen for a wide array of halide combinations to identify potential halide coupling partners. Conditions for the 96-well HTE set-up is shown in **Scheme 36**. The scope of electrophilic coupling partners reported by Lin et al. in the electrochemically-driven XEC of alkyl halides provided a starting point for substrate selection. To do this, 6 substrates were chosen as 1e$^-$ electrophiles were chosen, alongside 2 substrates as 2e$^-$ electrophiles. For 1e$^-$ electrophiles, α-functionalized halides were chosen based on the ability of the functional group to stabilize a radical or anion upon cleavage of the C–X bond. These included α-halo pinacol boronate ester (Bpin) substrates (**1** and **2**), as well as different substituted benzyl chlorides (**3-6**). For the 2e$^-$ electrophiles, a primary alkyl chloride (**A**) and a primary alkyl bromide (B**)** were selected due to their ability to be S_N2 electrophiles (2e$^-$ electrophiles will also be referred to as S_N2 electrophiles). To add to the diversity of the plate, additional parameters were varied to include 2 bases (KO^{t}Bu

and KHMDS) and 4 silanes (TMDSO, $PhMe_2SiH$, $(EtO)_3SiH$, and pentamethyldisiloxane) to provide a total of 96 unique reaction combinations.

Scheme 36. HTE plate set-up for XEC discovery of electrophile coupling partners

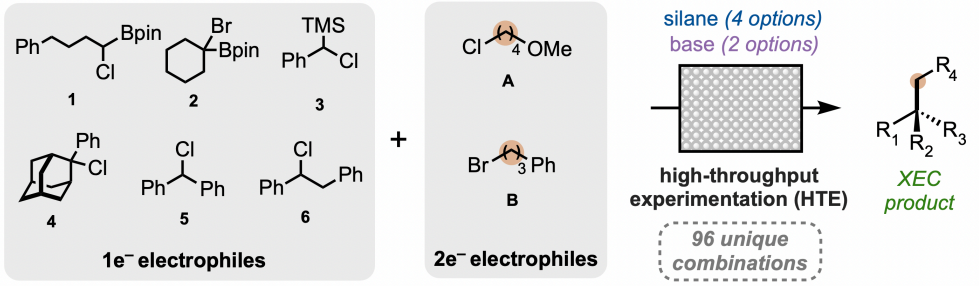

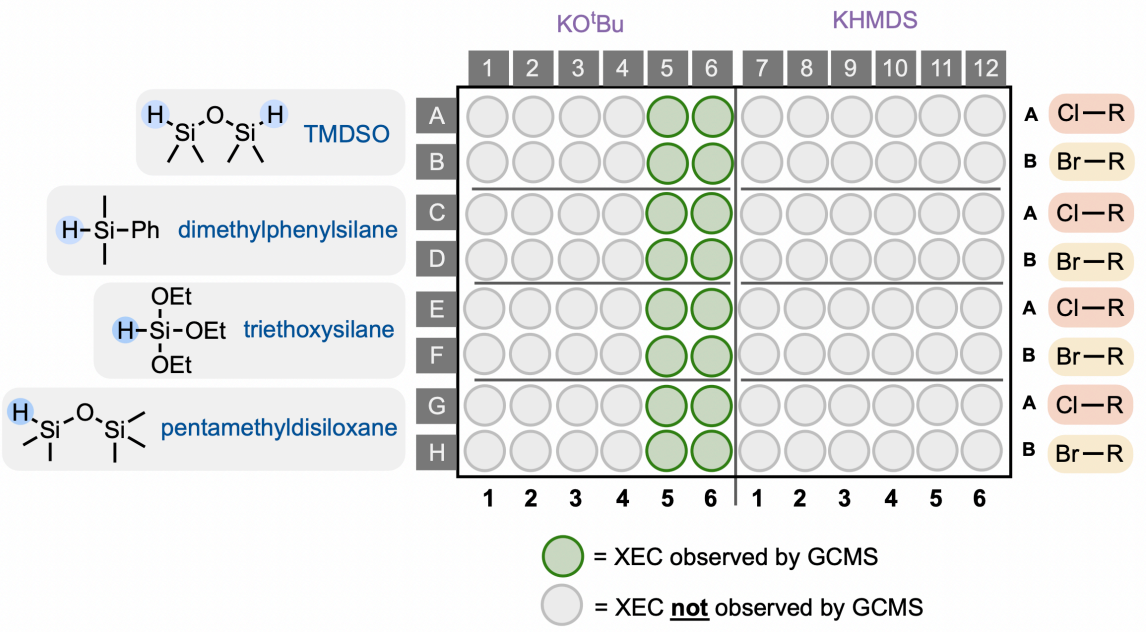

Results from this plate showed α-halo Bpin **1** and **2** did not undergo XEC, and instead decomposed to unidentified byproducts. In the hydroalkylation work, vinylarenes with boronic ester functional groups could not undergo hydroalkylation. This could allude to boronic esters not being tolerated in the harshly reductive system of TMDSO and KO^{t}Bu, resulting in a lack of reactivity for XEC. From this HTE screen, only diphenylchloromethane **5** and 1,2-diphenylchloroethane **6** were able to undergo XEC, despite there being other benzyl chlorides. Tertiary benzyl chloride **4** did not

participate in XEC, and instead resulted in a major product of phenyl adamantane, derived from reduction of the starting material. Interestingly, benzyl chloride with α-TMS group **3** was found to undergo alkylation, but with simultaneous cleavage of the TMS group. Based on these results, it was observed that only α-phenyl functionalized halides were compatible as the $1e^-$ electrophile. More importantly, substitution on the reactive carbon of the $1e^-$ electrophile also had a major influence on the success or failure of XEC, as benzyl chlorides **4** (α-adamantyl group) and **6** (α-TMS group) failed in XEC.

HTE hits were repeated on benchtop to ensure its success can be reproduced outside of the HTE environment. Of specific interest, HTE reactions A5, A6, B5, B6 were repeated in batch (**Scheme 37**). Based on these low to moderate yields, optimization of the reaction conditions needed to be done.

Scheme 37. HTE hits reproduced on benchtop

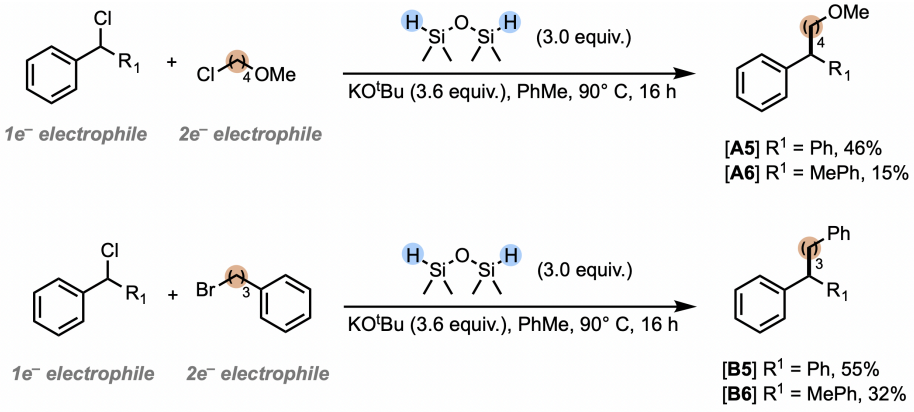

3.2.3 | Further reaction exploration and optimization

Based on the hits obtained from the HTE campaign, the combination of benzyl chloride and primary alkyl halide was a highly promising and exciting transformation to learn more about. However, the reaction conditions may be optimized to provide higher yields. To do this, the new

conditions needed to prioritize cross-coupling of the two electrophiles rather than the homocoupling of benzyl chloride. Additionally, reduction of the benzyl chloride was often observed as a side-product due to the strongly reductive conditions of TMDSO and KO^{t}Bu. These two alternate reactivity pathways provided most of the mass balance of starting material that did not participate in XEC. Therefore, optimization of reaction conditions focused on minimizing these two side-products.

As mentioned in Chapter 3.1, traditional XEC requires matching the rates of radical generation and capture of the first electrophile, as well as addition to the second electrophile. One strategy to favor cross-selectivity over homocoupling of halides is to use an excess of one reagent. Statistically, the activated species of the limiting reagent would be far more likely to encounter the other electrophile rather than itself, increasing cross-selectivity. To do this, the equivalents of the S_N2 electrophile can be in excess relative to the $1e^-$ electrophile. Furthermore, stoichiometry and ratio of base and silane could be varied to observe for improved XEC activity.

Considering yields of XEC using chloro(phenyl)(alkyl)methane (**Scheme 37**, A6 and. B6) were noticeably lower than with diaryl analogues (**Scheme 37**, A5 and B5), benzyl chlorides with one aryl stabilizing group became the main target for optimization for the goal of improving yield and minimization of homocoupling. For this, chloro(cyclohexyl)(phenyl)methane **3.1** (**Table 1**) was used as the substrate for optimization.

Numerous reactions needed to be set-up to observe the influence of changing equivalents of S_N2 electrophile (referred to as the alkyl bromide), base, and silane. To ease this process, a 24-well plate was employed to allow for parallel reactions to run. By this method, an array of differing stoichiometry loadings of alkyl halide, base, and silane can be tested. Increasing alkyl halide

equivalents from 1 to 3 had a positive effect on yield. This result aligns with the common strategy for XEC where having an excess of one electrophile over the other can promote cross-selectivity over homocoupling of electrophiles.

Table 1. Influence of increasing alkyl halide, base, and silane equivalents and ratios*

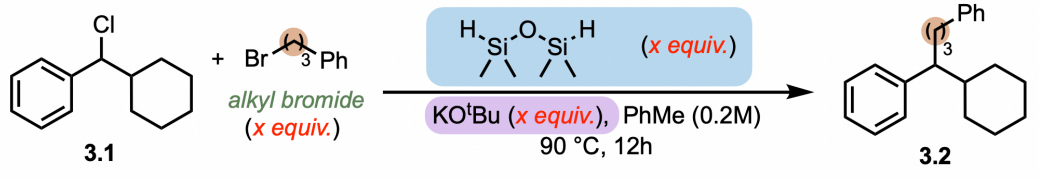

	Alkyl bromide (1 equiv)			Alkyl bromide (2 equiv)					Alkyl bromide (3 equiv)	
Base / Silane	1 equiv	2 equiv	3 equiv	1 equiv	2 equiv	3 equiv	4 equiv	5 equiv	4 equiv	5 equiv
1 equiv	<5	<5	<5	<5	<5	<5				
2 equiv	<5	<5	7	<5	6	10				
3 equiv	<5	<5	7	<5	<5	9				
4 equiv							26	24	22	**33**
5 equiv							25		23	

* NMR yields

Additionally, increasing equivalents of both base and silane proved to be beneficial for reactivity. In particular, using 2 equivalents of alkyl bromide, the increase from 3:3 equivalents of base:silane to 4:4 showed a dramatic increase in yield from 7% to 26%. Secondly, the ratio of base:silane was improved when the base was in excess relative to the silane, wherein a ratio of 5:4 base:silane resulted in 33% yield in the presence of 3 equivalents of alkyl bromide. The increase in reactivity with increasing equivalents of base and silane suggest that both of the components are key for generating the active nucleophilic species. Having the base in excess relative to the silane may be beneficial to drive the silane activation step. Ultimately,

stoichiometry of 3 equivalents alkyl halide, 5 equivalents of base, and 4 equivalents of silane were kept for next reactions.

Next, reaction parameters such as selection of base, silane, solvent, time, and temperature were tested. Based on the hydroalkylation work, it was observed that mainly ethereal or aromatic solvents were compatible with the TMDSO and KO^{t}Bu system. To screen for solvents that can influence the yield for XEC, a selection of ethereal and aromatic solvents were tested (**Table 2**). In Chapter 2, toluene was ultimately chosen as the best solvent for optimized hydroalkylation yield. In the case of XEC, toluene resulted in approximately double of the homocoupling product compared to the XEC product. Interestingly, dioxane showed the opposite result, favoring XEC while minimizing the amount of homocoupling.

Table 2. Screening of solvents and concentration

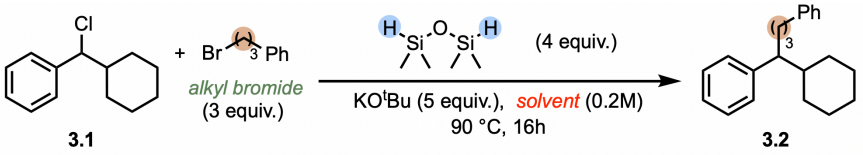

Entry	Change to conditions	%A
1	toluene	33
2	**dioxane**	**40**
3	dioxane:PhMe 1:1	28
4	dioxane, 1 M	31
5	THF	31
6	2-MeTHF	35
7	CPME	26
8	dibutyl ether	23
9	m-xylene	24
10	PhF	35

11	neat	24

The selection of bases were varied to include other *tert*-butoxides, other potassium bases, and no base as control (**Table 3**). Based on the results, it appeared that potassium as a counterion remained imperative for reactivity, which is consistent with all other prior work with the TMDSO and KO^tBu reagent pair as well as other hydrosilane-base systems. This alludes to the importance of potassium ion size and coordination behavior for the reaction to be successful. No other *tert*-butoxide bases, such as NaO^tBu or AlO^tBu, could harness the same reactivity as KO^tBu. Sodium and aluminium cations differ significantly in Lewis acidity and ion-pairing strength, which could have prevented the formation of the reactive silane species. In addition to this, when KO^tBu is combined with 18-c-6, no reactivity was observed, further highlighting the importance of potassium as the counterion. Other potassium bases, including KOAc, KOPh, KOTf, K_2CO_3, KF, KOEt, KHMDS were tested.

From these potassium bases, only KHMDS and KOEt were able to yield XEC product, with KOEt showing improved yields compared to KO^tBu. These observations further highlight that not only the counterion choice was important, but base identity influences reactivity. These unsuccessful potassium salts may have lacked sufficient basicity or appropriate nucleophilicity to activate the hydrosilane, while stronger and more alkoxide-like bases such as KHMDS and KOEt are much more effective for reactivity. Lastly, omitting a Lewis-base altogether showed no reactivity, confirming the fact that the hydrosilane requires a base for XEC to proceed. From the screening of various bases, KOEt was selected as the best base for XEC.

Table 3. Screening of various bases

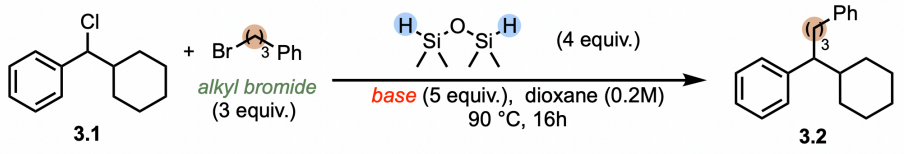

Entry	Base	%A
1	KO^{t}Bu	33
2	NaO^{t}Bu	0
3	AlO^{t}Bu	0
4	KO^{t}Bu + 18-c-6	0
5	KOAc	0
6	KOPh	0
7	KOTf	0
8	K_2CO_3	0
9	KF	0
10	KOH	0
11	**KOEt**	**40**
12	KHMDS	24
13	LiHMDS	0
14	NaHMDS	0
15	no base	0

A variety of silanes were tested to screen for options that may provide better XEC yields than TMDSO. Included in this screen were a wide variety of siloxanes (**Table 4, 1-6**). HMDSO (**Table 4, 4**) provides a unique example as it lacks a Si–H bond, and its success or failure in conducting XEC may indicate the necessity of an H-atom or hydride for the reaction. Phenyl silanes (**Table 4, 7-9**) are also included as they have weak Si–H bonds and used as often reducing agents in other reactions. Lastly, alkyl silanes were also included (**10-11**).

Table 4. Screening of various silanes

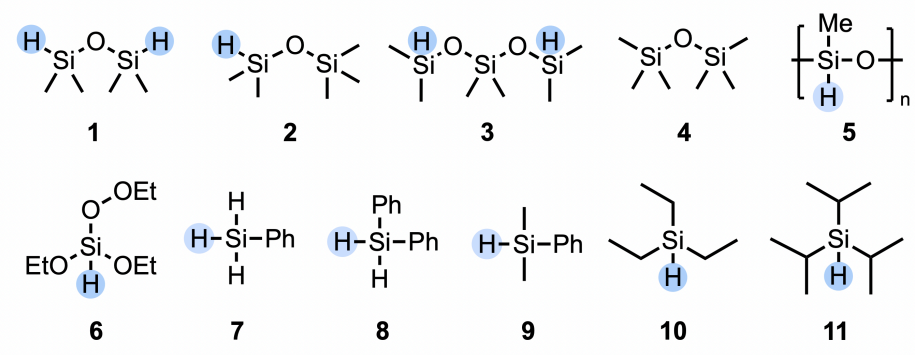

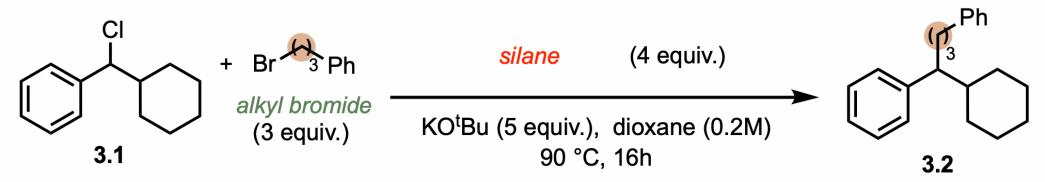

Entry	Silane	%A
1	**TMDSO**	**33**
2	pentamethyldisiloxane	18
3	hexamethyltrisiloxane	27
4	hexamethyldisiloxane (HMDSO)	0
5	PMHS	21
6	triethoxysilane	12
7	phenylsilane	35
8	diphenylsilane	23
9	dimethylphenylsilane	17
10	triethylsilane	0
11	triisopropylsilane	0
12	no silane	0

Of the silanes tested, siloxanes **1**, **2**, **3**, **5**, and **6** were effective in facilitating XEC. HMDSO (entry **6**) did not lead to XEC, confirming that activation of the Si–H bond is necessary for XEC to proceed. Alkyl silanes (entries **10** and **11**) were not effective for XEC. Et_3SiH (entry **10**), of which combined

with KO^tBu forms the Grubbs-Stoltz reagent system, showed to be ineffective at XEC. This indicates that the XEC of alkyl halides via the TMDSO and KO^tBu system offers complementary reactivity to that of the Grubbs-Stoltz system, and cannot be done using Et_3SiH as the silane. Although hexamethyltrisiloxane (entry **3**) was able to produce a higher yield, TMDSO was kept as the preferred silane due to its much cheaper cost.

Same as with the hydroalkylation work, all reactions were run in 1-dram vials. When TMDSO is added to a vial containing solvent and KO^tBu, the solution bubbles rapidly and vigorously. Considering this pressure build-up, one option to observe for a change in yield could be changing the reaction vessel to allow for more headspace to change the pressure in the tube. Upon switching the 1-dram vial out to an 8 mL reaction tube, no major change in yield was detected. Furthermore, varying time or temperature did not majorly influence yield. As a result, these three parameters–reaction vessel, temperature and time–were kept the consistent for the next steps in optimization.

Different combinations of the best bases, silanes, and solvents were carried out via 24-well plate (**Scheme 38**). In this way, each parameter is optimized within its own category, as well as coupled with other parameters. Best results from this plate showed a ceiling yield of ~48-50% (wells A2 and A6), where dioxane was consistent as the best solvent, both TMDSO, phenyl silane, and hexamethyltrisiloxane were the best silanes, and KOEt as the best overall base. The final optimized conditions are shown in **Scheme 39**, where these conditions were used for scope expansion discussed in the next section.

Scheme 38. 24-well plate for optimization of base, silane, and solvent (NMR yields)

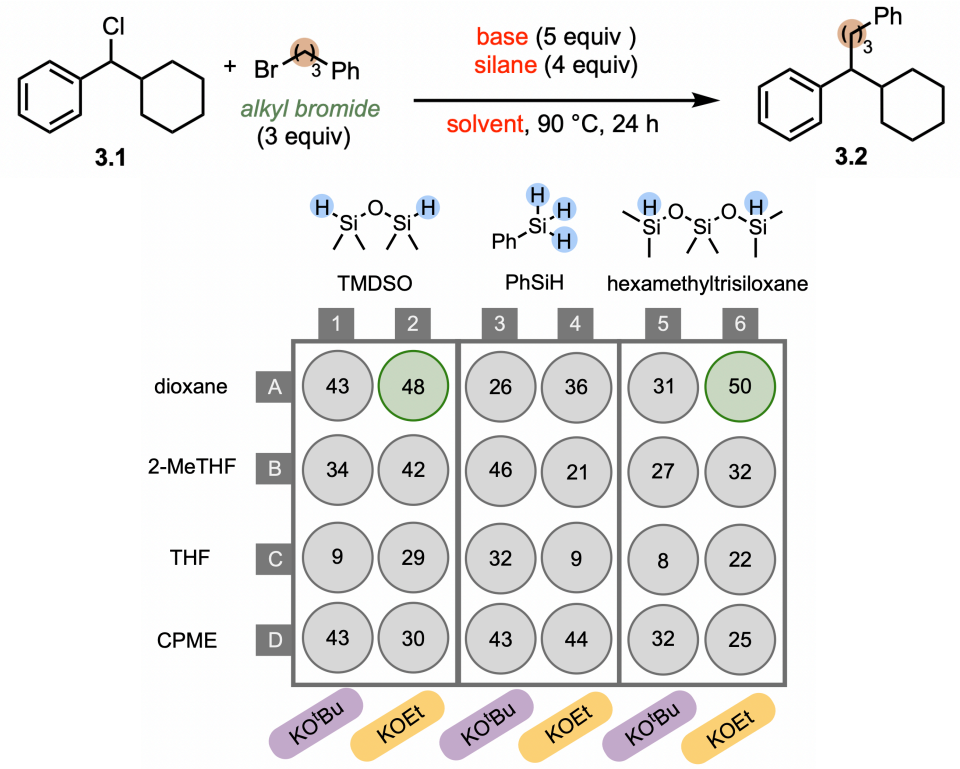

Scheme 39. Final optimized conditions for scope study

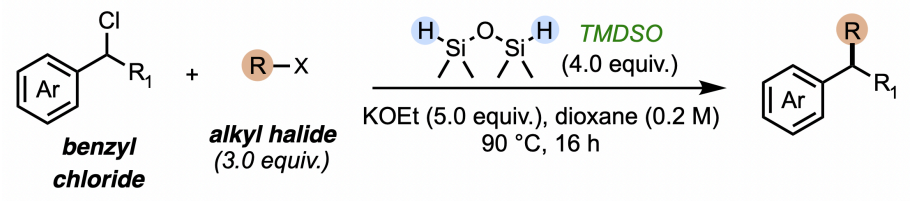

3.2.4 | Scope

The rigorous optimization campaign successfully improved yields of benzyl chlorides with one aryl stabilizing group. Following this, a scope of benzyl chlorides were created with these new conditions to ensure reactivity was not exclusive to the optimization substrates. Benzyl chlorides in scope included a number of diaryl methyl chlorides and benzyl chlorides with one aryl stabilizing group.

Four entries of diaryl methyl chloride scope examples are shown in **Scheme 40**. XEC was achieved with diphenyl methyl chloride an alkyl bromide (entry **3.3**) with 63%. When the phenyl groups

were *p*-fluoro substituted (entry **3.4**), reactivity was maintained and yields were not affected. The main side product of these scope examples were identified by NMR and GC-MS to be the reduced benzyl chloride and homocoupling of the benzyl chloride. In an interesting example, entry **3.6** observed XEC with a pyridine substituted benzyl chloride. In this example, dialkylation of the benzyl chloride was seen, leading to the hampered yield. This product may be derived from **3.6** undergoing a deprotonation facilitated by TMDSO and KOEt, and excess alkyl halide leads to a second alkylation event. Overall, additional scope examples with various functional group substitutions on the phenyl groups or other heterocycles will be needed to identify their tolerance and any reactivity patterns.

Scheme 40. Scope of XEC with chloro(diaryl)methanes as 1e⁻ electrophile

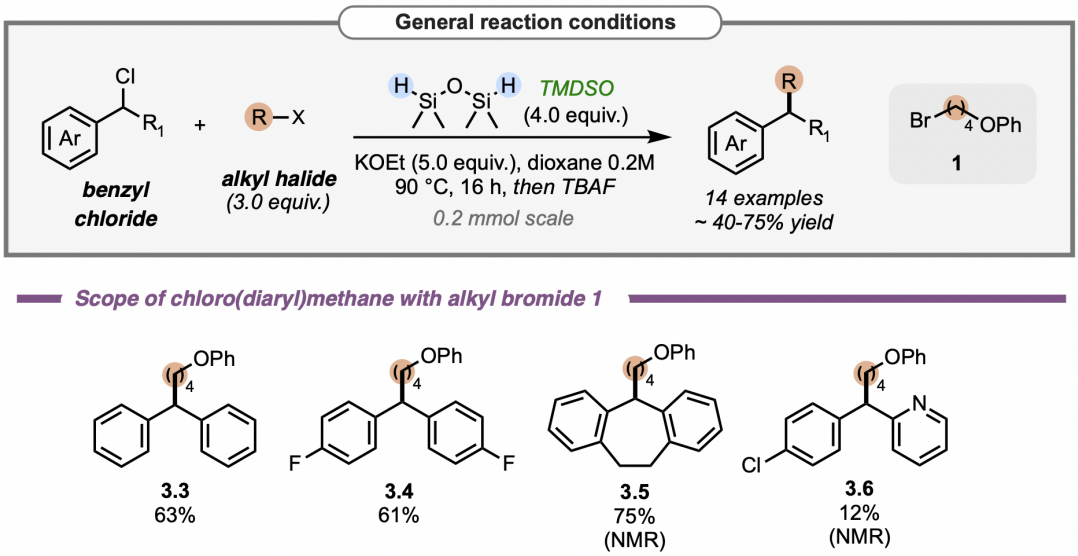

Aside from chloro(cyclohexyl)(phenyl)methane, other monoaryl methyl chlorides were successful in XEC, where most in scope were chloro(aryl)(alkyl)methanes (secondary benzyl chlorides) (**Scheme 41**). Despite optimization attempts, these examples have lowered yields compared to that of the diaryl analogues. Chloro(cyclohexyl)(phenyl)methane (entry **3.7**) was

observed to undergo XEC with an alkyl bromide with 61% yield, while other secondary benzyl chlorides entries **3.8** and **3.9** had yields of 39% and 45% respectively. Interestingly, primary benzyl chloride **3.10** was seen to undergo XEC, although in trace yields and detected qualitatively by GC-MS. Similar to their diaryl analogues, major side products of these secondary and primary benzyl chlorides were reduced benzyl chloride and homocoupling of the benzyl chloride, though to a greater extent. With the primary benzyl chloride example (entry **3.10**), most of the mass balance was observed to be the homocoupling of the benzyl chloride, suggesting rapid dimerization of the reactive benzylic intermediate facilitated by the lack of steric hindrance for C–Cl cleavage.

Scheme 41. Scope of XEC with chloro(aryl)methanes as 1e⁻ electrophile

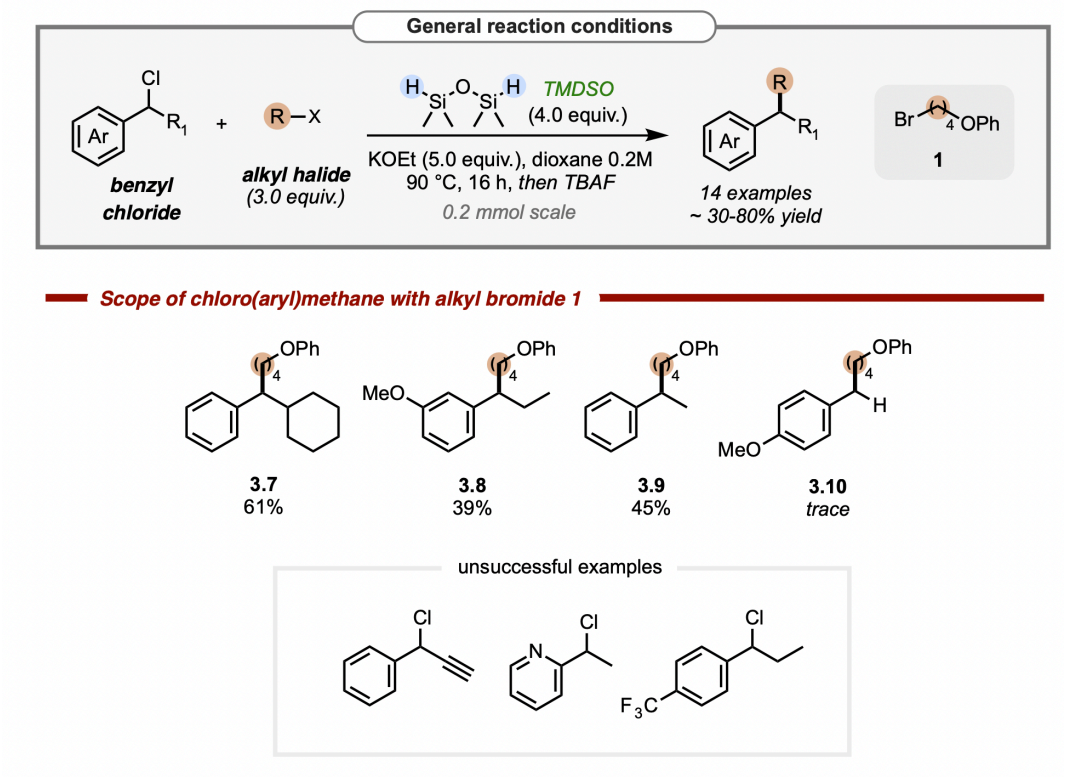

Failed substrates included para-substituted CF_3 chloro(aryl)(propyl)methane, α-pyridine, and α-alkyne benzyl chloride. This may be due to their reducibility in the harsh conditions provided by

TMDSO and KOEt. Furthermore, these functional groups may contribute to the destabilization of any reactive benzyl radical or anionic intermediates and hamper C–Cl activation.

Lastly, a scope of alkyl halides as S_N2 partners with diphenyl methyl chloride was also compiled (**Scheme 42**). Diphenyl methyl chloride was able to undergo XEC with both alkyl bromide and chlorides. However, entry **3.14** showed that yield was slightly higher with the alkyl bromide compared to that of the alkyl chloride. This can allude to S_N2 reactivity, where the alkyl bromide is a better electrophile due to having a better leaving group (Br^-) compared to the alkyl chloride (Cl^-).

Scheme 42. Scope of XEC with diphenylchloromethane as $1e^-$ electrophile

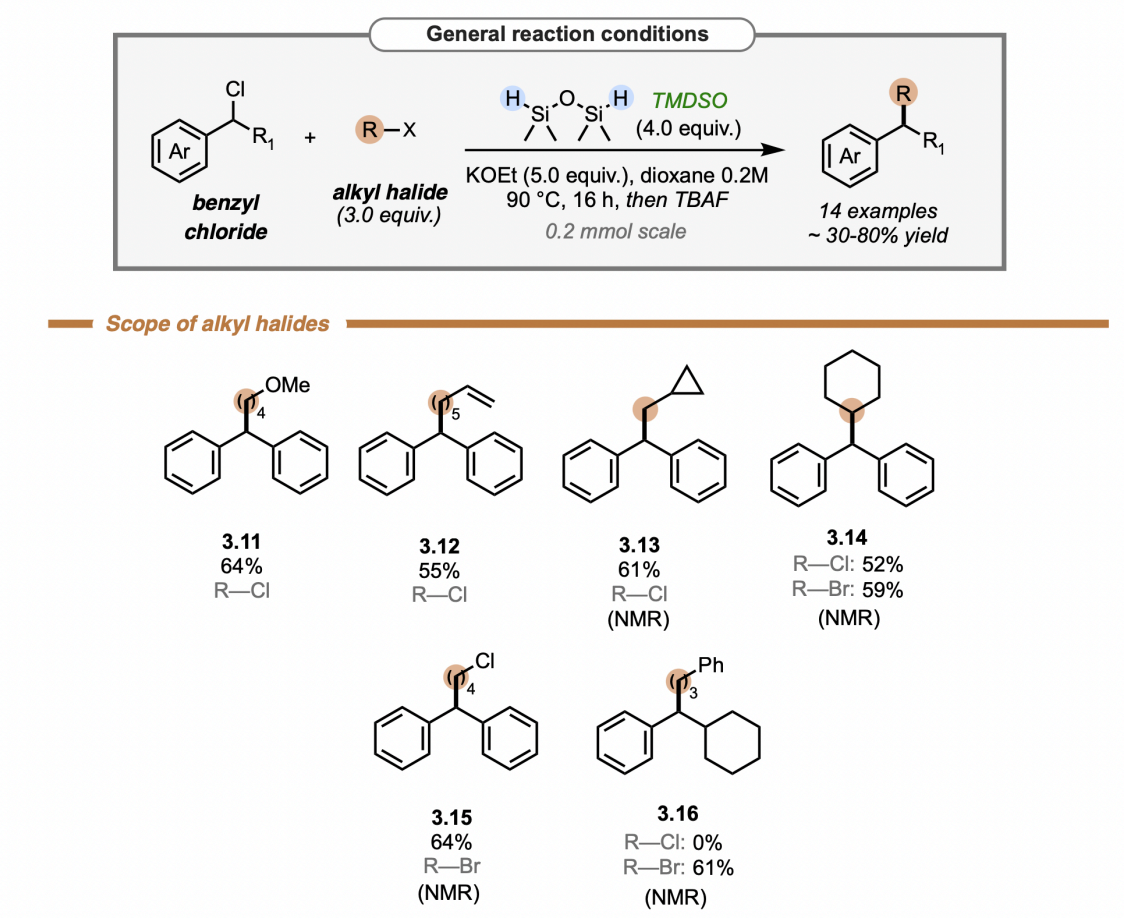

Additionally, entry **3.15** showed that XEC with 1-chloro-4-bromo butane as the S_N2 electrophile preferentially occurred with the alkyl bromide instead of the alkyl chloride with 64% yield. A minor side product observed by GC-MS was identified to be the product of alkylation with the alkyl chloride, but lacking the alkyl bromide moiety, suggesting that the harshly reductive conditions with TMDSO and KOEt may have dehalogenated the product. This scope example further highlights that although both alkyl bromide and chloride are compatible for XEC reactivity, the preference of reactivity lies with alkyl bromide instead of alkyl chloride. However, and important distinction was noted where in contrast to their diaryl counterparts, chloro(aryl)(alkyl)methane **3.16** can only undergo XEC with alkyl bromide as the S_N2 partners, with the reaction failing to proceed if the S_N2 electrophile was an alkyl chloride.

Similar to the hydroalkylation work, isolation in this study was also difficult due to the presence of silicon oligomers, which tend to co-elute with the desired product. These impurities were hard to eliminate, likely due to their varying lengths and insolubility in hexanes. In order to remove these silane derived byproducts, tetrabutylammonium fluoride (TBAF) was added to the mixture and stirred for an additional 2 hours. With this change, silicon-containing byproducts could be eliminated from the mixture. This scope study showed a number of successful examples of XEC between benzyl chloride and alkyl halide. Selected examples were isolated for characterization by ^{1}H NMR and ^{13}C NMR (**Appendix B**).

3.2.5 | Mechanistic investigations

The discovery an RRPC pathway to the hydroalkylation of vinylarenes described in Chapter 2 prompted a search for other transformations that can be done with the TMDSO and KO^{t}Bu reagent system. It was hypothesized that other reactions reported in literature to undergo RRPC

may be replicated in the TMDSO and KO^{t}Bu system. Through multiple discovery campaigns, the XEC of benzyl chloride and alkyl halide was found. This transformation was reported by Lin et al. where the cross-coupling was electrochemically driven. Through controlled electron transfer events, the 1e$^-$ electrophile could be selectively reduced to carbon-centered radical, followed by a second electron transfer event to form a carbanion. In the presence of an S_N2 electrophile, nucleophilic attack can occur, yielding the XEC product. Despite the overall transformation to be identical, further mechanistic studies on the XEC of alkyl halides by TMDSO and KOEt needed to be done to verify if the RRPC pathway is the key to this transformation.

Mechanistic probes were synthesized in order to detect for radical or anion character on the benzylic carbon. To test for benzylic anion character, diphenylchloromethane was charged with bromomethyl cyclopropane (**Scheme 43**). If the reactive intermediate involves a benzylic anion, alkylation with bromomethylcyclopropane should proceed via S_N2 and no ring-opening of the cyclopropane should be seen in the final XEC product structure. On the other hand, if the reactive intermediate involves a benzyl carbon-centered radical, a possible outcome can be alkylation with bromomethylcyclopropane through radical recombination. This method would require homolytic cleavage of the C–X bond with the alkyl halide to leave a primary radical, which lead to the ring-opening of the cyclopropane to release strain. The resulting radical would then recombine with the benzyl radical to yield a XEC product the cyclopropane is not retained.

Running this probe resulted in the retention of the cyclopropane, which supports the claim that the reactive benzylic carbon was less likely to be a carbon-centered radical and had more anionic character that could conduct alkylation in the presence of an alkyl bromide via S_N2.

Scheme 43. Benzyl anion probe with bromomethylcyclopropane

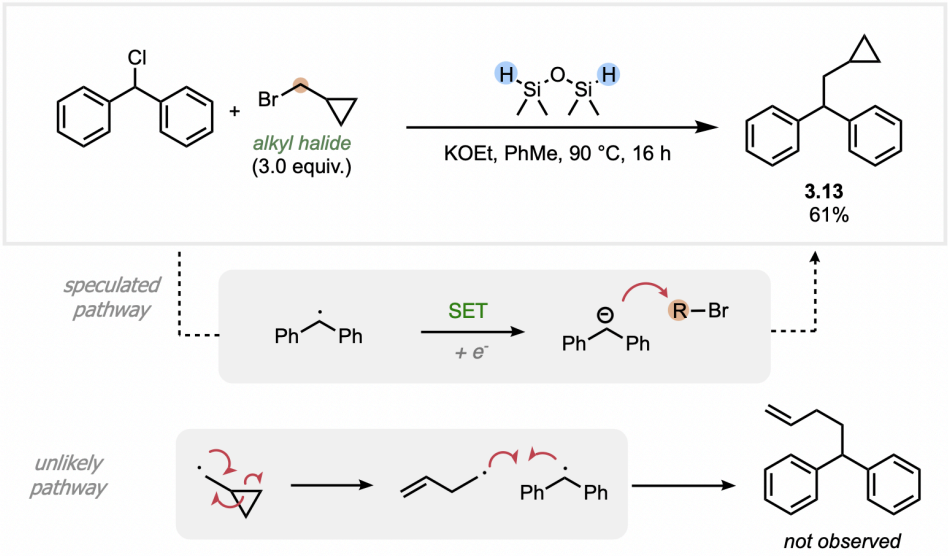

Homocoupling of benzyl chloride was described as a recurring issue during optimization as it hampered yields, so efforts were placed to minimizing this side reaction. The lack of cross-coupling of the benzyl chloride can be due to a number of hypothesized reasons. The prevalence of homocoupling in mono aryl benzyl chlorides (primary and secondary benzyl chloride) appeared higher than in diaryl benzyl chlorides. This may indicate that with each additional phenyl group connected to the benzylic carbon, it increases the extent of resonance as it allows for greater delocalization of the unpaired electron across more π-orbitals. However, with adamantyl benzyl chloride (from HTE plate), the main product of the reaction was its reduction to phenyladamantane. This may be due to steric hindrance from the adamantyl group, which can make alkylation difficult. Additional probes to test for radical character on the benzyl nucleophile have not yet been done.

With prior knowledge of RRPC activity in previous work, mechanistic hypotheses can still be made on the RRPC-mediation of XEC. Prior literature records the presence of silyl radicals in situ with

the combination of hydrosilane and base. These silyl radicals are reported to conduct XAT.[3] In one hypothesis, XAT can conduct C–Cl cleavage to yield a benzyl radical. Following this, as precedence of HAT and SET by TMDSO and KO^{t}Bu is established, two routes can occur: SET to afford the benzyl anion via RRPC subsequent alkylation, or HAT to lead to the reduced starting material (**Scheme 44**)

Scheme 44. Hypothesis for the XEC of alkyl halides by hydrosilane and base by XAT

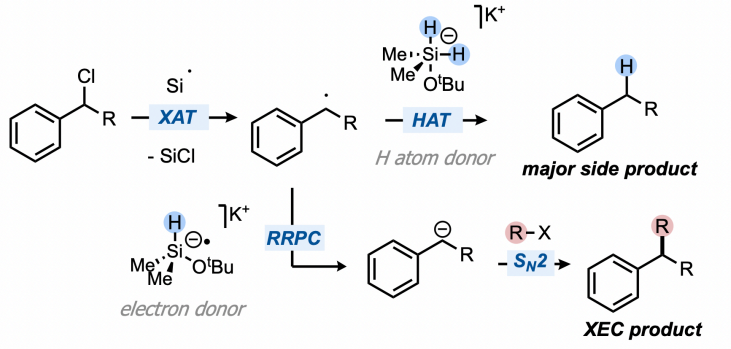

In a second hypothesis, an alternate reactive pathway may be derived from SET by the silicon electron donor complex towards the benzyl chloride, forming a radical anion.[7] This would then lead to fragmentation of the complex, resulting in a benzyl radical and chloride ion. From this point, the benzyl radical can proceed via HAT to afford the reduced starting material, or RRPC to afford a carbanion for subsequent alkylation (**Scheme 45**).

Scheme 45. Hypothesis for the XEC of alkyl halides by hydrosilane and base by benzyl radical anion

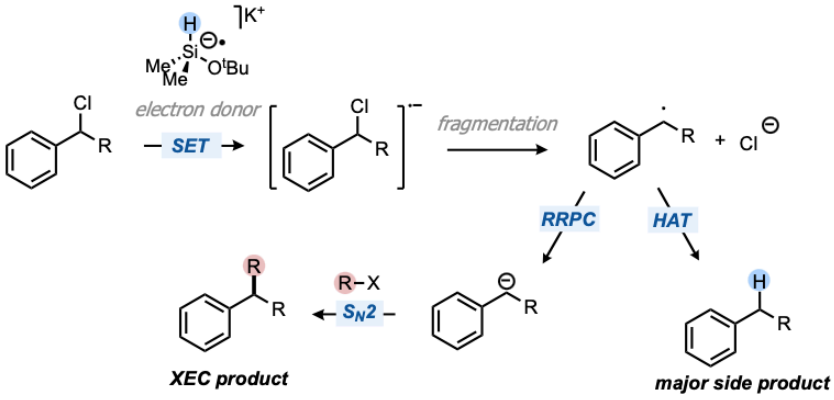

3.3: Summary and future work

In summary, a novel route to the cross-electrophile coupling of benzyl chloride with alkyl bromide and chloride via potassium alkoxide base and TMDSO was achieved. While KO^{t}Bu proved to be the base of choice of previous work in this field, KOEt proved to be the better base for supplying higher yield XEC. In chapter 2, this unusual combination of reagents was hypothesized to form a hypervalent silicon complex, facilitating the hydroalkylation of vinylarenes by initiating HAT subsequent SET to the radical enables RRPC.

While the mechanism for XEC is still speculated, anionic character of the benzylic carbon can already be argued, with further studies needing to be done to verify radical character. Experiments showed a scope where diaryl benzyl chlorides can participate in XEC better than their monoaryl counterparts. Overall, this study provides an introduction into the transition metal-, photochemical-, and electrochemical-free XEC of alkyl halides, with success in the hard-to-achieve C(sp^3)–C(sp^3) bond formation.

Additionally, the scope of functional group tolerance can be further explored. Selectivity is extremely dependent on matching the rates of activation of both coupling partners, meaning that coupling electrophiles of very different reactivity can prove to be difficult (such as Ar–Cl with alkyl-I). Other categories or combinations of electrophiles could be tested for XEC reactivity, which can include electrophiles with similar reducibility and stability as benzyl chloride.

.

3.4: References

(1) Hassan, J.; Sévignon, M.; Gozzi, C.; Schulz, E.; Lemaire, M. Aryl−Aryl Bond Formation One Century after the Discovery of the Ullmann Reaction. *Chem. Rev.* **2002**, *102*, 1359–1470.

(2) Everson, D. A.; Weix, D. J. Cross-Electrophile Coupling: Principles of Reactivity and Selectivity. *J. Org. Chem.* **2014**, *79*, 4793–4798.

(3) Zhang, P.; Le, C. "Chip"; MacMillan, D. W. C. Silyl Radical Activation of Alkyl Halides in Metallaphotoredox Catalysis: A Unique Pathway for Cross-Electrophile Coupling. *J. Am. Chem. Soc.* **2016**, *138*, 8084–8087. https://doi.org/10.1021/jacs.6b04818.

(4) Zhang, W.; Lu, L.; Zhang, W.; Wang, Y.; Ware, S. D.; Mondragon, J.; Rein, J.; Strotman, N.; Lehnherr, D.; See, K. A.; Lin, S. Electrochemically Driven Cross-Electrophile Coupling of Alkyl Halides. *Nature* **2022**, *604*, 292–297.

(5) Lu, L.; Wang, Y.; Zhang, W.; Zhang, W.; See, K. A.; Lin, S. Three-Component Cross-Electrophile Coupling: Regioselective Electrochemical Dialkylation of Alkenes. J. Am. Chem. Soc. **2023**, 145, 22298–22304.

(6) Smith, A. J.; Young, A.; Rohrbach, S.; O'Connor, E. F.; Allison, M.; Wang, H.-S.; Poole, D. L.; Tuttle, T.; Murphy, J. A. Electron-Transfer and Hydride-Transfer Pathways in the Stoltz–Grubbs Reducing System (KO^tBu/Et_3SiH). *Angew. Chemie Int. Ed.* **2017**, *56*, 13747–13751.

(7) Fontanesi, C.; Baraldi, P.; Marcaccio, M. On the Dissociation Dynamics of the Benzyl Chloride Radical Anion. An Ab Initio Dynamic Reaction Coordinate Analysis Study. *J. Mol. Struct. THEOCHEM* **2001**, *548* (1), 13–20.

Chapter 4: CONCLUSION

In this work, two new routes of synthesis using the reagent combination TMDSO and KO^{t}Bu were discovered and developed. In chapter 2, the hydroalkylation of vinyl arenes was reported. Through mechanistic hypotheses and investigations, reductive radical-polar crossover was deemed as a potential pathway for hydroalkylation. This work is now published in *Angewandte Chemie International Edition* **2025**, *64* (10), e202421077. Following this discovery, another transformation facilitated by the TMDSO and KO^{t}Bu reagent system was found. In chapter 3, the cross-electrophile coupling of benzyl chloride and alkyl halides was discussed.

The identification of these two reactions add to the perplexing and underexplored field of base-activated hydrosilane mediated reactions. With simple reagents such KO^{t}Bu, a common base, and TMDSO, often used as a reducing agent, these materials are inexpensive and accessible. Further work in this field may continue to discover other transformations that can be done using this reagent system and can give better insight to how the activation of the base and silane is able to facilitate diverse reactions.

Chapter 5: EXPERIMENTAL INFORMATION

5.1: Experimental Conditions

5.1.1 | General Considerations

General Experimental Conditions:

All reactions were set up inside the glove-box, or outside of the glove-box under a N_2 atmosphere using balloons and oven-dried glassware and stir-bars. Column chromatography was done either manually or using Combi-flash R_f automated chromatography both using Silicycle F60 40-63 µm silica gel. Thin- layer chromatography (TLC) was performed using aluminum-backed EMD Millipore Silica Gel 60 F254 pre-coated plates, and a UV lamp was used to visualize TLC plates.

Instrumentation:

GCMS data was collected using an Agilent Technologies 7890B GC with a 30 m x 0.25 mm HP-5 column. ^{1}H and ^{13}C NMRs were obtained using a Bruker Avance II 500 MHz spectrometer, a Bruker Avance II 400 MHz spectrometer, a Bruker Avance II 300 MHz spectrometer, or Bruker Avance I 300 MHz spectrometer. ^{1}H NMR yields were calculated using either 1,3,5-trimethoxybenzene or 1,2,4,5-tetramethylbenzene as an internal standard. ^{1}H NMR spectra were calibrated using $CDCl_3$ (7.26 ppm), and ^{13}C NMR spectra were calibrated using $CDCl_3$ (77.16 ppm). Reported NMR data is as follows: chemical shift (δ ppm), multiplicity (where s = singlet, d = doublet, t = triplet, q = quartet, quin = quintet, sext = sextet, m = multiplet), coupling constants in Hz (where applicable), and relative proton integration.

Materials:

Organic solvents were degassed using nitrogen and were then filtered through a PureSolv solvent purification system (SPS) to maintain dryness. Unless stated otherwise, all starting materials were purchased from Combi-blocks and used as received. Alkyl halides 2-(4-chlorobutyl)-2-methyl-1,3-

dioxolane, 1-(4-chlorobutyl)-1H-indole, 1-(4-bromobutyl)-1H-indole, N-(4-bromobutyl)phthalimide, 5-Ethenyl-1,3-benzodioxole, (4-Chlorobutoxy)(1,1-dimethylethyl)dimethylsilane were synthesized according to literature reported protocols.

5.1.2 | Procedure for high-throughput experimentation (HTE)

96 well-plate preparation: All 96 well-plates were run in an aluminum block assembly (Analytical Sales and Services, cat. no. 96973). Glass inserts (8 × 40-mm, 1.2-mL vials; Chemglass Life Sciences, cat. no. CV-2103-0840) were loaded into the wells with a pair of clean tweezers. Micro stir bars (Parylene-coated micro stir bars, VP Scientific, cat. no. VP 712-1) were dispensed into the 96-well plates using a stir bar dispenser (VP Scientific, cat. no. VP-711A-1S/D).

Heating the plates: Plates were sealed by placing a PFA sheet (Analytical Sales and Services, cat. no. 96967) and two rubber gaskets (Analytical Sales and Services, cat. no. 96965) on top of the aluminum block followed by screwing in the plate lid with 1.5" stainless steel screws.

24-well plate in Chapter 2

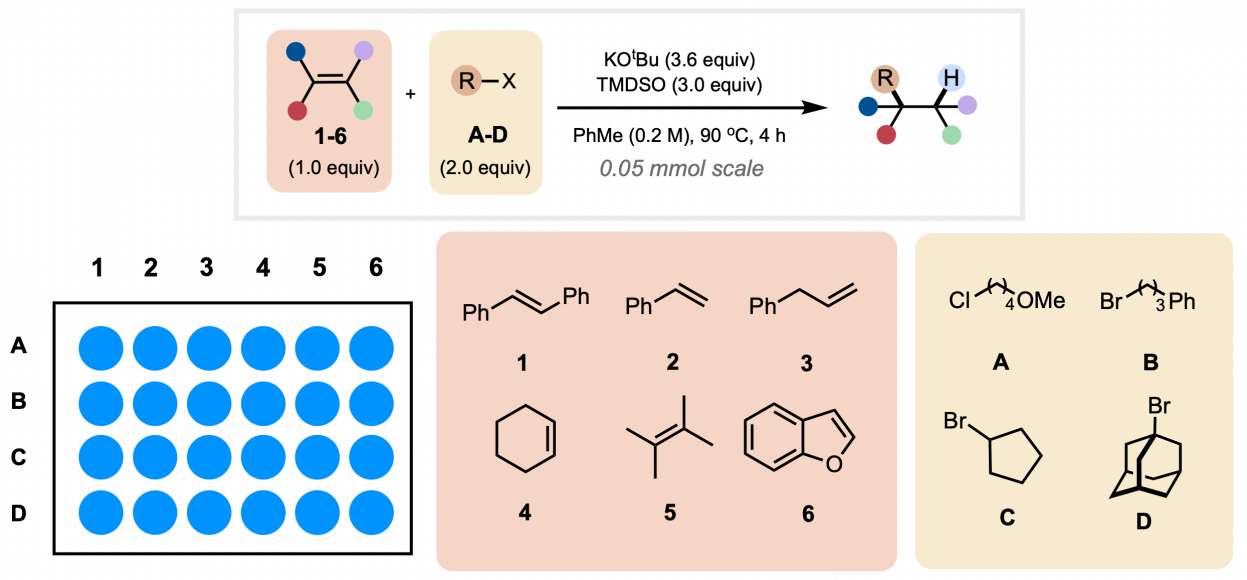

The high-throughput experiment was done under nitrogen atmosphere in 1.2 mL 8 x 40 mm glass vials enclosed within an aluminum 96-well plate. In the glove box, 0.18mmol of KO^tBu was added to 24 vials (4 rows x 6 columns). Stock solutions were made for the alkene substrates (0.05mmol) and alkyl halides (0.1mmol). Each alkene stock solution **1-6** was loaded into its respective column, and TMDSO (0.15mmol) was added to all vials. Then, each row was charged with its corresponding alkyl halide **A-D**. The plate was then taken out of the glove box and heated on a Heidolph magnetic stirrer/hotplate at 90^oC for 4 hours. All vials were quenched with EtOAc, and filtration was conducted manually by passing 15 µL aliquots of each reaction mixture through a short plug of Silicycle F60 40-63 µm silica gel, filtering into a second 96-well plate. For qualitative GCMS analysis, each vial was charged with 0.2M 1,3,5-trimethoxybenzene as internal standard. The peak corresponding to the target product was integrated relative to the internal standard, and the ratio of target product to internal standard was obtained.

96-well plate in Chapter 3

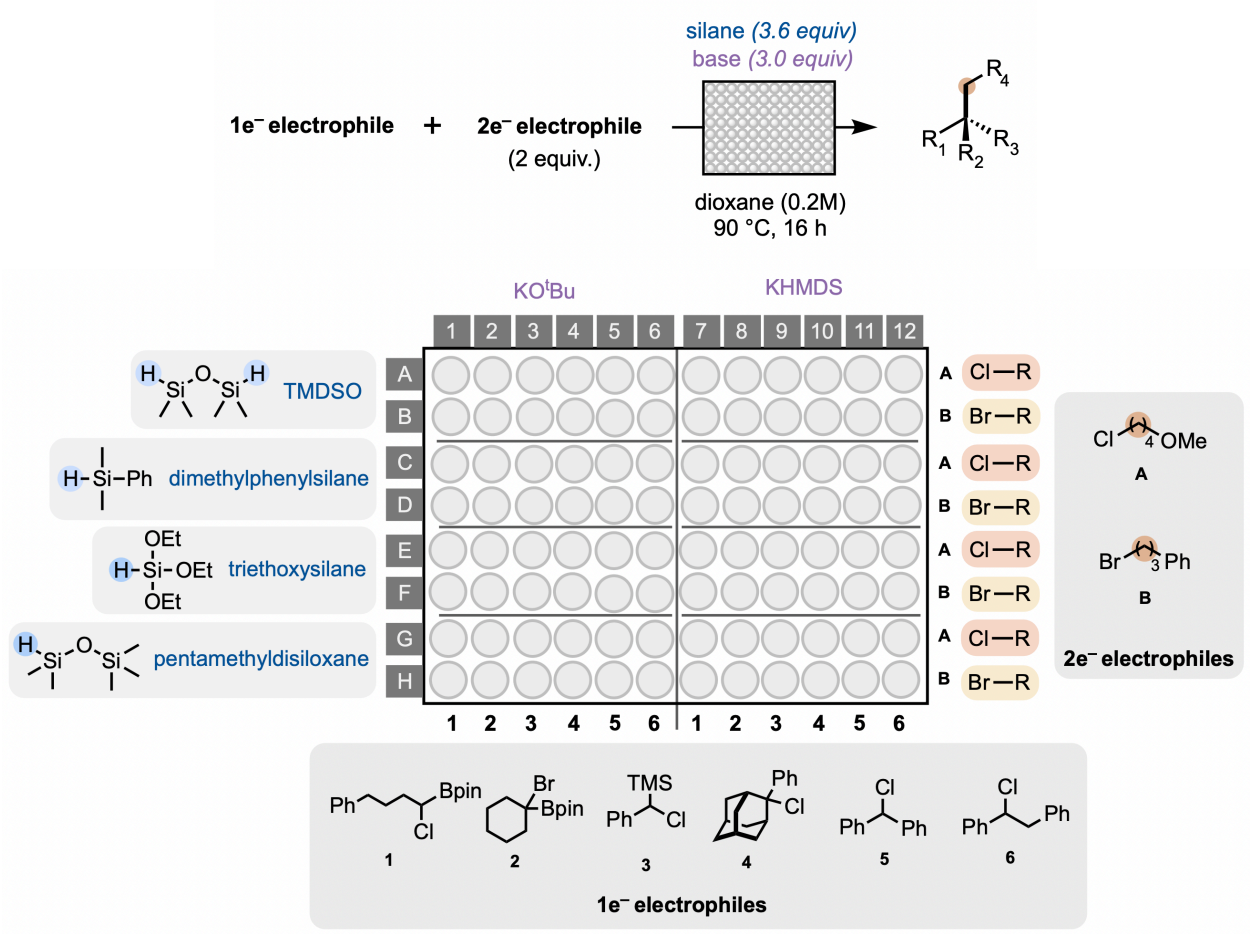

The high-throughput experiment was done under nitrogen atmosphere in 1.2 mL 8 x 40 mm glass vials enclosed within an aluminum 96-well plate. In the glove box, base (3.0 equiv) was added to the columns according to the figure above, where KO^{t}Bu was added to column 1-6 and KHMDS was added to columns 7-12. Stock solutions were made for each 1e$^-$ electrophile **1-6** (0.05mmol) and 2e$^-$ electrophiles **A** and **B** (0.1mmol). Stock solutions for each 1e$^-$ electrophile **1-6** were loaded into its respective column depicted in the figure. Then, stock solutions of alkyl halide **A** was added to rows A, C, E, G, and alkyl halide **B** was added to rows B, D, F, H. Lastly, the 4 silanes (3 equiv) were added to each vial according to the figure above. The plate was screwed closed with the lid and taken out of the glove box and heated on a Heidolph magnetic stirrer/hotplate at 90^{o}C for

16 hours. All vials were quenched with EtOAc, and filtration was conducted manually by passing 15 µL aliquots of each reaction mixture through a short plug of Silicycle F60 40-63 µm silica gel, filtering into a second 96-well plate. For qualitative GCMS analysis, each vial was charged with 0.2M 1,3,5-trimethoxybenzene as internal standard. The peak corresponding to the target product was integrated relative to the internal standard, and the ratio of target product to internal standard was obtained.

<u>24-well plate in Chapter 3</u>

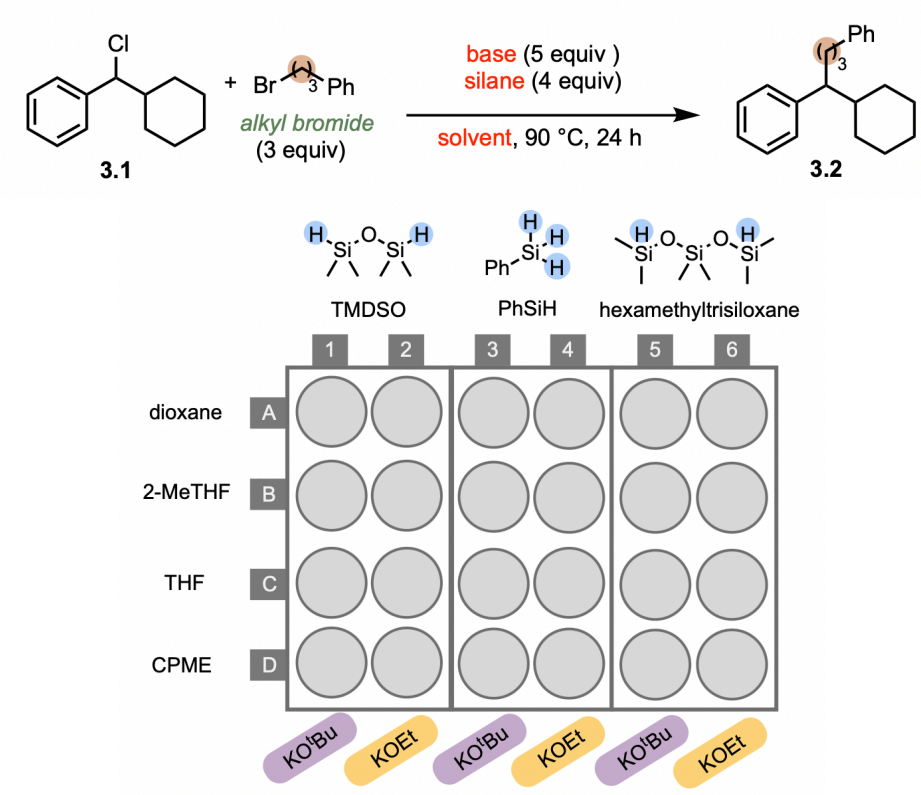

The high-throughput experiment was done under nitrogen atmosphere in 1-dram vials in and aluminum 24-well plate. In the glove box, base (5 equiv) was added to the corresponding columns. Stock solution was made for **3.1** (0.05mmol) in each solvent **A-D**, and added to the corresponding rows. Lastly, each column was charged with its corresponding silane: TMDSO in columns 1 and 2, PhSiH in columns 3 and 4, and hexamethyltrisiloxane in columns 5 and 6. Each

vial waws screwed closed with a cap. The plate was taken out of the glove box and heated on a Heidolph magnetic stirrer/hotplate at 90°C for 4 hours. All vials were quenched with EtOAc and filtered through silica gel using a glass fritted funnel. A small amount of the crude sample was analyzed by GCMS and concentrated on the rotary evaporator. The crude sample was dissolved in $CDCl_3$ and charged with ~5.0mg of 1,3,5-trimethoxybenzene as an internal standard (unless otherwise stated) for ^1H NMR analysis. To quantify NMR yield, the sextet peak at approximately 2.65 ppm corresponding to the benzylic proton was integrated relative to the singlet peak at 2.19 ppm from 1,2,4,5-tetramethylbenzene accounting for 12 protons.

5.1.3 | General procedure for scope discovery in Chapter 2

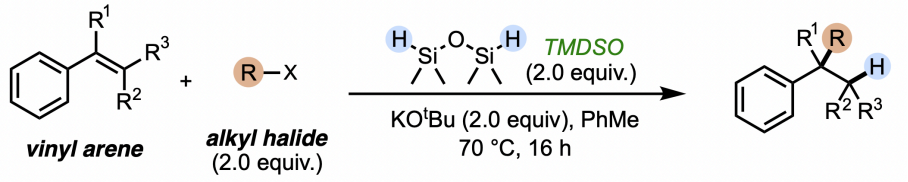

Reactions were set up outside of the glove box under a N_2 atmosphere using balloons and a 1-dram screw-cap vial, sealed with a Teflon/silicone septum. The vial was equipped with a stir bar and charged with KO^tBu (0.4 mmol). The vial was sealed with the cap and septum and purged with N_2 for 10 minutes. Once sufficiently purged, PhMe (1 mL) was added using a syringe, followed by the vinylarene (0.2 mmol), TMDSO (0.4 mmol), and alkyl halide (0.4 mmol) respectively. The N_2 source was removed, and the vial was then placed in an oil bath heated to the appropriate temperature and stirred for 16 hours. After the reaction time was complete, 0.8mL of TBAF was added to the vial and stirred for an additional 2 hours. The reaction mixture was quenched with EtOAc and filtered through silica gel using a glass fritted funnel. A small amount of the crude sample was analyzed by GCMS and concentrated on the rotary evaporator.

The crude sample was dissolved in $CDCl_3$ and charged with ~5.0mg of 1,2,4,5-tetramethylbenzene as an internal standard (unless otherwise stated) for ^1H NMR analysis. To quantify NMR yield, the sextet peak at approximately 2.65 ppm corresponding to the benzylic proton was integrated relative to the singlet peak at 2.19 ppm from 1,2,4,5-tetramethylbenzene accounting for 12 protons. TLC analysis of the crude sample was done to evaluate purity and determine the solvent system required for purification by column chromatography. Crude samples were then isolated by column chromatography, and the mass of the target product was measured for quantifying isolated yield. A final ^1H NMR in $CDCl_3$ as well as ^{13}C NMR was obtained for characterization of the pure compound.

Chapter 2 – Product Characterization

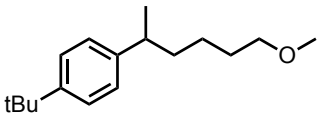

1-tert-butyl-4-(6-methoxyhexan-2-yl)benzene: Compound **4** was prepared from 4-tertbutylstyrene and 4-chloro-1-methoxybutane following the general procedure in 5.1.3. The crude residue was purified via automated column chromatography using 10% EtOAc:hexanes and a clear oil was obtained. (18.5mg, 37% yield). **^{1}H NMR** (500 MHz, $CDCl_3$) δ 7.30 (d, J = 8.3 Hz, 2H), 7.11 (d, J = 8.2 Hz, 2H), 3.33 (t, J = 6.7 Hz, 2H), 3.31 (s, 3H), 2.66 (sext, J = 7.1 Hz, 1H), 1.63 – 1.49 (m, 4H), 1.32 (s, 9H), 1.30 – 1.25 (m, 2H), 1.23 (d, J = 6.9 Hz, 3H).**^{13}C NMR** (500 MHz, $CDCl_3$) δ 148.58, 144.77, 126.67, 125.25, 73.00, 58.66, 39.45, 38.50, 34.46, 31.58, 29.90, 24.46, 22.27.

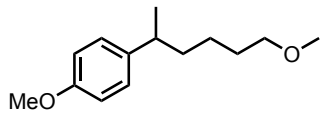

1-methoxy-4-(6-methoxyhexan-2-yl)benzene: Compound **5** was prepared from 4-methoxystyrene and 4-chloro-1-methoxybutane following the general procedure in 5.1.3. The crude residue was purified via automated column chromatography using a gradient of 10-20% EtOAc:hexanes and a clear oil was obtained. (4.7mg, 10% yield). **^{1}H NMR** (500 MHz, $CDCl_3$) δ 7.09 (d, J = 8.6 Hz, 2H), 6.83 (d, J = 8.7 Hz, 2H), 3.79 (s, 3H), 3.32 (t, J = 6.7 Hz, 2H), 3.30 (s, 3H), 2.63 (sext, J = 7.0 Hz, 1H), 1.53-1.58 (m, 4H), 1.31 – 1.25 (m, 2H), 1.21 (s, 3H). **^{13}C NMR** (500 MHz, $CDCl_3$) δ 157.82, 139.98, 127.93, 113.82, 73.00, 58.67, 55.38, 39.20, 38.60, 29.87, 24.43, 22.64.

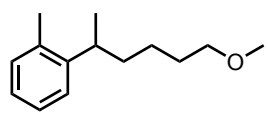

1-(6-methoxyhexan-2-yl)-2-methylbenzene: Compound **6** was prepared from 4-methoxystyrene and 4-chloro-1-methoxybutane following the

general procedure in 5.1.3. The crude residue was purified via automated column chromatography using 10% EtOAc:hexanes and a clear oil was obtained. (24.2mg, 59% yield) **^{1}H NMR** (500 MHz, $CDCl_3$) δ 7.18 (dd, J = 6.6, 1.8 Hz, 2H), 7.13 (d, J = 7.5 Hz, 1H), 7.08 (d, J = 2.2 Hz, 1H), 3.34 (t, J = 6.9 Hz, 2H), 3.31 (s, 3H), 2.97 (sext, J = 7.0 Hz, 1H), 2.33 (s, 3H), 1.67 – 1.62 (m, 2H), 1.56 (dt, J = 14.6, 7.2 Hz, 2H), 1.34 – 1.28 (m, 2H), 1.21 (d, J = 6.9 Hz, 3H). **^{13}C NMR** (500 MHz, $CDCl_3$) δ 146.01, 135.41, 130.30, 126.29, 125.54, 125.34, 72.97, 58.69, 37.78, 34.56, 29.99, 24.48, 21.70, 19.71.

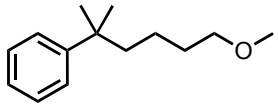

(6-methoxy-2-methylhexan-2-yl)benzene: Compound **7** was prepared from alpha-methyl styrene and 4-chloro-1-methoxybutane following the general procedure in 5.1.3. The crude residue was purified by column chromatography using a gradient of 0-10% EtOAc:hexanes and a clear oil was obtained. (19.3mg, 47% yield). **^{1}H NMR** (500 MHz, $CDCl_3$) δ 7.35 – 7.30 (m, 3H), 7.20 – 7.15 (m, 2H), 3.28-3.30 ppm (m, 5H), 1.66 – 1.55 (m, 2H), 1.48 (p, J = 7.0 Hz, 2H), 1.30 (s, 3H), 1.12 (tdd, J = 10.0, 7.8, 5.2 Hz, 2H). **^{13}C NMR** (500 MHz, $CDCl_3$) δ 149.69, 128.15, 125.92, 125.47, 72.98, 58.65, 44.65, 37.80, 30.46, 29.05, 21.55. Triplet (2H) and singlet peak (3H) are overlapping at 3.28-3.30 ppm.

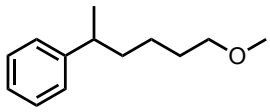

(6-methoxyhexan-2-yl)benzene: Compound **10** was prepared from styrene and 4-chloro-1-methoxybutane following the general procedure in 5.1.3. The crude residue was purified via column chromatography first using a gradient of 10-15% EtOAc:hexanes, then again with 2-4% EtOAc:hexanes to eliminate the dimer. A clear oil was obtained. (12.3mg, 32% yield). **^{1}H NMR** (400 MHz, $CDCl_3$) δ 7.31 (dd, J = 8.1, 6.9 Hz, 2H), 7.23 – 7.16 (m, 3H), 3.34 (t, J = 6.6 Hz, 2H), 3.32 (s, 3H), 2.71 (sext, J = 7.1 Hz, 1H), 1.63 – 1.56 (m, 4H), 1.36 – 1.32 (m, 2H), 1.27 (d, J = 6.9 Hz, 3H). **^{13}C NMR** (400 MHz, $CDCl_3$) δ 147.79, 128.40, 127.07, 125.91, 72.92, 58.62, 40.05, 38.40, 29.85, 24.41, 22.41.

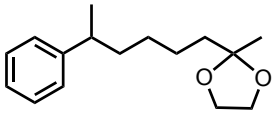

2-methyl-2-(5-phenylhexyl)-1,3-dioxolane: Compound **11** was prepared from styrene and 2-(4-chlorobutyl)-2-methyl-1,3-dioxolane following the general procedure in 5.1.3. The crude residue was purified via automated column chromatography using a gradient of 0-10% EtOAc:hexanes and a clear oil was obtained. (13.0mg, 26% yield). **^{1}H NMR** (300 MHz, $CDCl_3$) δ 7.30 (d, J = 7.8 Hz, 2H), 7.21 – 7.14 (m, 3H), 3.99 – 3.82 (m, 3H), 2.67 (sext, J = 7.1 Hz, 1H), 1.65 – 1.51 (m, 6H), 1.38 – 1.30 (m, 2H), 1.28 (s, 3H), 1.23 (d, J = 6.9 Hz, 3H). **^{13}C NMR** (500 MHz, $CDCl_3$) δ 128.46, 128.40, 127.10, 126.00, 64.74, 63.86, 43.84, 39.93, 38.27, 29.98, 27.40, 23.99, 22.48. Peak at 3.99 – 3.82 is missing one proton.

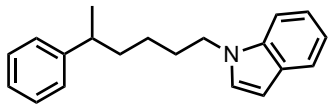

1-(5-phenylhexyl)-1H-indole: Compound **12** was prepared from styrene and 1-(4-chlorobutyl)-1H-indole following the general procedure in 5.1.3. The crude residue was purified via column chromatography using 10% EtOAc:hexanes and a clear oil was obtained. (18.0mg, 32% yield). **^{1}H NMR** (500 MHz, $CDCl_3$) δ 7.64 (d, J = 7.9 Hz, 1H), 7.32 – 7.30 (m, 2H), 7.24 – 7.15 (m, 5H), 7.13 – 7.09 (m, 1H), 7.04 (d, J = 3.2 Hz, 1H), 6.48 (d, J = 3.1 Hz, 1H), 4.06 (td, J = 7.1, 4.4 Hz, 2H), 2.67 (sext, J = 7.1 Hz, 1H), 1.82 (dt, J = 9.6, 2.7 Hz, 2H), 1.66 – 1.55 (m, 2H), 1.35 – 1.29 (m, 2H), 1.24 (d, J = 6.9 Hz, 3H). **^{13}C NMR** (500 MHz, $CDCl_3$) δ 147.49, 136.01, 128.69, 128.49, 127.86, 127.08, 126.07, 121.40, 121.05, 119.27, 109.48, 100.97, 46.41, 39.96, 38.09, 30.36, 25.23, 22.35.

5.1.4 | General procedure for scope discovery in Chapter 3

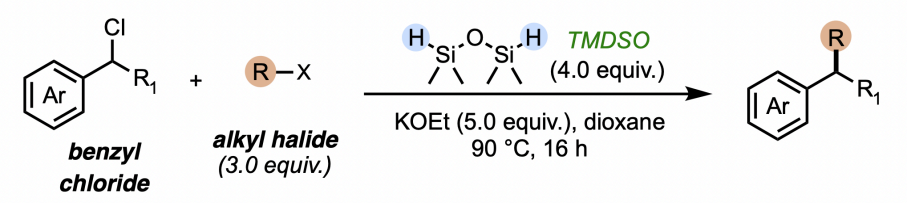

Reactions were set up outside of the glove box under a N_2 atmosphere using balloons and a 1-dram screw-cap vial, sealed with a Teflon/silicone septum. The vial was equipped with a stir bar and charged with KOEt (1.0 mmol). The vial was sealed with the cap and septum and purged with N_2 for 10 minutes. Once sufficiently purged, dioxane (1 mL) was added using a syringe, followed by alkyl halide (0.6 mmol) and TMDSO (0.8 mmol). Once bubbling ceased, benzyl chloride (0.2 mmol) was added into the vial using a syringe. The N_2 source was removed, and the vial was then placed in an oil bath heated to the appropriate temperature and stirred for 16 hours. After the reaction time was complete, 0.8mL of TBAF was added to the vial and stirred for an additional 2 hours. The reaction mixture was quenched with EtOAc and filtered through silica gel using a glass fritted funnel. A small amount of the crude sample was analyzed by GCMS and concentrated on the rotary evaporator. The crude sample was dissolved in $CDCl_3$ and charged with ~5.0mg of 1,2,4,5-tetramethylbenzene as an internal standard (unless otherwise stated) for ^{1}H NMR

analysis. To quantify NMR yield, the sextet peak at approximately 2.65 ppm corresponding to the benzylic proton was integrated relative to the singlet peak at 2.19 ppm from 1,2,4,5-tetramethylbenzene accounting for 12 protons. TLC analysis of the crude sample was done to evaluate purity and determine the solvent system required for purification by column chromatography. Crude samples were then isolated by column chromatography, and the mass of the target product was measured for quantifying isolated yield. A final ^{1}H NMR in $CDCl_3$ as well as ^{13}C NMR was obtained for characterization of the pure compound.

Glove-box set up:

The same reactions that were set up outside of the glovebox could also be prepared inside the glovebox without affecting reactivity, and was a faster method to use when running a larger number of reactions at a time. Inside the glovebox, a 1-dram screw-cap vial was equipped with a stir bar and charged with KOEt (1.0 mmol) and suspended in dioxane (1 mL), followed by the addition of alkyl halide (0.6 mmol) and TMDSO (0.8 mmol). The vial was promptly sealed with sealed with a Teflon/silicone septum to stop gas from leaving. Once bubbling ceased, the cap was quickly reopened, and benzyl chloride (0.2 mmol) was added before sealing the vial once again. The vial was taken out of the glovebox and placed in an oil bath heated to the appropriate temperature and stirred for 16 hours. After the reaction time was complete, 0.8mL of TBAF was added to the vial and stirred for an additional 2 hours. The reaction mixture was quenched with EtOAc and filtered through silica gel using a glass fritted funnel. A small amount of the crude sample was analyzed by GCMS and concentrated on the rotary evaporator. The crude sample was dissolved in $CDCl_3$ and charged with ~5.0mg of 1,2,4,5-tetramethylbenzene as an internal standard (unless otherwise stated) for ^{1}H NMR analysis. To quantify NMR yield, the sextet peak

at approximately 2.65 ppm corresponding to the benzylic proton was integrated relative to the singlet peak at 2.19 ppm from 1,2,4,5-tetramethylbenzene accounting for 12 protons. TLC analysis of the crude sample was done to evaluate purity and determine the solvent system required for purification by column chromatography. Crude samples were then isolated by column chromatography, and the mass of the target product was measured for quantifying isolated yield. A final ^{1}H NMR in $CDCl_3$ as well as ^{13}C NMR was obtained for characterization of the pure compound.

Chapter 3 – Product Characterization

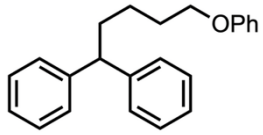

5,5-diphenyl-1-phenoxypentane: Compound **3.3** was prepared from diphenylchloromethane and 4-chloro-1-methoxybutane following the general procedure in 5.1.4. The crude residue was purified by column chromatography using 2% EtOAc in hexanes and a clear oil was obtained. **^{1}H NMR** (400 MHz, $CDCl_3$) δ 7.31 – 7.27 (m, 5H), 7.19 – 7.10 (m, 5H), 7.02 – 6.91 (m, 5H), 4.01(t, 2H), 3.92 (t, 1H), 2.16 – 2.05 (m, 3H), 1.99 – 1.93 (m, 2H), 1.87 – 1.79 (m, 1H). **^{13}C NMR** (400 MHz, CDCl3) δ 158.98, 145.16, 129.60, 128.56, 127.98, 126.24, 120.87, 114.59, 66.82, 51.44, 33.61, 29.64, 28.06.

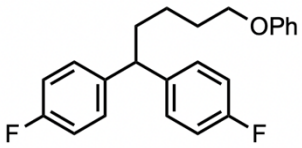

1,1-bis(4-fluorophenyl)-5-phenoxypentane: Compound **3.4** was prepared from chlorobis(4-flurophenyl)methane and 4-chloro-1-methoxybutane following the general procedure in 5.1.4. The crude residue was purified by column chromatography using 2% EtOAc in hexanes and a clear oil was obtained. **^{1}H NMR** (400 MHz, $CDCl_3$) δ 7.28 – 7.22 (m, 3H), 7.14 – 7.12 (m, 2H), 6.90 – 6.82 (m, 8H), 3.98 (t, J = 8.1 Hz, 2H), 3.89 (t, J = 6.0 Hz, 1H), 2.09 – 2.00 (m, 3H), 1.96 – 1.94 (m, 2H), 1.82 – 1.75 (m, 1H). **^{13}C NMR** (400 MHz, $CDCl_3$) δ 158.99, 140.69, 140.65, 129.61, 129.20, 120.88, 115.51, 114.60, 66.83, 49.86, 33.62, 29.65, 28.07.

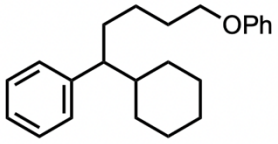

1-cyclohexyl-5-phenoxy-1-phenylpentane: Compound **3.7** was prepared from cyclohexylphenylmethylchloride and 4-chloro-1-methoxybutane following the general procedure in 5.1.4. The crude residue was purified by column chromatography using 2% EtOAc in hexanes and a clear oil was obtained.**^{1}H NMR** (400 MHz, $CDCl_3$) δ 7.30 – 7.25 (m, 5H), 7.20 – 7.16 (m, 1H), 6.91 – 6.85 (m, 3H), 6.85 – 6.83 (m, 2H), 3.85 (t, J = 6.4 Hz, 2H), 2.31 (td, 1H), 1.81 – 1.75 (m, 5H), 1.71 – 1.62 (m, 4H), 1.43 – 1.25 (m, 4H), 1.43 8 s, 4H), 1.10 – 1.08 (m, 4H), 0.82 – 0.75

(m, 1H). **^{13}C NMR** (101 MHz, $CDCl_3$) δ 159.19, 144.70, 129.50, 128.69, 128.09, 125.87, 120.57, 114.63, 67.90, 52.29, 43.42, 32.44, 31.58, 31.24, 29.50, 26.75, 24.42.

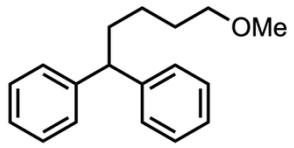

5,5-diphenyl-1-methoxypentane: Compound **3.11** was prepared from diphenylchloromethane and 4-chloro-1-methoxybutane following the general procedure in Chapter 5.1.4. The crude residue was purified by column chromatography using 2% EtOAc in hexanes and a clear oil was obtained. **^{1}H NMR** (400 MHz, $CDCl_3$) δ 7.31 – 7.24 (m, 8H), 7.20 – 7.16 (m, 2H), 3.91 (t, J = 7.8 Hz, 1H), 3.34 (t, J = 6.7 Hz, 2H), 3.31 (s, 3H), 2.9 (dt, 2H), 1.63 (p, J = 6.9 Hz, 2H), 1.34 (t, J = 7.8 Hz, 2H). **^{13}C NMR** (400 MHz, $CDCl_3$) δ 145.26, 128.53, 127.97, 126.18, 72.83, 58.65, 51.49, 35.71, 29.77, 24.78.

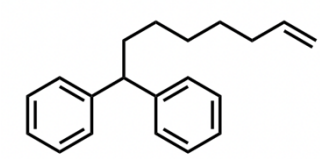

5,5-diphenyloct-1-ene: Compound **3.11** was prepared from diphenylchloromethane and 7-bromo-1-heptene following the general procedure in Chapter 5.1.4. **^{1}H NMR** (400 MHz, $CDCl_3$) δ 7.30 – 7.26 (m, 3H), 7.25 (s, 2H), 7.24 – 7.19 (m, 3H), 7.18 – 7.13 (m, 2H), 5.78 (ddt, J = 16.9, 10.2, 6.7 Hz, 1H), 5.02 – 4.87 (m, 2H), 3.89 (t, J = 7.8 Hz, 1H), 2.09 – 1.96 (m, 4H), 1.35 (td, J = 7.1, 3.1 Hz, 4H), 1.25 (d, J = 6.6 Hz, 2H). **^{13}C NMR** (400 MHz, $CDCl_3$) δ 145.45, 139.22, 128.00, 126.14, 114.35, 51.50, 42.09, 35.81, 33.87, 29.24, 28.87, 27.99.

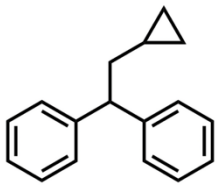

2,2-diphenylethyl-cyclopropane: Compound **3.13** was prepared from diphenylchloromethane and bromomethylcyclopropane following the general procedure in 5.1.4. The crude residue was purified by column chromatography using 2% EtOAc in hexanes. Diphenylmethane side product was inseparable from the resulting mixture. **^{1}H NMR** (500 MHz, $CDCl_3$) δ 7.30 (s, 5H), 7.20 (s, 3H), 7.18 – 7.15 (m, 2H), 4.05 (t, J = 7.7 Hz, 1H), 1.94 (dd, J = 7.7, 6.9 Hz, 2H), 0.88 (q, J = 6.6 Hz, 2H), 0.65 – 0.55 (m, 1H), 0.38 (dd, J = 8.2, 1.6 Hz, 2H). **^{13}C NMR** (126 MHz, CDCl3) δ 141.26, 129.08, 128.60, 126.21, 51.80, 42.09, 9.87, 4.88.

Appendix A: ^{1}H NMR and ^{13}C NMR for Chapter 2

1-tert-butyl-4-(6-methoxyhexan-2-yl)benzene. $CDCl_3$, 500 MHz

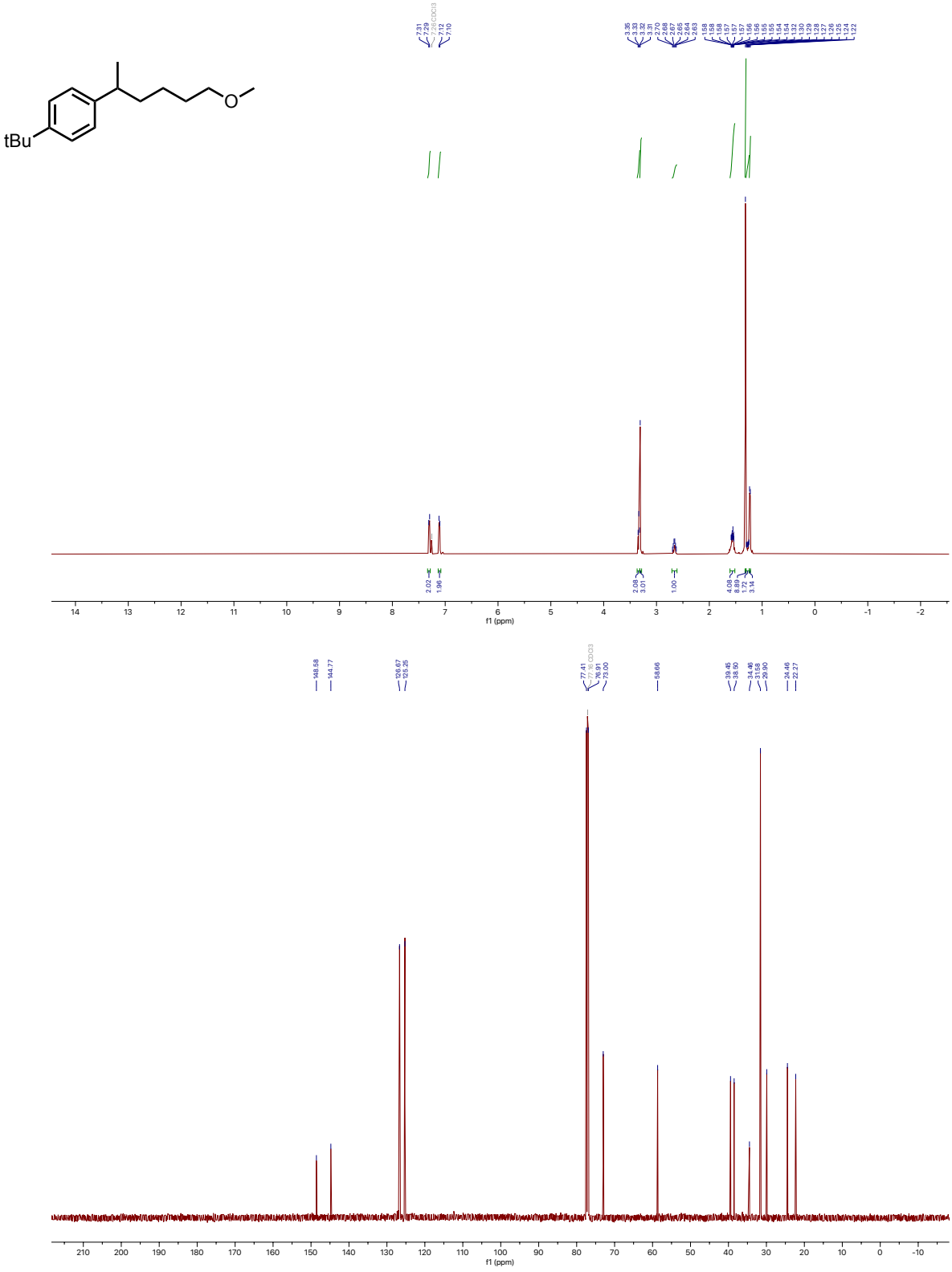

1-methoxy-4-(6-methoxyhexan-2-yl)benzene. $CDCl_3$, 500 MHz

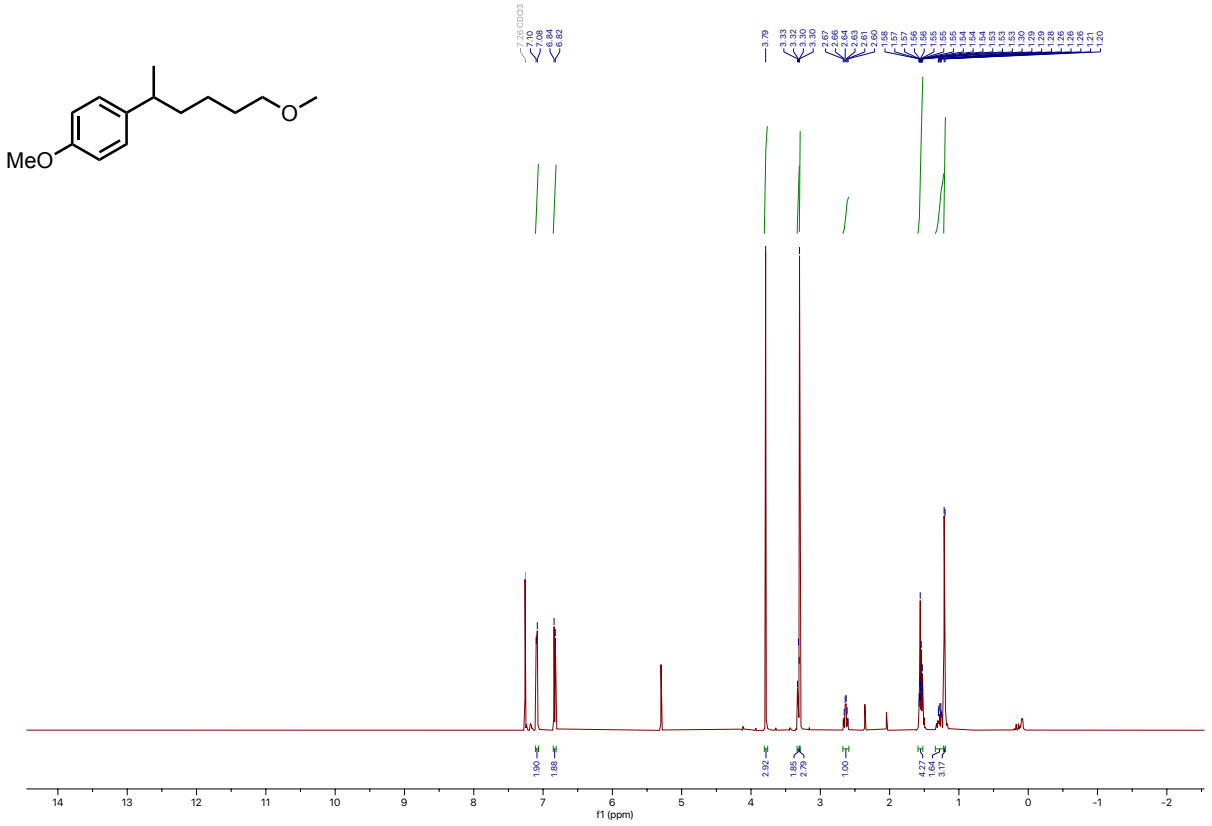

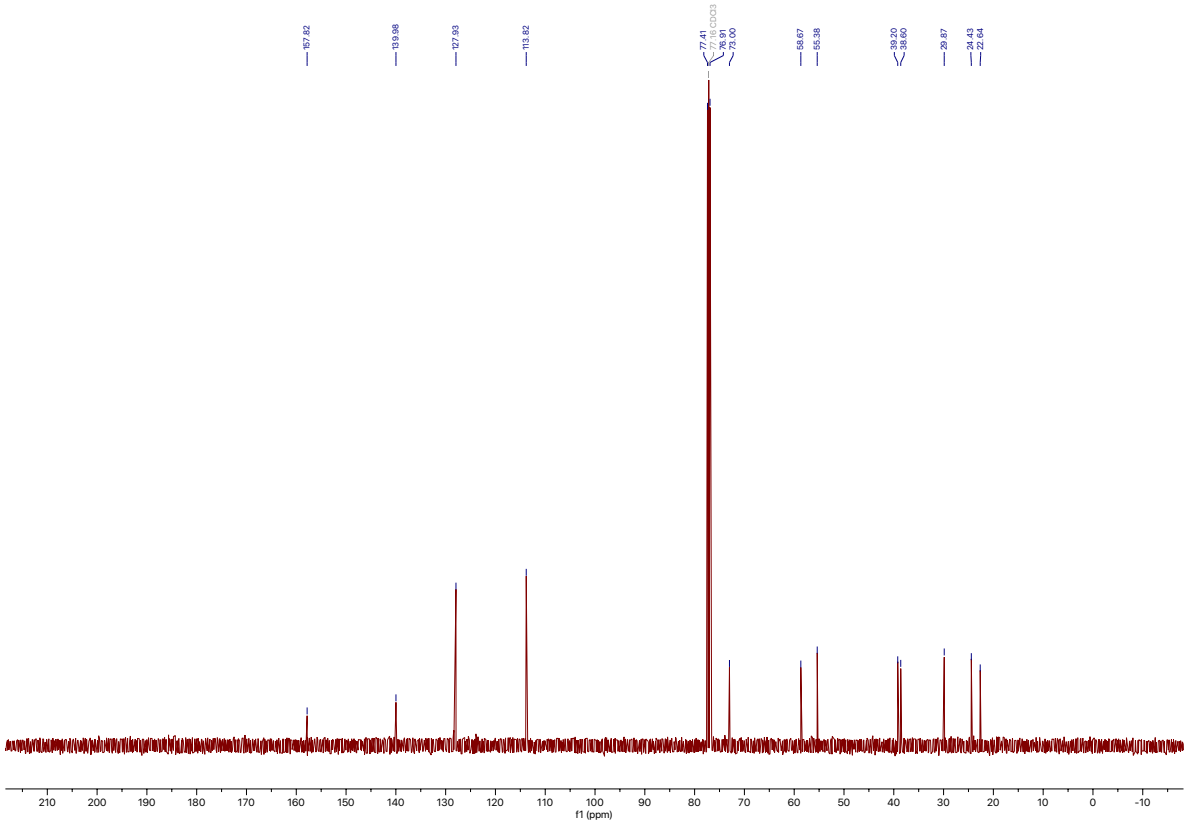

1-(6-methoxyhexan-2-yl)-2-methylbenzene. $CDCl_3$, 500 MHz

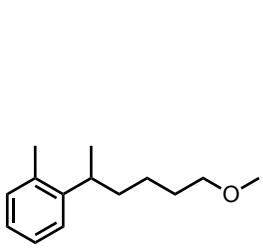

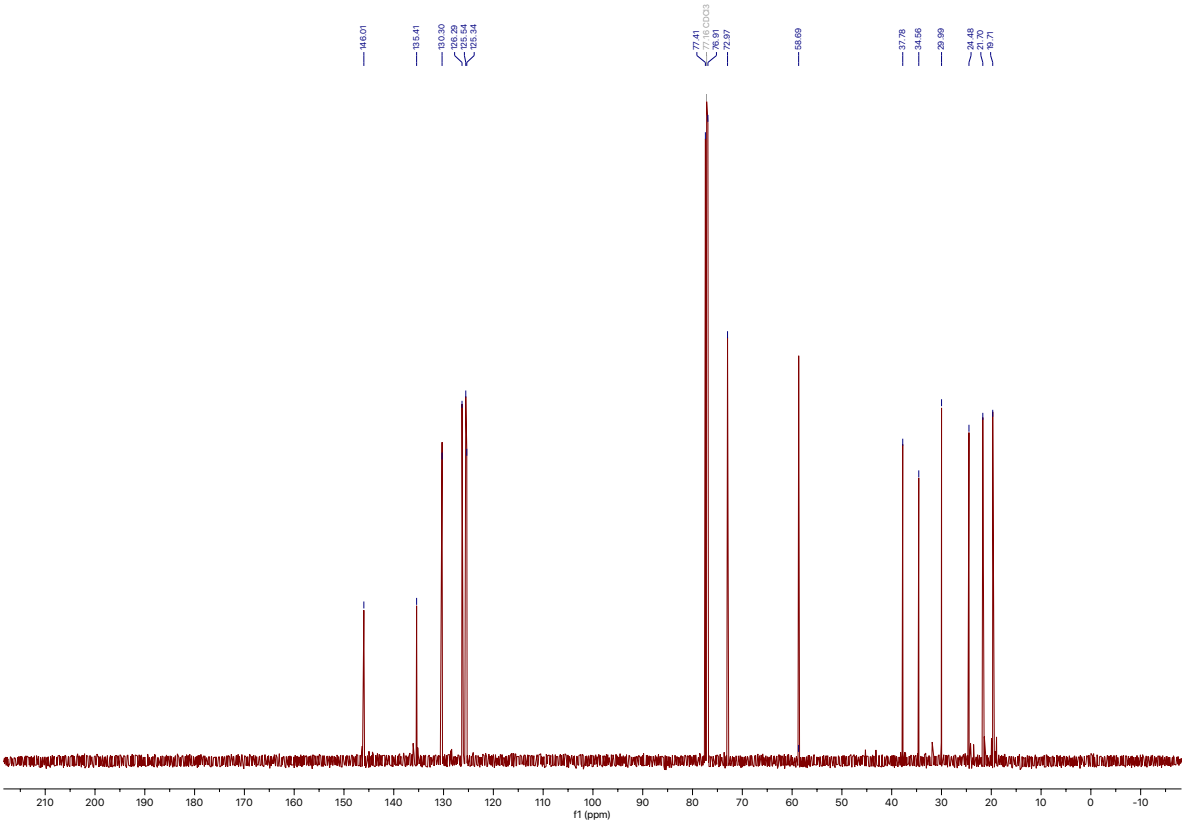

(6-methoxy-2-methylhexan-2-yl)benzene. $CDCl_3$, 500 MHz

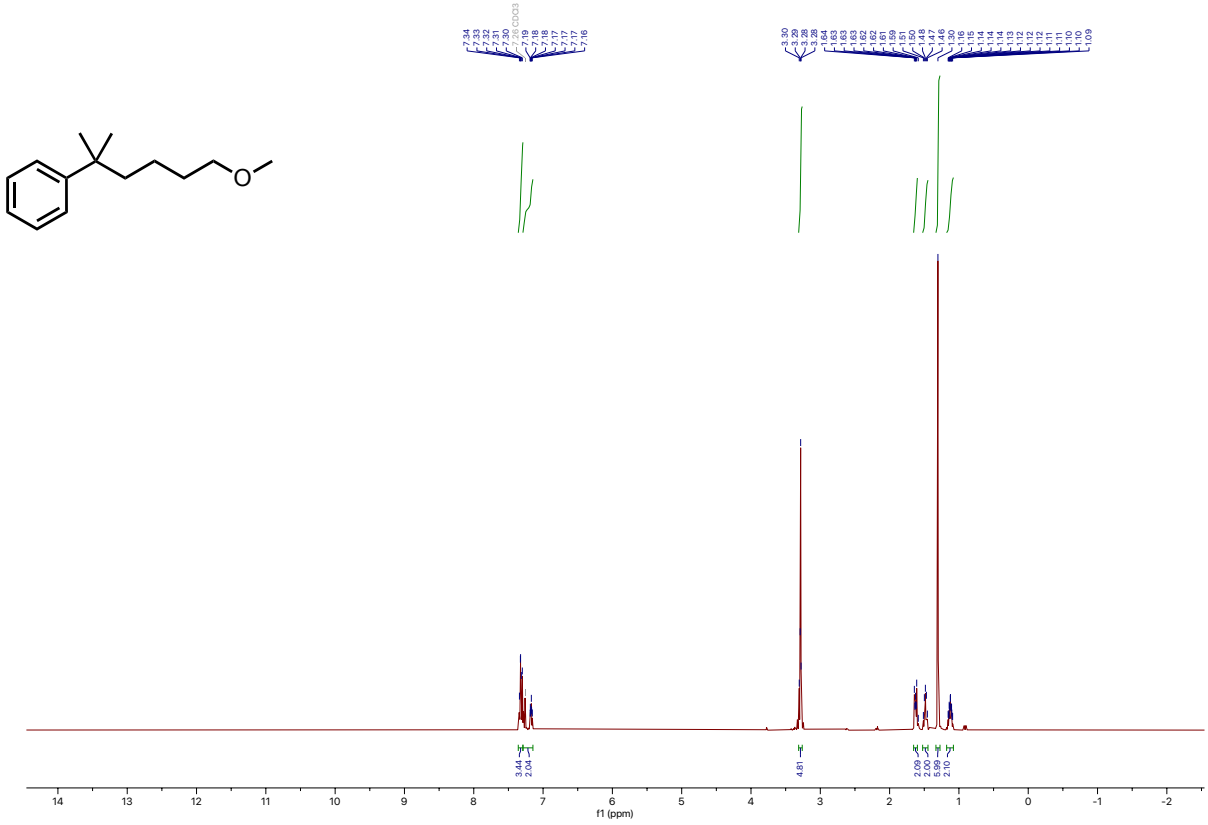

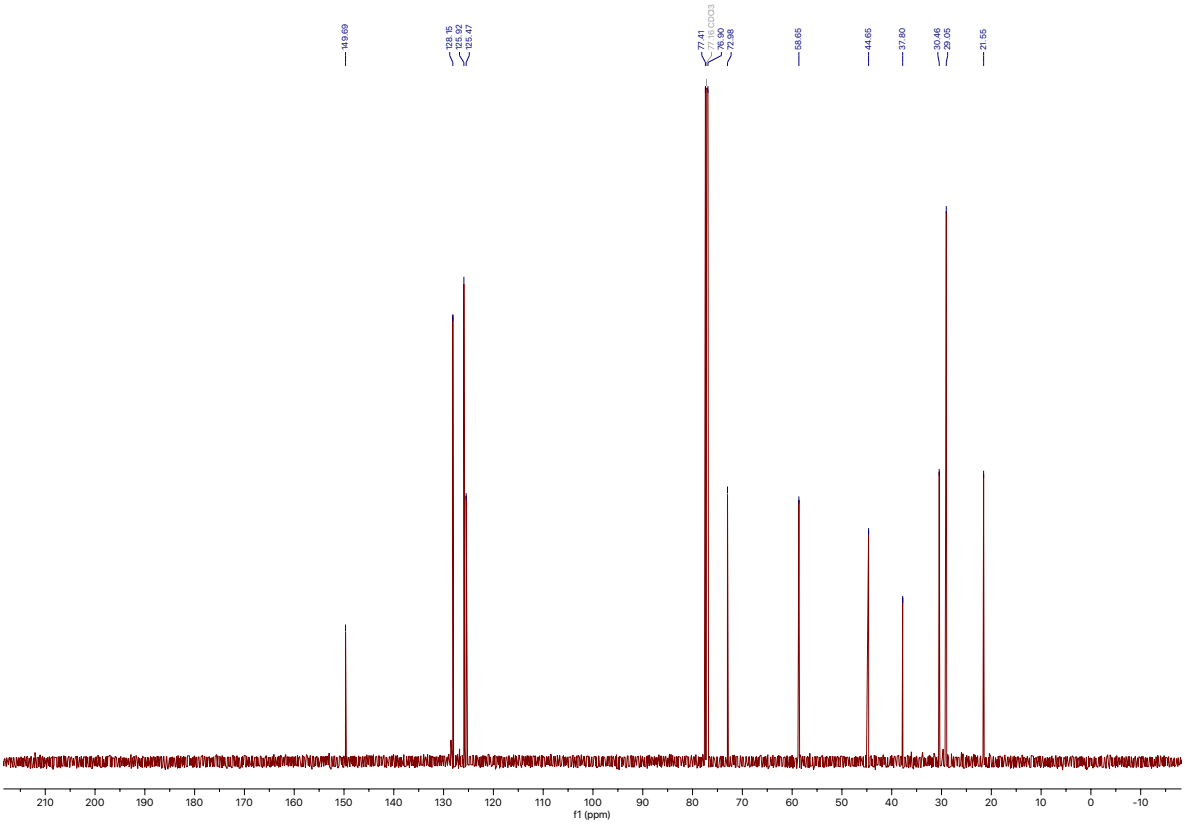

(6-methoxyhexan-2-yl)benzene. $CDCl_3$, 500 MHz

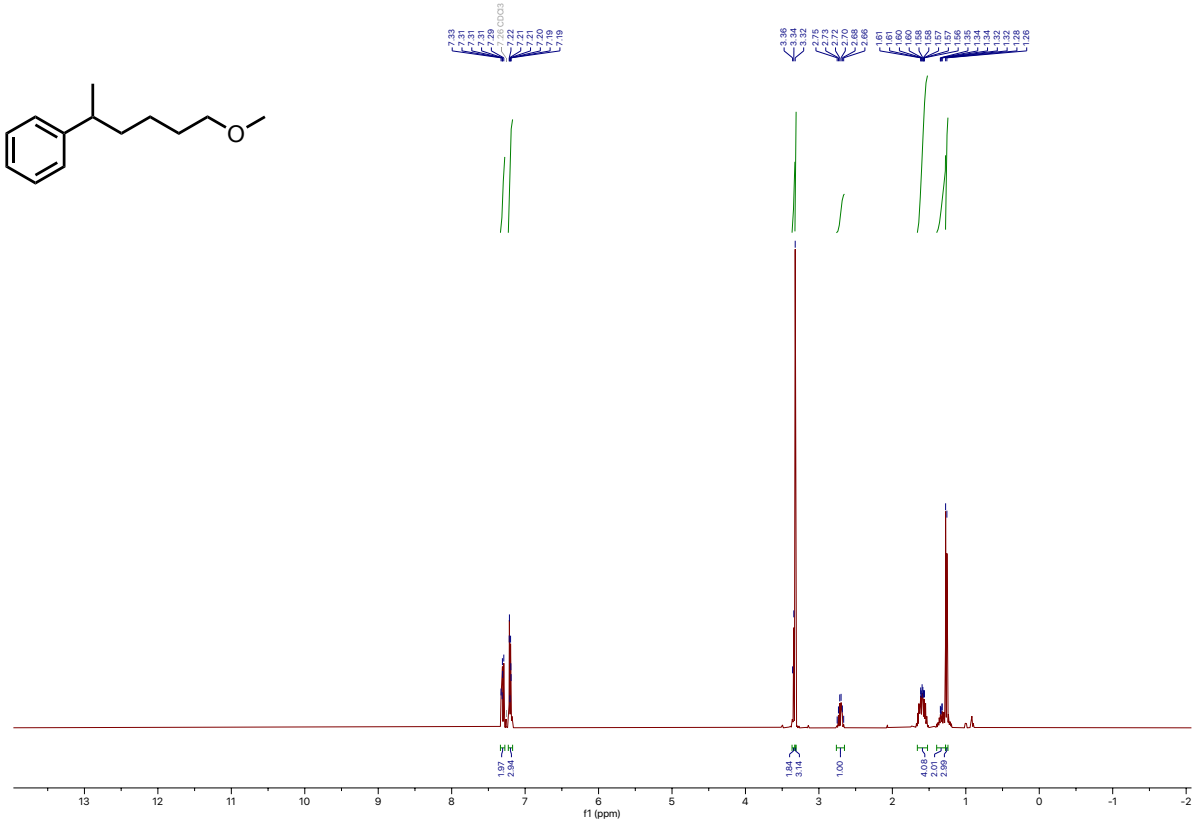

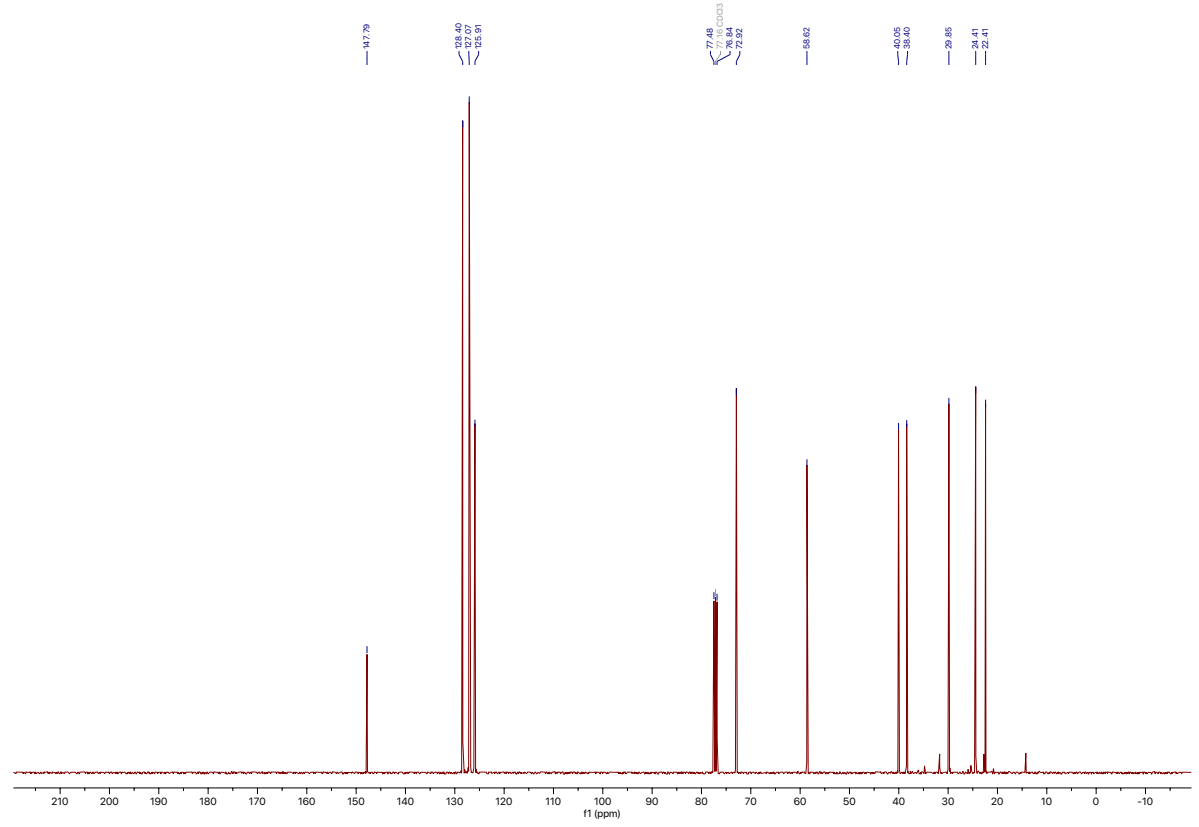

2-methyl-2-(5-phenylhexyl)-1,3-dioxolane. $CDCl_3$, 500 MHz

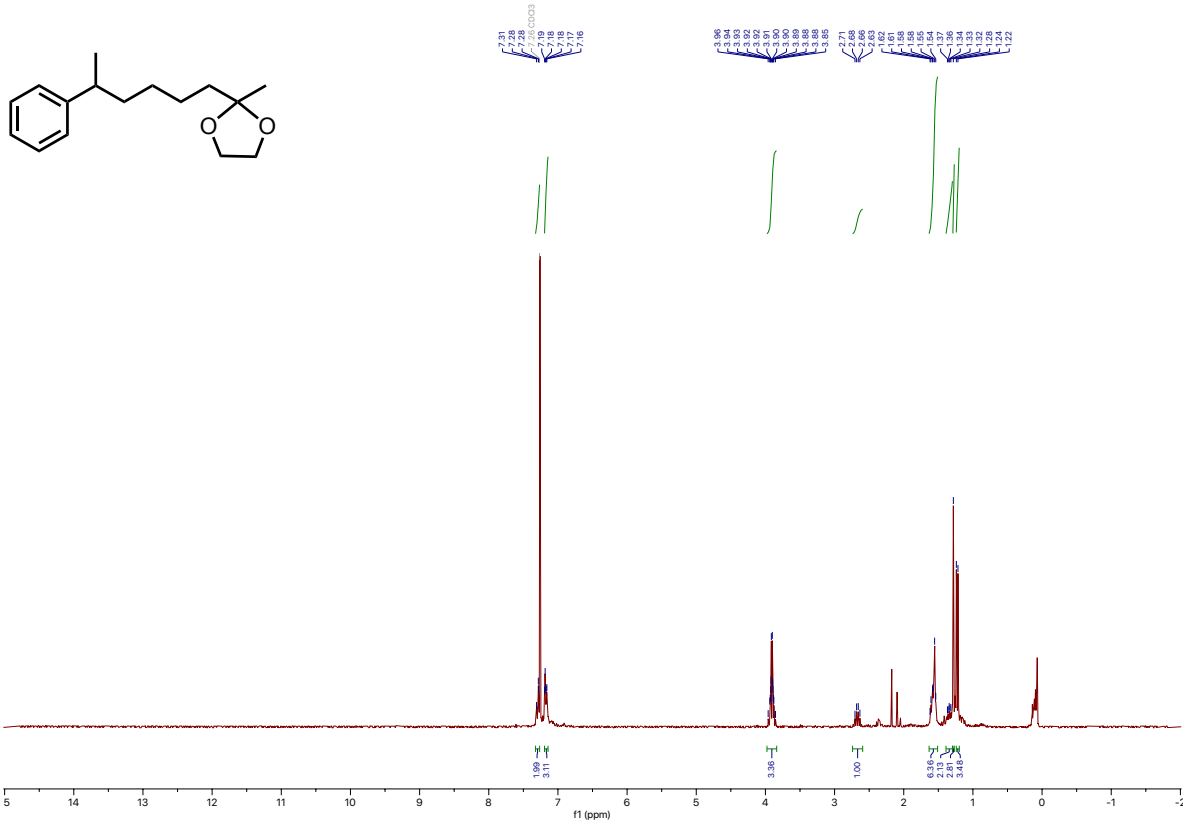

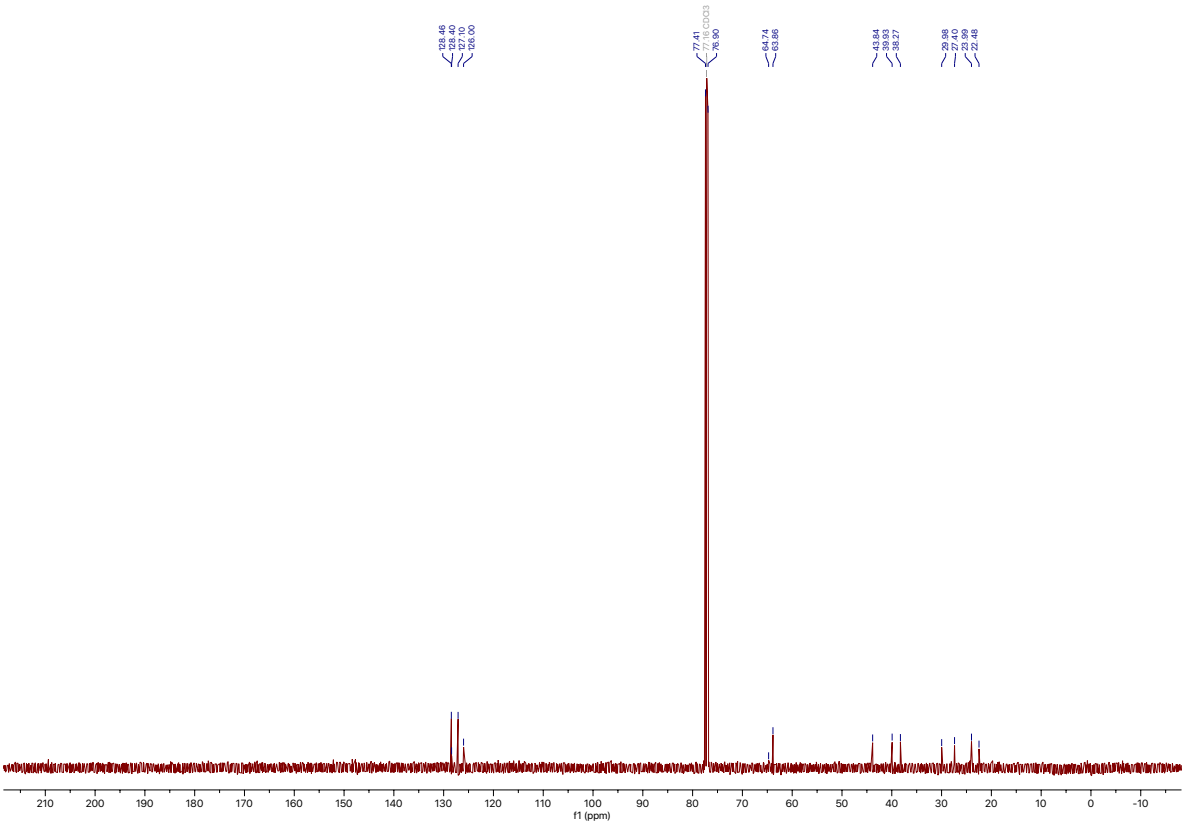

1-(5-phenylhexyl)-1H-indole. $CDCl_3$, 500 MHz

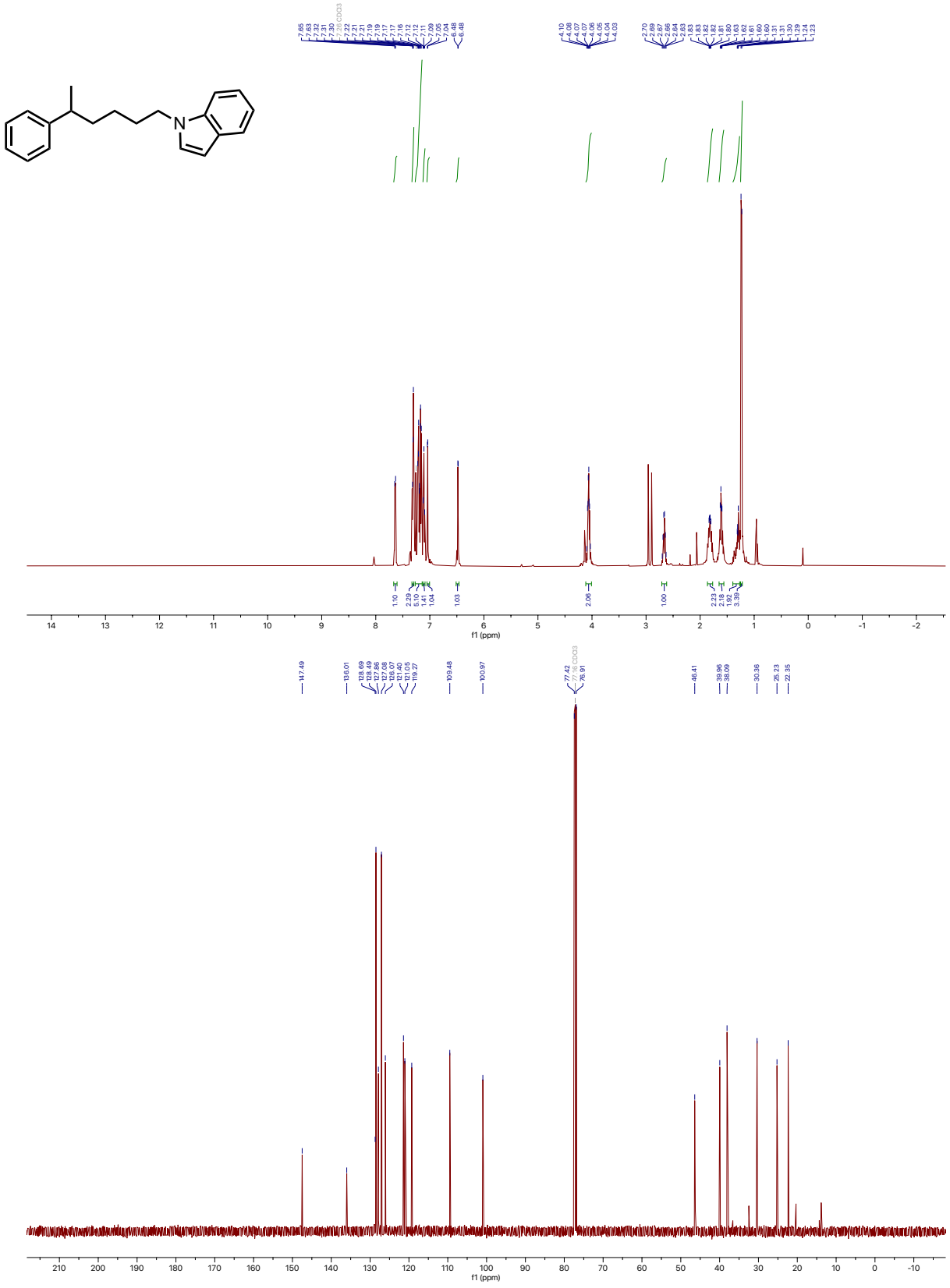

Appendix B: ^{1}H NMR and ^{13}C NMR for Chapter 3

5,5-diphenyl-1-phenoxypentane. $CDCl_3$, 400 MHz.

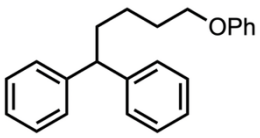

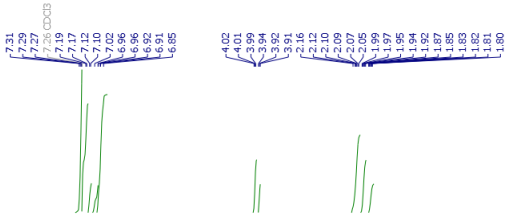

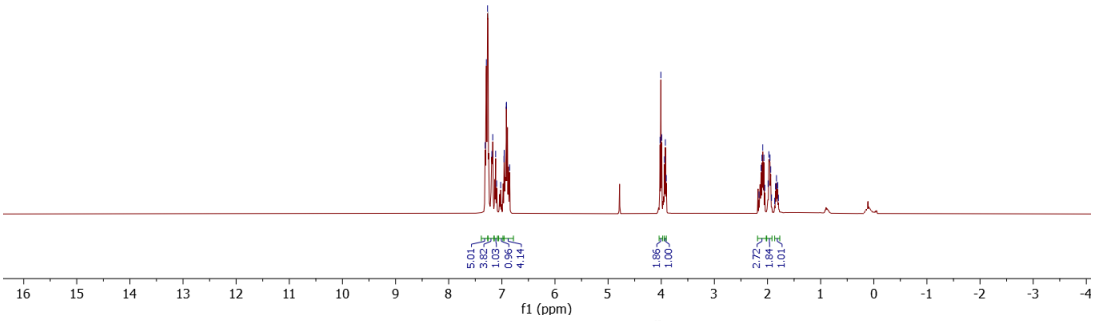

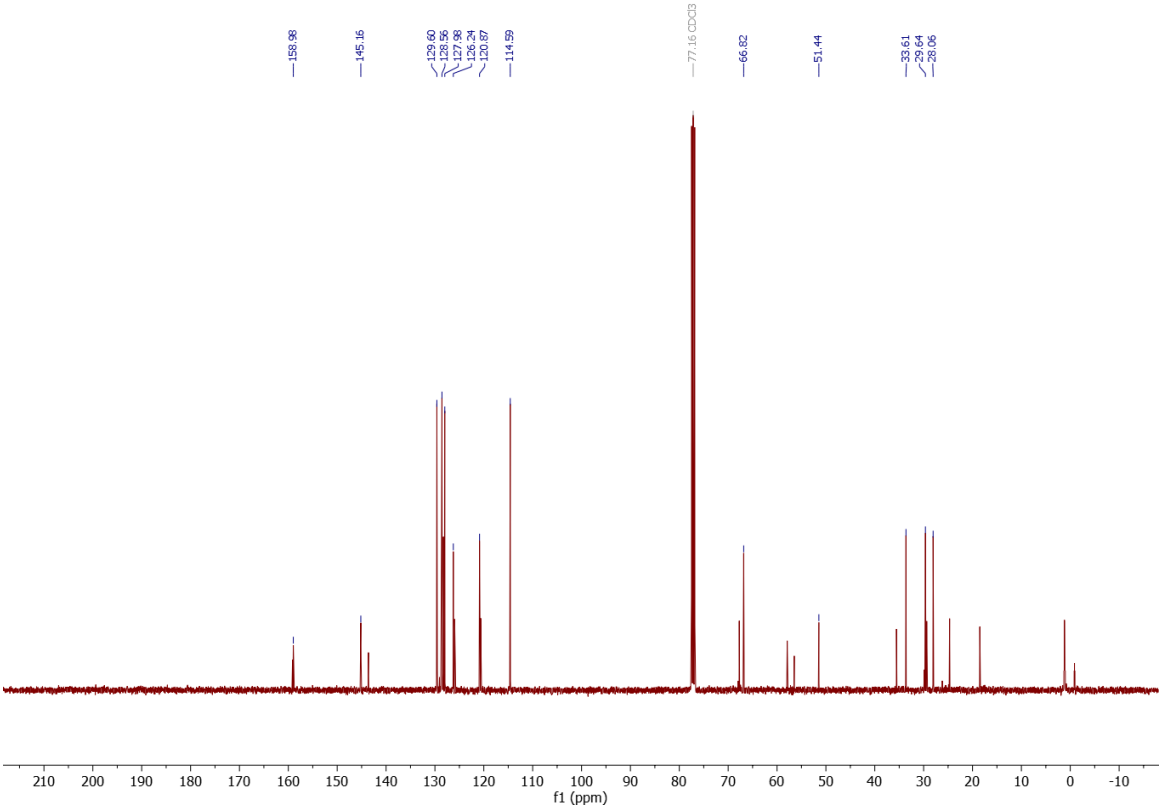

(5,5-bis(4-fluorophenyl)-pentyl)-phenyl ether. $CDCl_3$, 400 MHz.

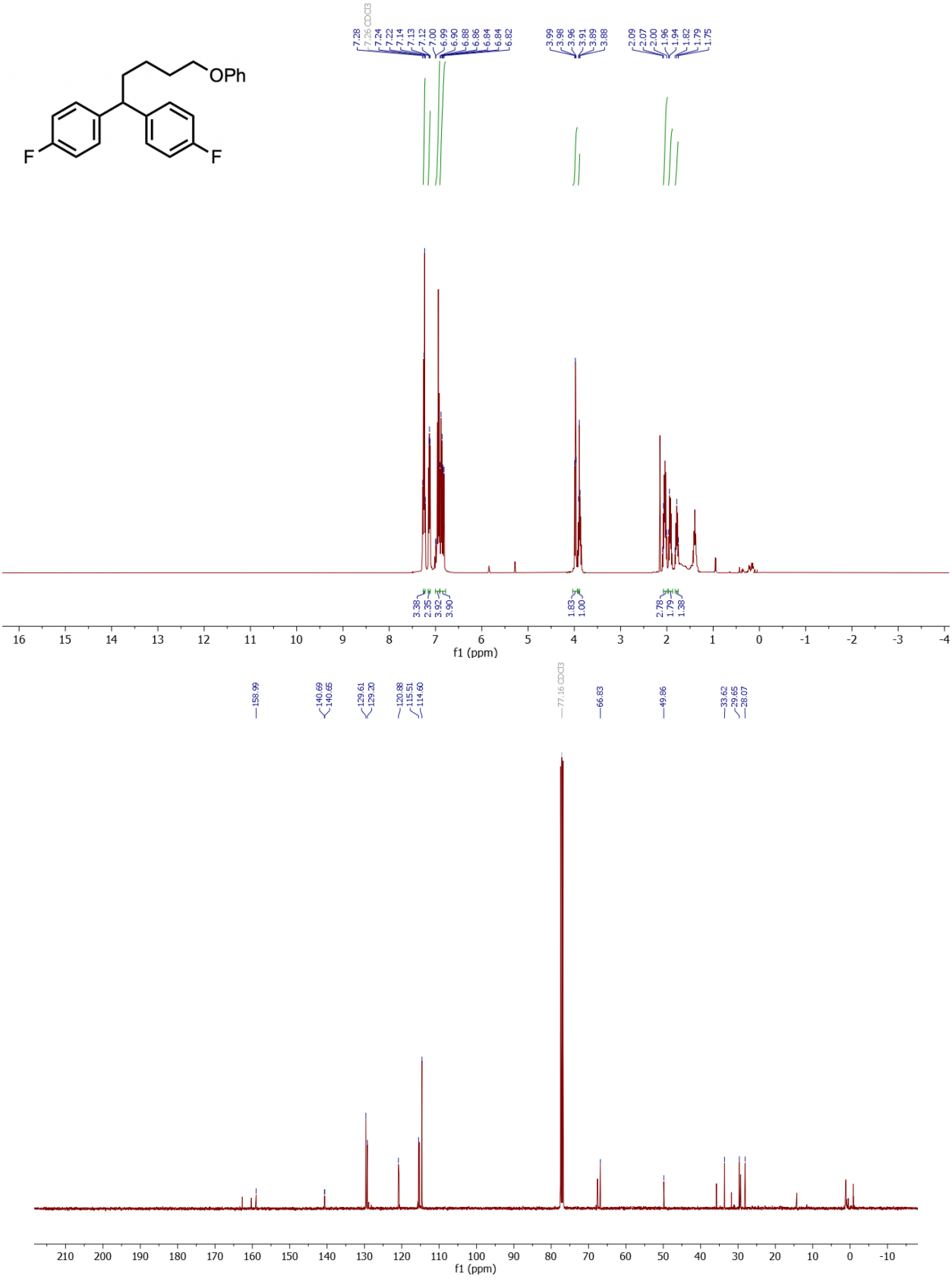

1-cyclohexyl-5-phenoxy-1-phenylpentane. $CDCl_3$, 400 MHz

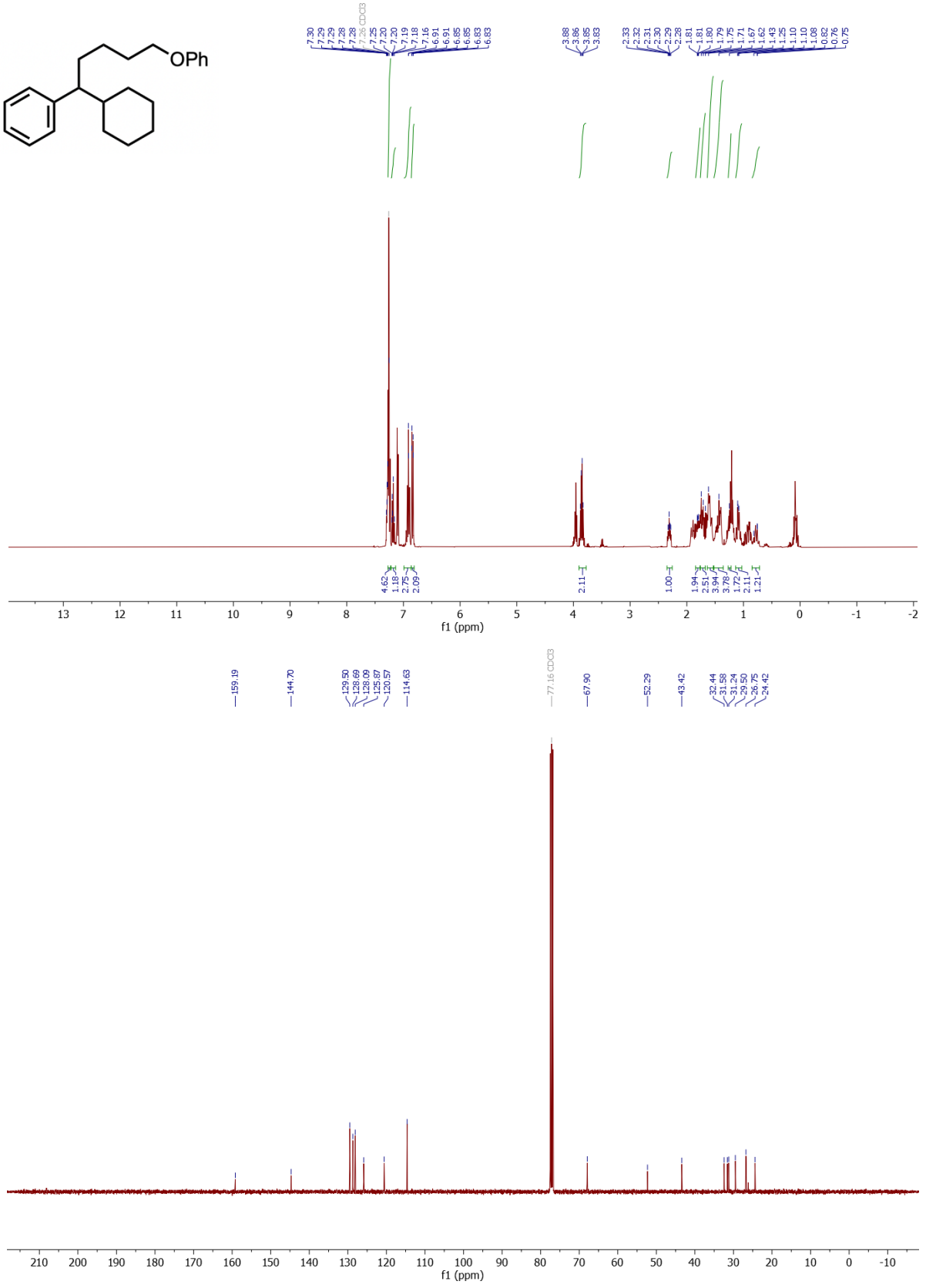

5,5-diphenyl-1-methoxypentane. $CDCl_3$, 400 MHz

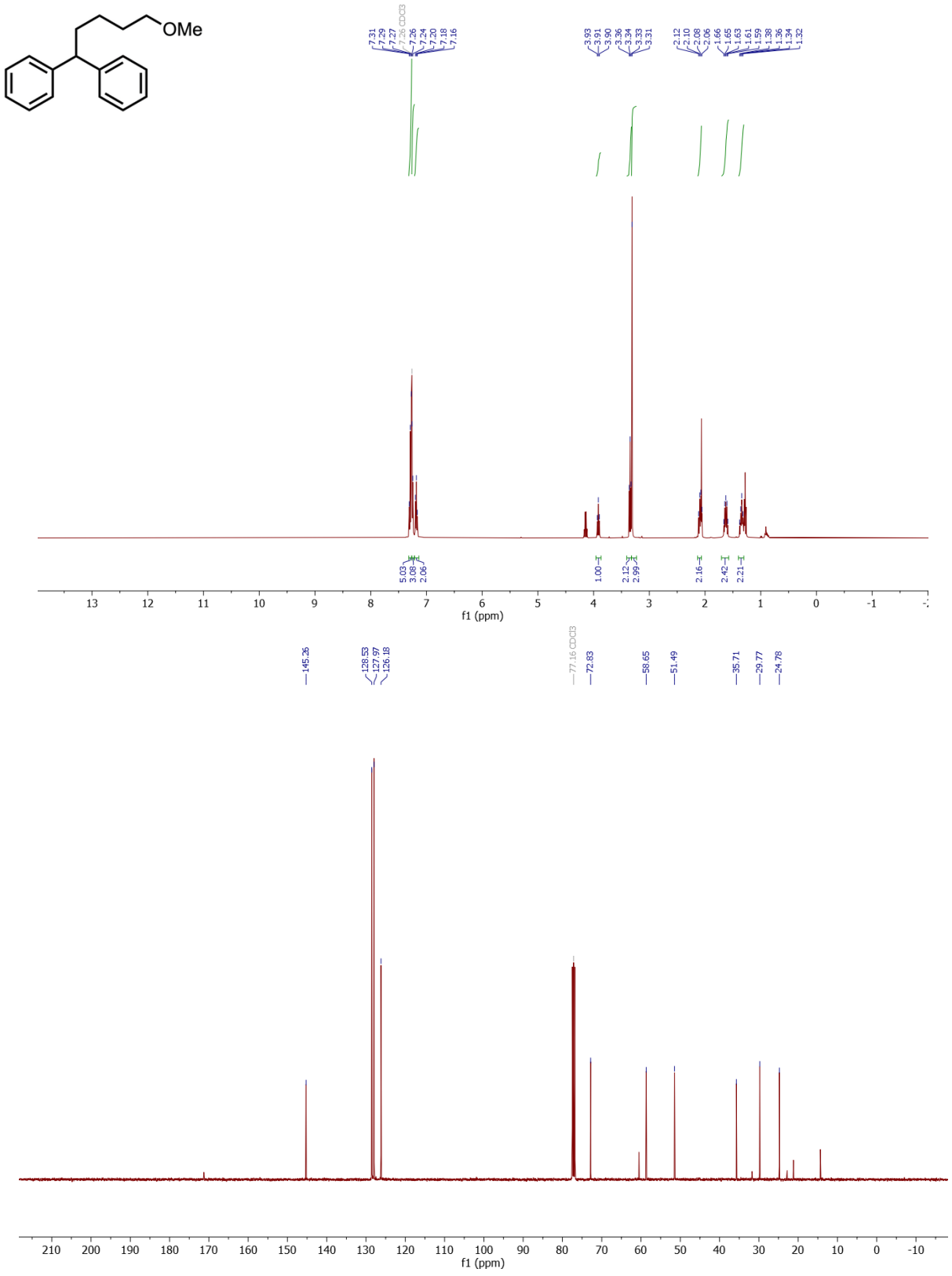

5,5-diphenyloct-1-ene. $CDCl_3$, 400 MHz

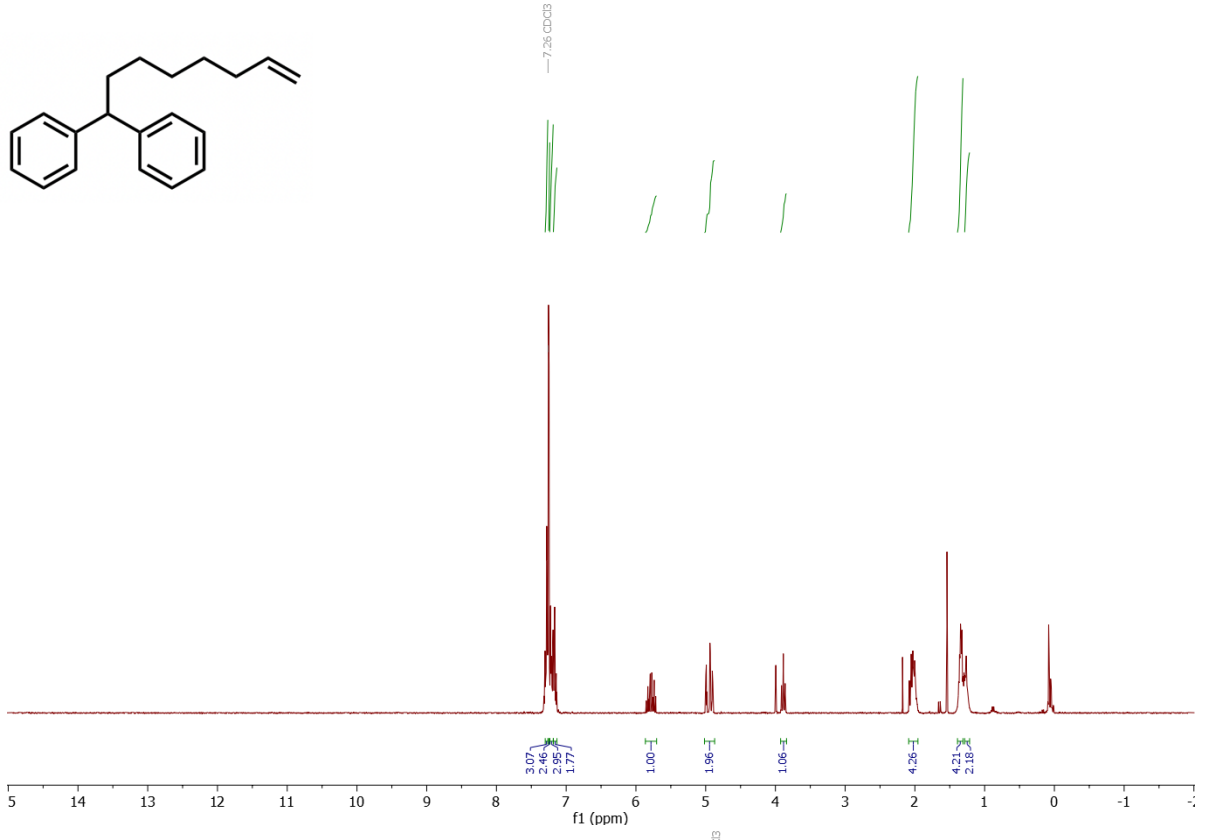

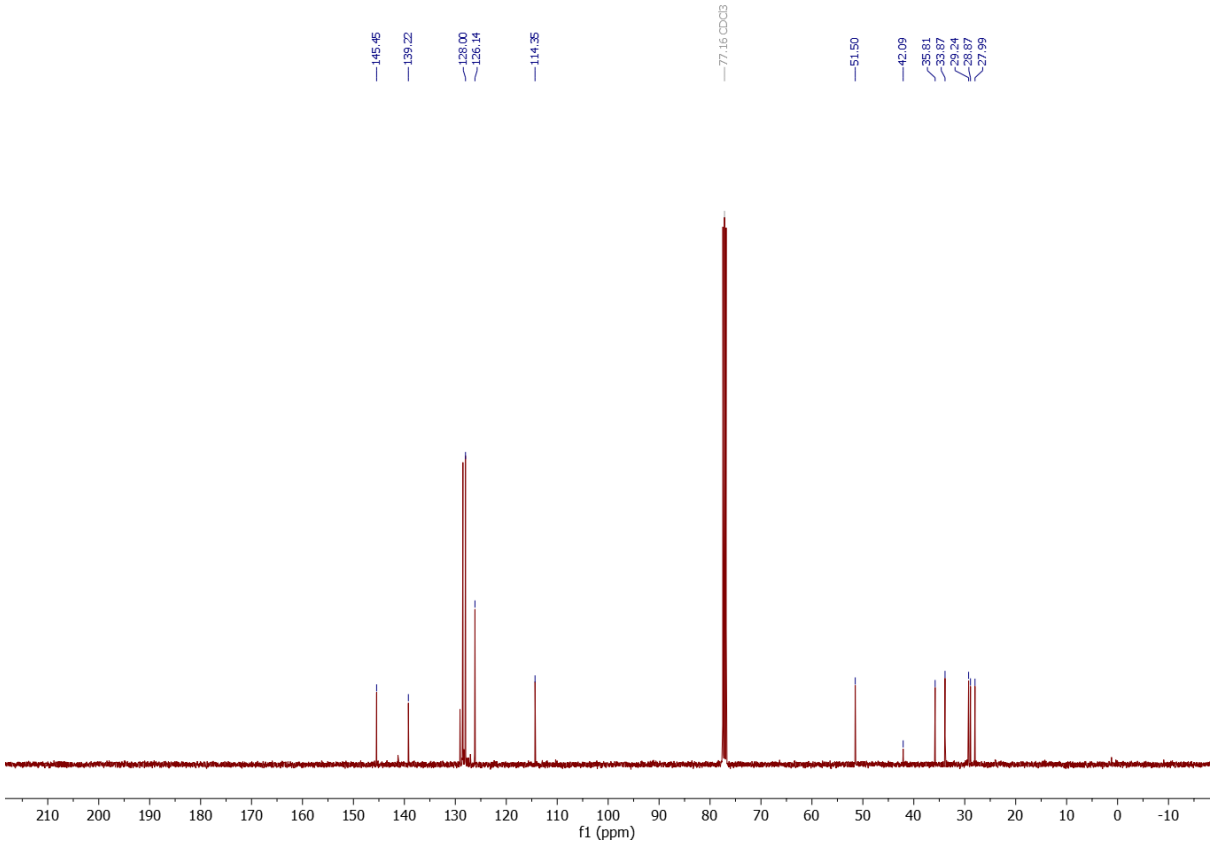

2,2-diphenylethyl-cyclopropane. $CDCl_3$, 400 MHz